UNIVERSITÀ DEGLI STUDI DI UDINE

FACOLTÀ DI INGEGNERIA

Dipartimento di ingegneria elettrica, gestionale e meccanica
Dottorato in ingegneria industriale e dell'informazione
-XXIV ciclo-

Tesi di dottorato

Advances in Centerless Grinding Technology

Relatore:
Dr.Ing. Marco Sortino

Dottorando:
Michele Pascolo

Coordinatore:
Prof. Paolo Gardonio

Anno Accademico 2011 - 2012

Contents

Summary

Nowadays, the competitive level of manufacturing industries depends on one's capacity to increase productivity, reduce production costs whilst assuring high production quality. Among machining processes, centerless grinding permits high production rates, high levels of automation and close tolerances but can be particularly tedious due to the multitude of parameters involved.
This research focuses on the investigation and development of innovative tools aimed to furnish a quick response to the development need of a centerless production cycle, to be integrated with the experimental phase. Firstly, an analysis of infeed centerless model available in literature has been carried out, with a particular attention on tool characteristics and resulting process variances. Secondly, based on practical rules of thumb and predictable variances from geometrical stability analysis an innovative approach has been implemented for the quick determination of set up parameters. Thirdly, effects of main process parameters on roundness components were investigated. Inline monitoring devices (acoustic emission and power sensor) investigated main process characteristics. Whilst the AE signal gave promising correlation with high demanding roughness and the power sensor permitted to investigate system time constant, the relationship between roundness components and AE analysis did not incur in any statistically significant results.

Introduction

In the field of manufacturing with geometrically undefined cutting edge, grinding takes a special place due to its removal possibilities combined with the possibility to fulfill demanding accuracies. Amongst grinding techniques, a special position is held by centerless grinding process which, thanks to its particular features, permits high production rates, high levels of automation and close tolerances. These characteristics focus on centerless grinding main application areas in high volume batches and mass production, particularly in bearing and automotive industries.
One of the mostly known issues of centerless grinding is related to high set up times. Despite some recent advance, the latter's drawback copes with the increasing necessity of flexibility and quick changeover.
Changeover durations are indeed due to the multitude of parameters and aspects involved in centerless grinding technology; anyway, the manufacturing cycle is often designed by time consuming trial-and-error approach or expert-based experience rather than a structured knowledge and awareness of possible inconveniences. A structured knowledge is at the same time indispensable considering the fulfillment of process performance characteristics, necessary requirements to cope with stochastic conditions actively involved in the manufacturing process.
In the centerless grinding process, a huge amount of research was carried out over the last fifty years. Research interest covered mainly problems related to three aspects: machine development, stability analysis and the development of simulation tools.
The development of simulation tools is getting an increasing importance in understanding the complexity of the various aspect involved in the centerless grinding system. The application of time domain simulations had permitted to analyze the impact of different process variables previously not investigable such as elastic deflections, continuous speed variations and others.
Despite this efforts, anyway, at the present time these tools appeared to be adequate for qualitative purpose only, particularly regarding the roundness characteristic.
With the aim of developing an highly integrated intelligent centerless grinding machine, the latter result to be an important issue. At the same time, whilst diameter and taper consistency are already provided in last generation production machines, roughness detection found promising results with AE monitoring.
This research work focuses on a deep understanding of the main aspect involved in the design and application of a robust centerless grinding cycle, from the main practical aspects to the development of tools for the process design and the set-up of main machining parameters.
The thesis is structured as follows.
In chapter 1 a brief introduction on the centerless infeed grinding process is given, from the definition of the grinding machining and its main geometric and kinematic parameters to the main aspects of the centerless grinding technologies.
In chapter 2 a review of the grinding dynamic model is carried out with a particular attention to the different issues involved in the centerless grinding tools with an

explanation their representative characteristics in the machining system and a collection of available data in literature.
In chapter 3 practical aspects of the centerless infeed grinding process are examined, with main indications of important parameters and rules of thumb for machine set-up and cycle time design.
In chapter 4 two innovative tools are developed with the aim of giving assistance for the design and set-up of proper infeed cycle, considering the possible variances in main geometrical and macro system characteristics.
In chapter 5 a practical investigation of macro system characteristics and outputs is carried out. A design of experiments is carried out to understand the effect of cycle parameters on roundness characteristics and system response characteristics through the application of in-line monitoring system (acoustic emission and absorbed power).

1 Grinding theory and centerless plunge grinding

1.1 Abrasive machining concept – generalities

Abrasive machining can be defined as a machining operation carried out through the use of geometrically undefined cutting edges.
DIN norm 8589 groups under the previous category the following:

- grinding
- honing
- lapping
- free abrasive grinding
- abrasive blast cutting

In order to cut, typically within the range of few μm, abrasive has to be harder than machined material. Abrasive is normally of crystalline and brittle material and it splinters as the machining operation goes on.
Comparing the machining action of abrasive grits to the one carried out by geometrically defined cutting edges, the following aspects have to be underlined (especially concerning grinding operation):

- the varying nature of the number of cutting edges in abrasive operations with bonded grits based on the applied machining parameters[1];
- the difference in orthogonal rake angle of cutting edge machining.

The number of cutting edges and their action vary depending on machining parameters (for the grinding process, on kinematical parameters, as shown in figure 1-1); therefore a distinction has to carried out between the number of protruding grits on the outer surface of the grinding wheel and the number of cutting grits (kinematic cutting grits).
For instance, in grinding operation, the number of bonded cutting grits engaging the part depends on the kinematic machining parameters (such as speed ratio[2] and depth

[1] It has to be reminded that a difference exists between number of cutting edges and the number of cutting grits. Based on abrasive grit properties (e.g. friability, sharpness) the number of cutting edge can be higher than the number of cutting grits. Anyway, in order to investigate kinematic parameter dependence easily, the dependence is reported for the number of cutting grits.
[2] The speed ratio is intended to be the ratio between the cutting edge speed and the cut surface [Tonshoff, 1992]..

of cut[3]) and on the conformity of the grinding wheel to the cut surface (generally included in the equivalent diameter[4]). A good example of kinematic cutting edge number variation based on previously cited parameters is shown in figure 1-2 [Tonshoff, 1992].

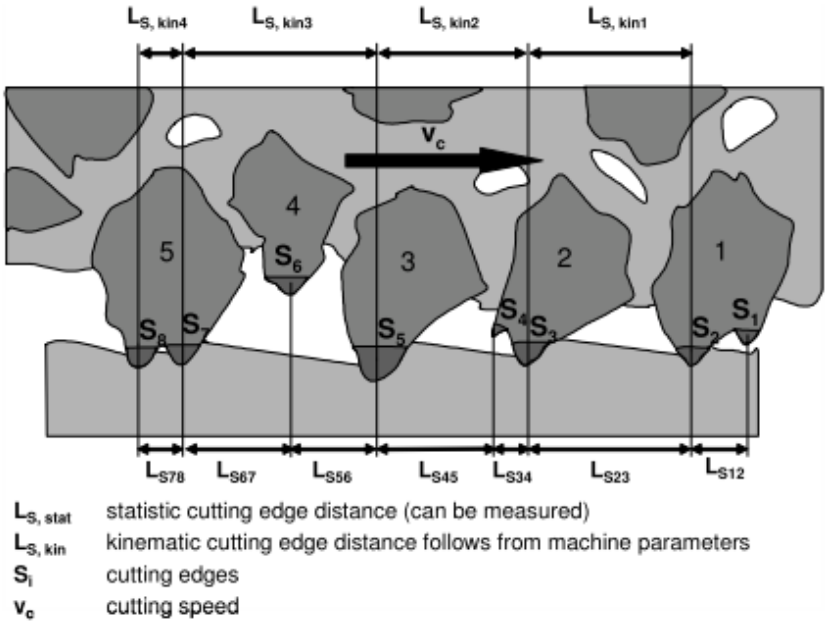

Figure 1-1 Difference between kinematical and static cutting edges [Klocke, 2009]

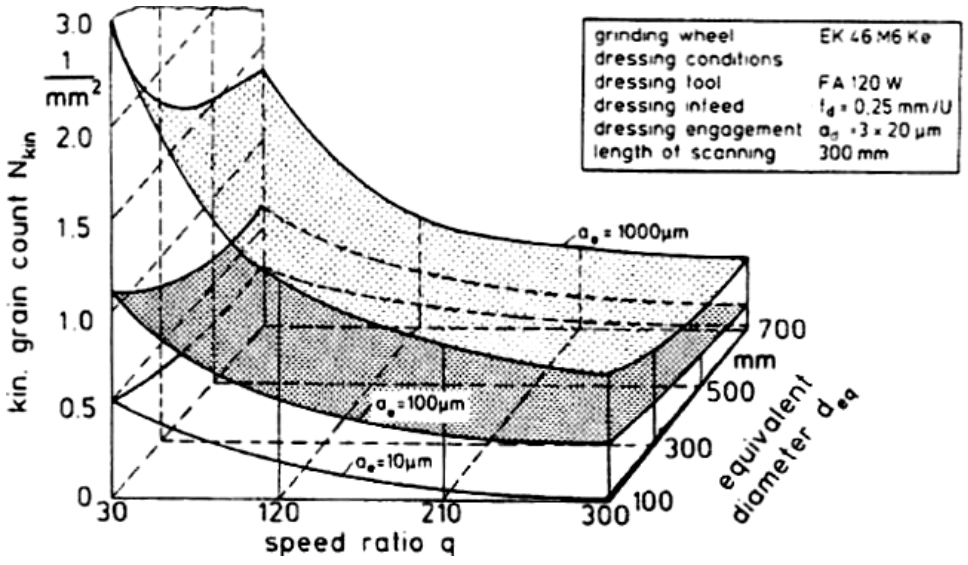

Figure 1-2 Variation of kinematic cutting edge as function of speed ratio *q*, conformity (equivalent diameter) d_e and depth of cut a_e for grinding operation [Tonshoff, 1992]

[3] The depth of cut is traditionally defined as the depth of removal carried out by the geometrically-ideal cut carried out by the grinding wheel shape on the workpiece (i.e. no deflections are taken in consideration) [Tonshoff, 1992]..

[4] The equivalent diameter is a geometrically defined parameter giving reason of geometrical conformity between the cut surface and the cutting wheel (particularly relevant when examining internal grinding) [Tonshoff, 1992].

Due to the shape of abrasive grits, the orthogonal tool rake angles are usually considered to be negative, up to -80°[5] .The cutting behaviour may be subjected to variation, due to frictional nature of the abrasive action (figure 1-3).

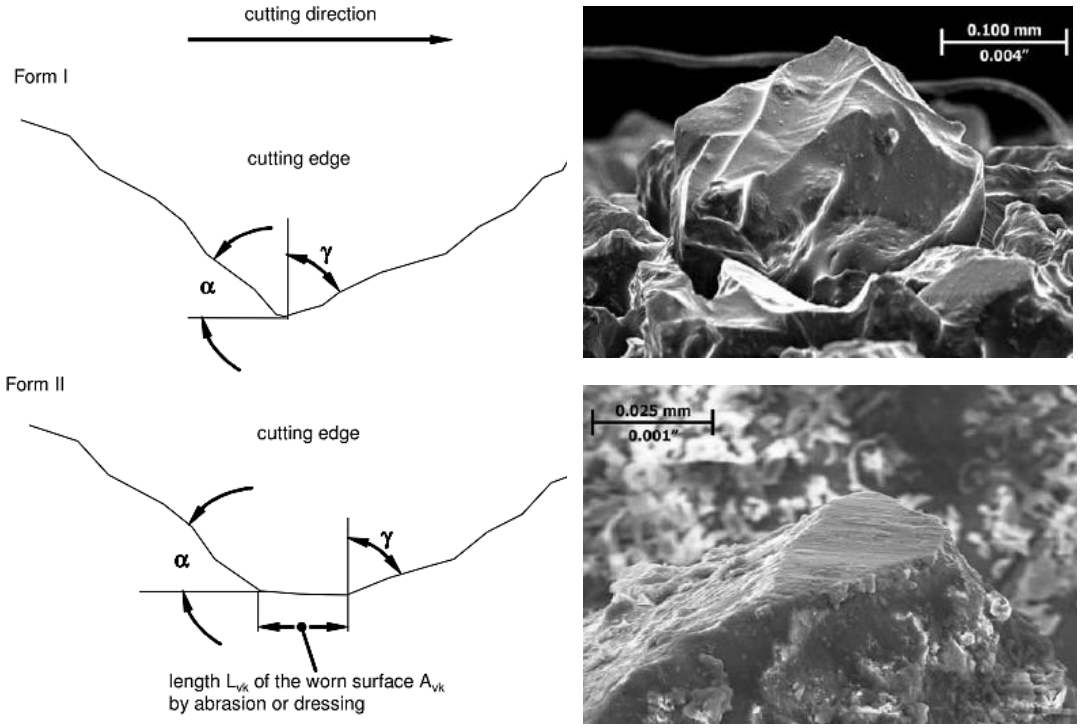

Figure 1-3 Example of cutting edge changing geometry due to wear for grinding operation [Klocke, 2009], [Badger, 2009]

1.2 Distinction of abrasive processes

Abrasive processes can also be classified based on the way the abrasive grit engages material [Klocke, 2009]. Four are the main engagement principles: energy-bound, force-bound, track-bound, space-bound (figure 1-4).
The energy bound system is the working principle involved in sand-blasting. The abrasive action (that varies based on the hardness of the machined material[6]) is determined by the impacting abrasive energy.
Other free abrasive applications are considered to be lapping and polishing. Free abrasive is usually suspended in a medium (fluid or paste/wax). In lapping (figure 1-5), grits are conveyed in movement trough a relative movement between pad and workpiece with resulting rolling and cutting action. So the free abrasive action is considered to be highly dependent on the imposed geometry gap (space bound principle).

[5] "…many researchers are of the opinion that the average grit resembles a tip of a rake angle of up to γ=-80°" [Klocke, 2009]
[6] In soft workpieces the impacting action of sand blasting result in small craters with hardening (similar to what happens with shot peening on hard parts) whilst abrasive chips the workpiece material in hard parts.

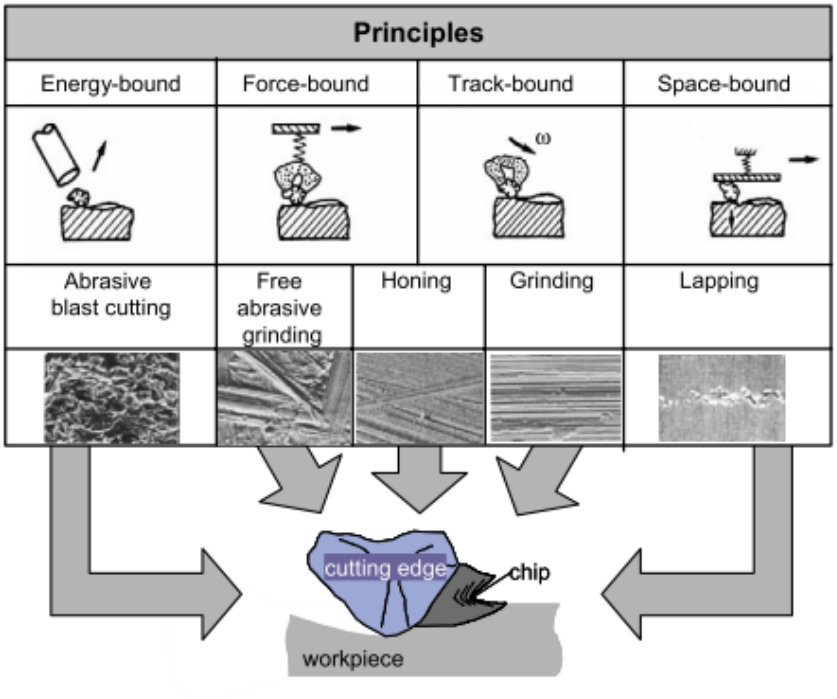

Figure 1-4 Abrasive processes and cutting principles [Klocke, 2009]

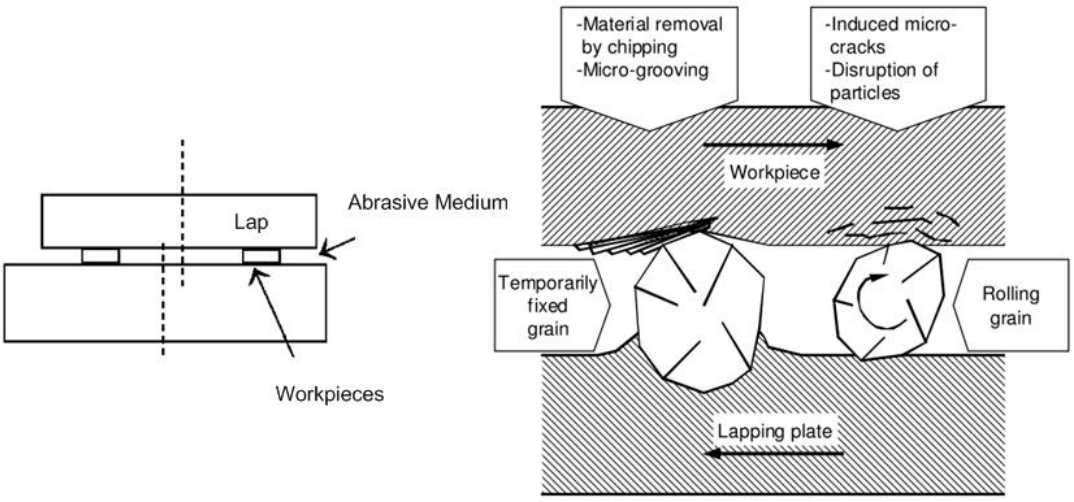

Figure 1-5 Schematic representation of lapping [Marinescu, 2004] and possible removal mechanism [Klocke, 2009]

In polishing, instead, the abrasive is not bonded in a determined gap with a rolling action but it is pressed with increasing force to the workpiece, with resulting fine scratches on it (force-bound principle) (figure 1-6).

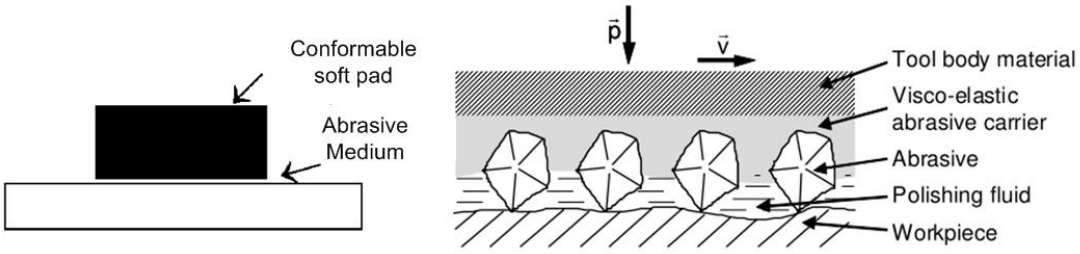

Figure 1-6 Schematic representation of polishing process [Marinescu, 2004] and material removal mechanism [Klocke, 2009]

Grinding process is carried out by abrasive grits held in a rigid tool, the grinding wheel. The cutting action of the abrasive grit is essentially determined by the trajectory of the cutting tool (track-bound principle) (figure 1-7).
The honing process (figure 1-7) can be considered as a process consequence of midway action between track bound and force bound principle. Abrasive grits are held in a rigid tool (abrasive stones) but the cutting action is performed in different ways: the cutting path is a combination of axial oscillation and of another relative movement (cross hatch); the removal action is determined by a pressure-controlled infeed movement.

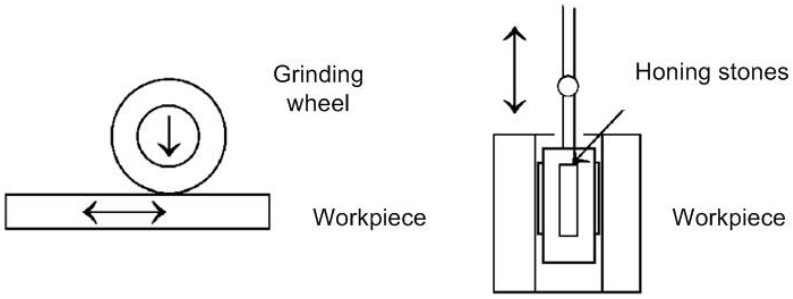

Figure 1-7 Schematic representation of grinding elements (left) and honing process (right) [Marinescu, 2004]

1.3 Grinding technology: brief overview

Formerly cited DIN 8589 carries out a subdivision of machining operations with geometrically undefined cutting edges, down to grinding operation, i.e. machining with rotating tools. Further, different grinding methods for different surface to be machined are distinguished.
From the kinematics of the machining operation and the feed movements, good distinction is reported in literature with corresponding parameters [Klocke, 2009] [Metcut R.A., 1980]. This distinction is particularly helpful in order to have a clear situation of different parameters involved in the machining operation with the aim of comparing different machining methods with the Q_w parameter, i.e. the volume of metal removed per unit of time. An example of distinction among different grinding operation is shown in figure 1-8.
Few parameters have to kept in consideration for a proper process design:

- v_s = grinding wheel cutting speed [m/s]
- v_w = work speed [rpm for OD machining,
- v_{fa} = infeed speed (traverse) [mm/min]
- v_{fr} = infeed speed (radial) [mm/min]
- b_s = grinding wheel width [mm]
- b_w = workpiece width [mm]
- a_p = depth of cut (traverse) [mm]
- a_e = depth of cut (radial) [µm].

As previously reported, an index of machining process performance is given by the stock volume removed per minute, namely Q_w [mm^3/min]. This parameter sometimes may be related to other general process performance indexes such as the G ratio (volume of stock removed per volume of wheel consumption), mostly used for very high removal rate machining operations,.

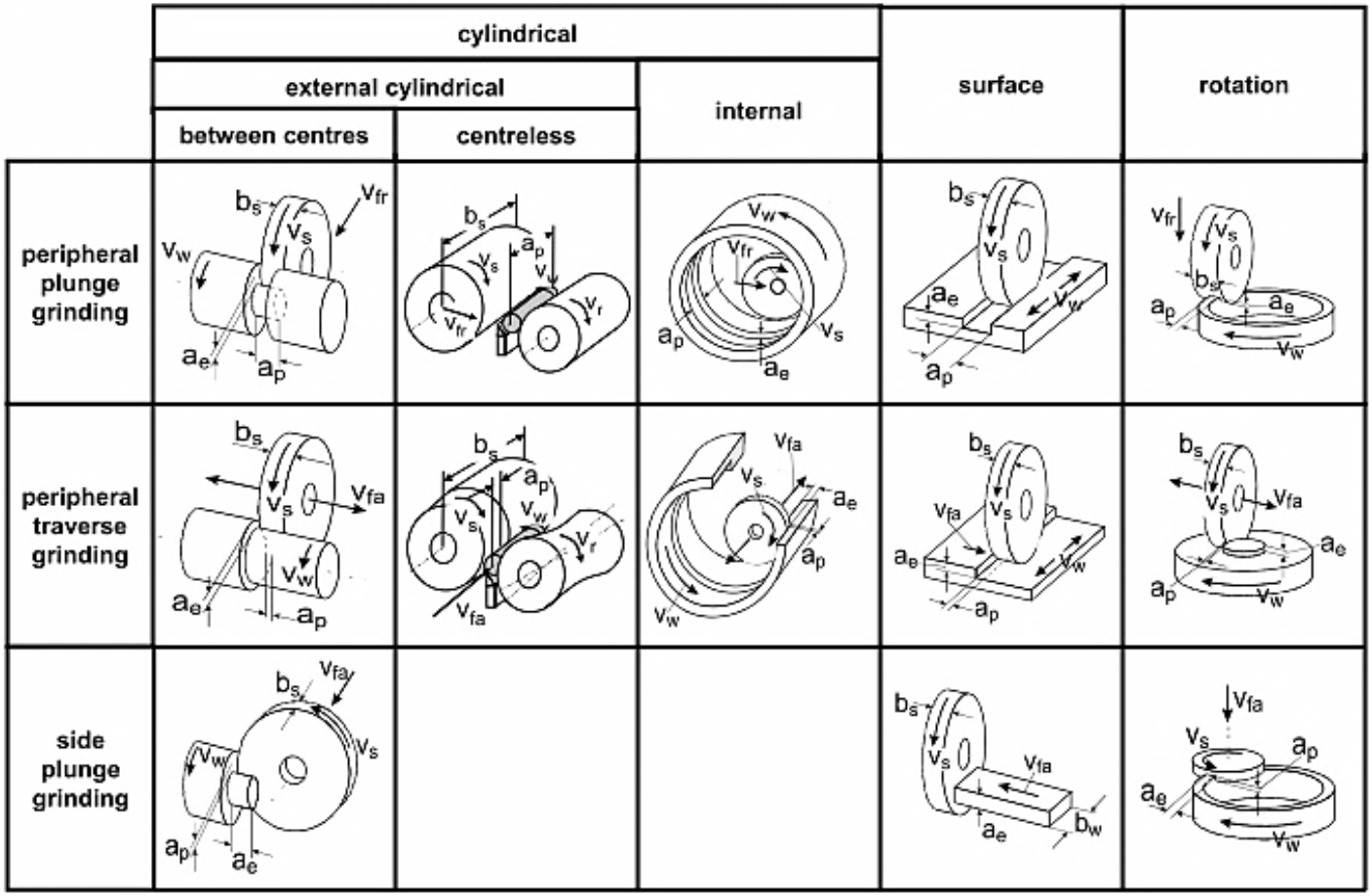

Figure 1-8 Types and configuration of grinding processes [Klocke, 2009]

Similarly, another helpful parameter is Q'_w, very used in plunge operation where the radial stock removal rate is considered to be uniform along the active grinding wheel width[7].

Considering tools, grinding operations are usually carried out by two main classes of abrasives: conventional abrasives (aluminium oxide) and superabrasives (cBN and diamond). These abrasives are held and constrained in their fixed path by the bonding agent (or simly 'bond') which commonly can be resinoid, vitrified or metallic (the latter only for superabrasive application).

The application of superabrasives may be particularly convenient in some application where high production volumes occur with minimal wheel re-shaping needs (i.e. dressing is not due to new geometry). Further, superabrasive grinding needs proper machine features (e.g. dressing disc unit, high speed spindles) to be economically convenient with resulting high first application investments. The latter is, in particular, a short term drawback that may be complicated to overcome. The major benefit of using superabrasives (especially cBN) consists in the increase of the achievable Q'_w (figure 1-9). This is due to different aspects such as superior sharpness-holding capability and thermal properties.

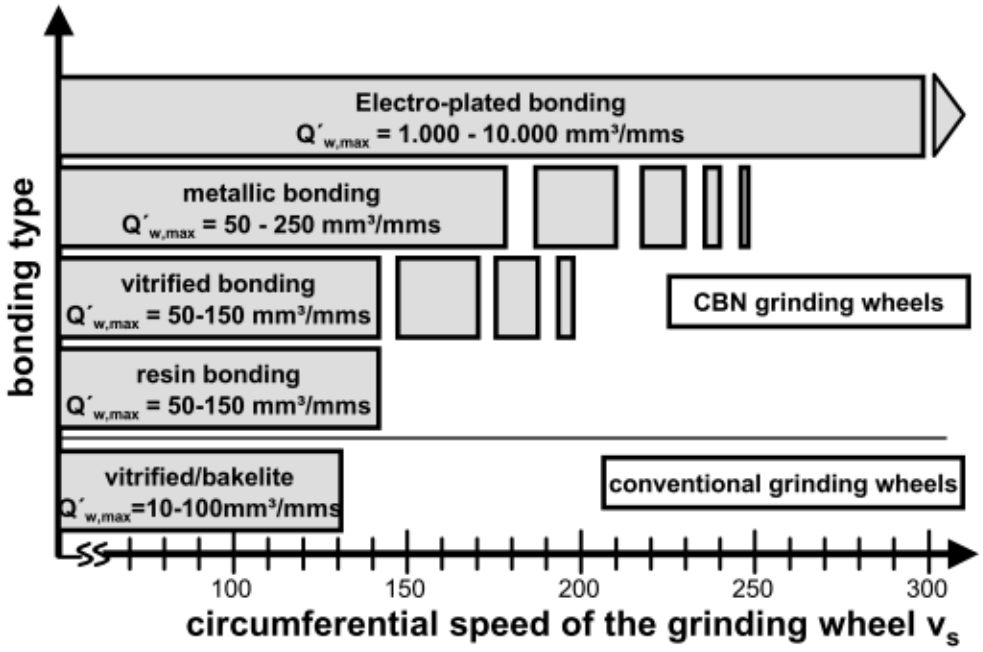

Figure 1-9 Machining speed and Q'_w application area based on tool technology [Webster, 2004]

Several machining operations reach different task of accuracy, coping with different stock removals. Indeed the stock removal quantity varies based on quality achieved by previous manufacturing operations; consequently, cycle time can be varied based on different needs.

Anyway, for common precision mechanics application, it is possible to find indicative application ranges in table 1-2.

[7] The active grinding wheel width is the cutting grinding wheel width. For example in cylindrical OD operation, plunge grinding, the active grinding wheel width equals the workpiece machined width; instead, in cylindrical OD traverse operation the active grinding wheel is just a small portion both along the wheel width and the workpiece machined width.

Table 1-1 Main parameters involved in grinding processes for different types of machining configurations [Klocke, 2009]

$Q_w = a_e \cdot a_p \cdot v_w$ $Q'_w = \frac{Q_w}{b_{s\,eff}}$	cylindrical			surface	rotation
	external		internal		
	between centres	centreless			
peripheral plunge grinding	$Q_w = \pi \cdot d_w \cdot v_{fr} \cdot a_p$ $v_{fr} = a_e \cdot n_w$ $a_p = b_s = b_{s\,eff}$	$Q_w = 1/2\ \pi \cdot d_w \cdot v_{fr} \cdot b_s$ $n_w = n_r \cdot \frac{d_r}{d_w}$ $v_{fr} = 2 \cdot a_e \cdot n_w$ $a_p = b_s = b_{s\,eff}$	$Q_w = \pi \cdot d_w \cdot v_{fr} \cdot a_p$ $v_{fr} = a_e \cdot n_w$ $a_p = b_s = b_{s\,eff}$	$Q_w = v_w \cdot a_p \cdot a_e$ $a_p = b_s = b_{s\,eff}$	$Q_w = v_w \cdot a_p \cdot a_e$ $v_w = \pi \cdot d_w \cdot n_w$ $v_{fr} = a_e \cdot n_w$ $a_p = \frac{d_{ws} - d_{wi}}{2} = b_{s\,eff}$
peripheral longitudinal grinding	$Q_w = \pi \cdot d_w \cdot v_{fa} \cdot a_e$ $v_{fa} = a_p \cdot n_w$ $a_p = b_{s\,eff}$	$Q_w = \pi \cdot d_w \cdot v_{fa} \cdot a_e$ $v_{fa} = n_r \cdot \pi \cdot d_r \cdot \sin\alpha_r$ $a_p = b_{s\,eff}$	$Q_w = \pi \cdot d_w \cdot v_{fa} \cdot a_e$ $v_{fa} = a_p \cdot n_w$ $a_p = b_{s\,eff}$	$Q_w = v_w \cdot a_p \cdot a_e$ $a_p = b_{s\,eff}$	$Q_w = a_e \cdot a_p \cdot v_w$ $v_w = \pi \cdot d_w \cdot n_w$ $a_p = \frac{v_{fa}}{n_w} = b_{s\,eff}$
side plunge grinding	$Q_w = \pi \cdot d_w \cdot v_{ft} \cdot a_p$ $v_{ft} = a_e \cdot n_w$ $a_e = b_{s\,eff}$			$Q_w = a_e \cdot b_w \cdot v_{fa}$ $b_{s\,eff}$ not defined	$Q_w = v_w \cdot a_p \cdot a_e$ $v_w = \pi \cdot d_w \cdot n_w$ $a_e = \frac{d_{ws} - d_{wi}}{2}$ $a_p = \frac{v_{fr}}{n_w} = b_{s\,eff}$

Table 1-2 Allowances and achievable accuracy values typical of some grinding processes [Tsasch, 2009]

Grinding technique	Allowance			Achievable accuracy	
	Maximum length of workpiece [mm]	Machining diameter/thickness of the part [mm]	Allowance related to diameter [mm]	Accuracy to size	Peak to valley height Rt [µm]
Flat	Up to 100	Up to 50	0.2-0.25	IT8-IT9 (IT5 – IT6)	3-8 (1-3)
	150-200	Up to 150	0.3-0.35		
Profile	20-100	-	Partially ground from solid	IT4- IT5	2-4
External cylindrical	Up to 150	Up to 50	0.2 -0.25	IT6 – IT8	5-10
	200-400	100-150	0.25-0.3		
Internal cylidrical	Up to 50	Up to 20	0.1-0.15	IT8 – IT10	10-20
	80-100	21-100	0.2-0.25		
Centerless	Up to 100	Up to 300	0.2-0.3	IT4-IT6	2-4
		31-100	0.2-0.3		

1.4 Centerless grinding

1.4.1 Introduction

Centerless grinding is an high production rate process that allows to grind parts within very narrow tolerances (table 1-2).
As reported in figure 1-8, there may be two main types of centerless grinding operation: OD through feed and OD plunge. Anyway other application are known such as ID grinding, ID-OD simultaneous grinding [Hashimoto,2012] and others. A more detailed classification of centerless grinding configurations is reported the in next section.

1.4.2 Advantages of centerless grinding

One of the highest advantage in centerless grinding concerns the absence of clamping fixtures and, hence, its error avoidance: the workpiece is not held and it is not clamped to a driving device trough centre holes (thus not affecting the final part quality and eventually decreasing production cost of the part): the workpiece location

is defined by the newly machined surface and its contact points with the other machine elements: grinding wheel, blade and regulating wheel.
This permits, generally speaking, to save time (using highly automated loading devices), saving manpower, performing very high production rates.
Another advantage of centerless grinding relates to the possibility of machining precisely very thin and brittle parts with high production rate (thanks to linear contact, pieces may be held on the whole length with limited bending torques).
It has to be remarked that grinding technology is strictly bonded to the machine technology used.
A recent paper by Hashimoto [Hashimoto,2012] use three major classification of centerless grinding methods:

- machine configuration based (by orientation and configuration): horizontal, slant, vertical;
- workpiece-feed direction based: infeed (plunge), troughfeed, tangential;
- work-supporting device based: regulating wheel and blade type, two shoes type, three rolls type, two roll-shoe type, two roll type, double disk type.

Further, it has to be remarked that, since it is an high production rate process (e.g. millions of parts per year), there is an huge amount of centerless grinders customized for single parts production with different solutions [Klocke, 2009] [Modler, 2005].
More commonly, centerless grinding machines are horizontal, distinguished in throughfeed and infeed type.
In these cases the machining operation consists of three major components (figure 1-10):

- grinding wheel;
- workrest (blade);
- control wheel.

The mutual position of latters plus the position of the workpiece during machining defines the grinding gap (see figure 1-10).
The control wheel and the workrest have two main tasks: holding the part and controlling the workpiece angular speed (avoiding its acceleration due to the grinding wheel friction).
Further, the control wheel has another aim: controlling of the axial position of the part. This is carried out in different manners, depending on through-feed or infeed grinding type.

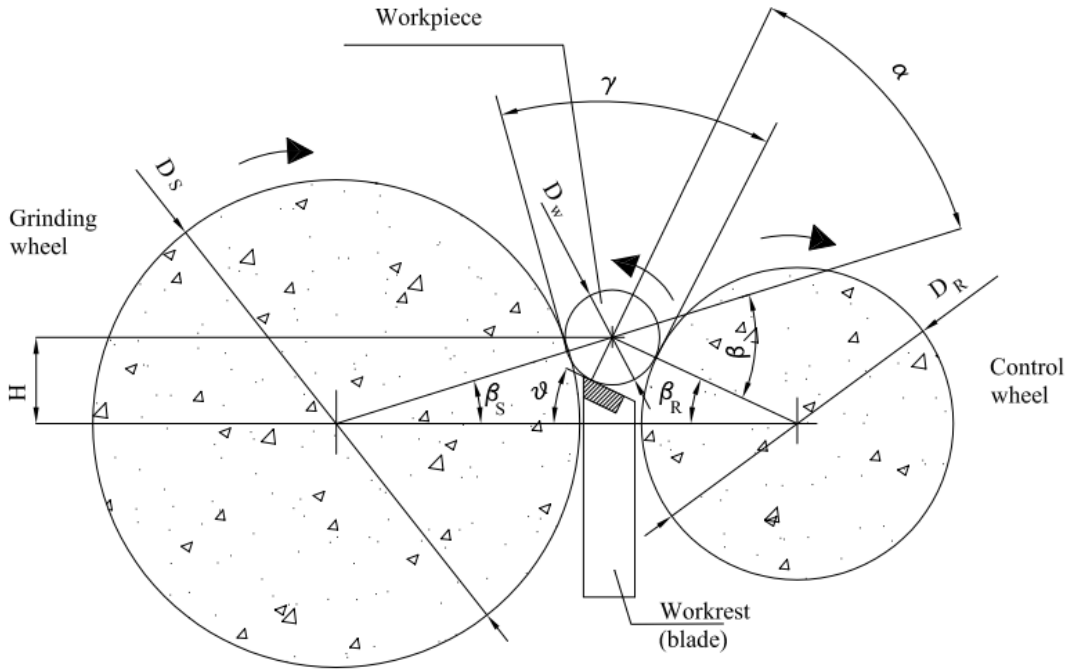

Figure 1-10 Centerless gap geometry

1.4.3 Throughfeed grinding

In troughfeed centerless grinding machined parts move along the blade due to the inclination of the control wheel.
Based on the desired cycle time, the control wheel is tilted by an inclination angle α_r. This is commonly set in the order of few degrees (2°-5°). If no slip occurs between workpiece and control wheel, the axial speed of the control wheel will be given by the axial component of the tangential speed of the control wheel determined by its inclination.

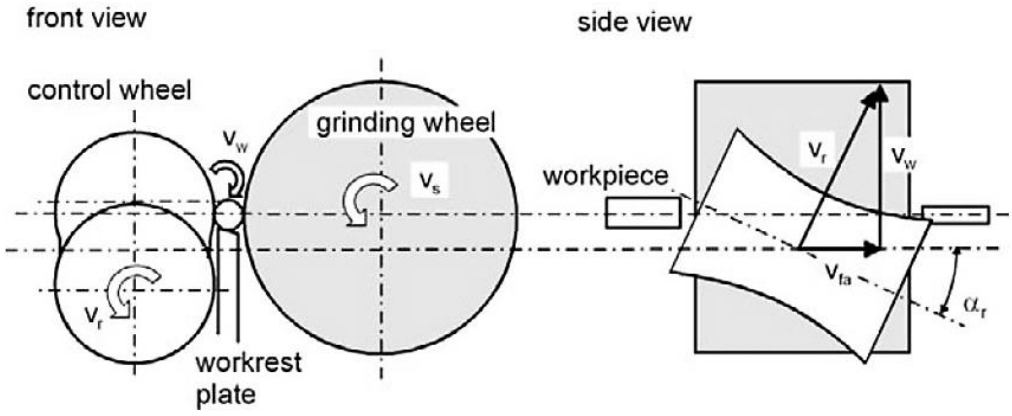

Figure 1-11 Troughfeed centerless grinding kinematic scheme [Klocke, 2009]

1.4.4 Infeed centerless grinding

During machining the parts are axially positioned through the use of an axial stop (figure 1-12). Since infeed grinding is essentially a multidiameter operation, there is the necessity of having an optimal matching between workpiece diameters and grinding wheel shape.

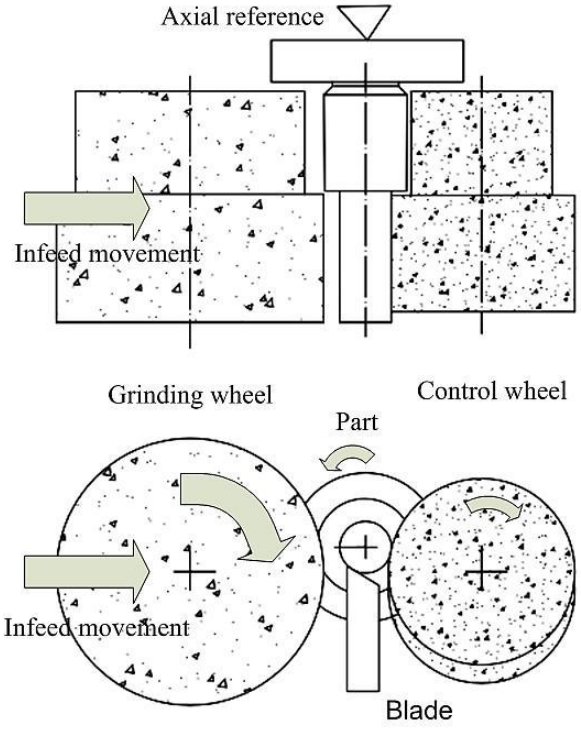

Figure 1-12 Infeed centerless grinding kinematic scheme

Commonly it is not possible to load the part in the exact final axial position due to loading devices limits. Then two possibilities are available:

- use an axial positioning device (e.g. pneumatic cylinder pushing the workpiece to the final position before the machining starts);

- use the friction action of control wheel (mostly used): during loading, a gap (few tenth of mm) is left between the axial stop and the end reference face of the workpiece; at the earliest machining stage the workpiece moves towards the axial stop, in the final axial position.

1.4.5 Centre height

Concerning the grinding gap, machining configurations may differ for the positioning of the workpiece centre respect to a reference line which links control wheel centre to grinding wheel centre.
Based on that, the workpiece may lie above the centre line ("above – centre configuration") or below the centre line ("below centre" configuration), as shown in

figure 1-13; the distance connecting the workpiece centre to the line connecting the parts is called “height” of the part on the centres.

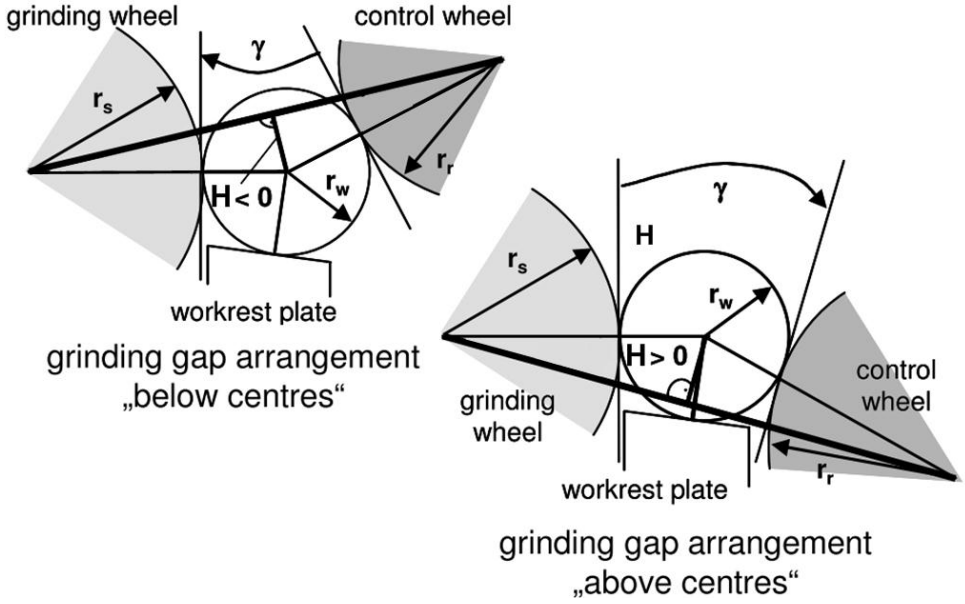

Figure 1-13 Grinding gap configuration: “below the centers” and “above the centers” [Klocke, 2009]

The Grinding gap configuration is defined (figure 1-10) as follows:

- H = distance between the workpiece centre to the connecting line between control and grinding wheel centres;
- D_s = grinding wheel diameter;
- D_w = workpiece diameter;
- D_r = control wheel diameter,

According to the above defined geometrical features, independently of the given dimensions of wheel and workpiece, the gap configuration can be defined based on the following angles:

- β_s = angle between the direction connecting grinding wheel and workpiece centres to the direction connecting the grinding and control wheel centres (clockwise direction)
- β_r = angle between the direction connecting control wheel and workpiece centres to the direction connecting the grinding and control wheel centre (counter-clockwise direction)
- ϑ = angle between the workpiece holding flat to the direction connecting control and grinding wheel centers (counter clockwise)

Another recurrent angle used for analysis purpose is the "centre height angle" γ [8]. The latter angles can be defined as follows:

$$\beta_s = \text{asin}\left(\frac{2 * h}{D_s / D_w}\right) \quad (1)$$

$$\beta_r = \text{asin}\left(\frac{2 * h}{D_r / D_w}\right) \quad (2)$$

$$\gamma = \beta_s + \beta_r \quad (3)$$

Equivalently, another notation is used to represent the grinding gap in literature, based on mutual angles among grinding wheel centre, workpiece centre, control wheel centre and blade.

$$\alpha = \frac{\pi}{2} - \vartheta - \beta_s \quad (4)$$

$$\beta = \gamma = \beta_s + \beta_r \quad (5)$$

1.4.6 Process instabilities

Centerless grinding has many advantages but one major disadvantage: due to its lack of motion-controlling devices the process is more prone to instabilities.
There are three main types of instabilities:

- Work holding: if the frictional action exerted by control wheel and blade is not strong enough, the workpiece is angularly accelerated by the grinding wheel cutting action. Since no slowing down occurs, the part speeds up risking to cause the jumping of the part out of the machining gap (in case of grinding above centers).

- Geometric instability: due to grinding gap geometrical configuration and deviations from perfectly round shape of workpiece, moving of its centre occurs; this movement makes the workpiece surface lobed, resulting often in a bad quality roundness. This type of instability is just due to the grinding gap configuration and, theoretically, could occur also on infinite stiffness machine [Hashimoto,2012].

[8] γ is defined as the angle spanned by the common tangent between workpiece and control wheel passing through their contact point to the common tangent between workpiece and grinding wheel passing through their contact point.

- Dynamic instability: a problem common to all machines, grows much faster in centerless grinding due to occurrence of work regenerative type vibration [Hashimoto,2012] [Gallego , 2007].

Since the latter aspects are about the "classic" instabilities considered in centerless grinding, it has to be reminded another aspect well known in industrial application: capabilities. While just few customized machines (e.g. Modler) dress the part after every machining cycle using very low-wear control wheels (assuring intrinsically-high process robustness), the most of them experiment variations due to:

- different behaviours during the time between dressing stint (i.e. shape capabilities);

- different wear rates at different workpiece diameters (i.e. size capabilities)

1.4.7 Work holding stability

Work holding stability concerns two main types of instability: flat band and spinning [Hashimoto,2012].
Flat band is a problem related to insufficient friction action exerted by the regulating wheel. Insufficient friction may cause an initial lack of rotation of the part. The workpiece starts to rotate only when the contacting force on the control wheel is high enough. Since force increase due to grinding action, the workpiece will have a flat band formed on its diameter before starting to rotate; this phenomenon could harm the roundness process capacity. It has to be remarked that the less the needed friction, the less the resulting flat band depth.
Spinner is the other problem related to the work holding configuration typical of centerless grinding. It concerns a sudden increase of the workpiece rotational speed due to the fact that grinding wheel friction is higher than friction exerted by control wheel.
This problem has been tackled by Takasu [Takasu, 1988], Hashimoto [Hashimoto, 1998], [Barrenetxea, 2009] and Zakharov [Zakharov, 2008]. Takasu and Barrextea studied rotational control issues in case of multidiameter shafts, while Hashimoto developed an intuitive model to predict problems related to rotational stability such as self- rotation (i.e. flat band) and upper critical force (i.e. spinners).
Hashimoto's stability study is based on general equations (for multi diameter parts) [Hashimoto, 1998] in following (figure 1-14):

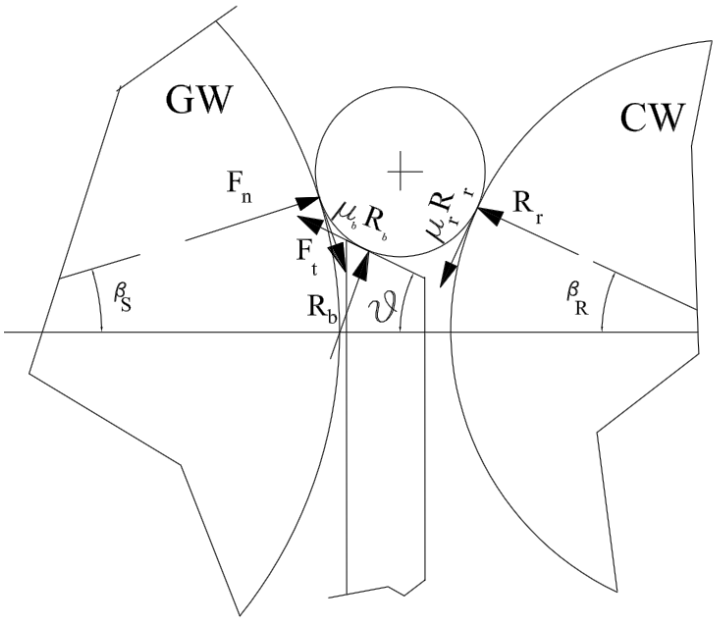

Figure 1-14 Parameters involved in rotational stability study

$$I_z * \dot{\Omega} = \sum_{i=1}^{N} R_i * L_i * \frac{(B_1 * \mu_{r_i} + B_2) * \lambda * F_{n_i} - (C_1 * \mu_{r_i} + C_2) * m_i}{A_1 * \mu_{r_i} + A_2} \quad (6)$$

$$\begin{cases} A_1 = \mu_{b_i} \cos(\theta - \beta_r) - \sin(\theta - \beta_r) \\ A_2 = \mu_{b_i} \sin(\theta - \beta_r) + \cos(\theta - \beta_r) \\ B_1 = A_1 - \mu_{b_i} (\sin(\beta) + \lambda^{-1} \cos(\beta)) - \begin{bmatrix} (1 + \lambda^{-1} * \mu_b) \sin(\theta - \beta_s) + \\ (\lambda^{-1} - \mu_b) \cos(\theta + \beta_s) \end{bmatrix} \\ B_2 = A_2 - \mu_{b_i} (cos\beta - \lambda^{-1} \sin\beta) \\ C_1 = \sin\theta - \mu_{b_i} (cos\beta - \lambda^{-1} \sin\beta_r) \\ C_2 = \mu_{b_i} \cos(\beta r) \end{cases} \quad (7)$$

where:

- μ_{b_i} kinetic friction coefficient between workpiece and blade at the part i-th diameter (totally, *N* diameters);
- μ_{r_i} friction coefficient between workpiece and regulating wheel at the part i-th diameter;
- λ is the cutting ratio (= F_t/F_n);
- I_z inertial mass moment of the workpiece.

From the above approximated equation the determination of the work holding stability condition is possible.
Two are the possible cases regarding the friction action of the control wheel in early machining stages:

- Self-rotation, i.e. the workpiece starts to rotate before the grinding operation begins;

- Induced rotation, i.e. the workpiece mass moment of inertia exceed the control wheel friction; the workpiece begins its rotation only after a minimum torque ("*lower critical tangential force")* has been applied due to the occurred cutting action[9].

An important result of the rotational stability study concerns the maximum possible friction exerted by the control wheel. The rotational control of the control wheel, combined with blade and grinding wheel friction action, leaded Hashimoto to the definition of the *"Upper critical tangential force"* f_U, identified as the maximum grinding tangential force to be applied in the whole cycle before spinning starts.
For simple cylindrical parts, f_U is expressed as [Hashimoto, 1998]:

$$f_U = \frac{C_1\,\mu_{r0} + C_2}{B_1\,\mu_{r0} + B_2} * m \qquad (8)$$

where:

- μ_{ro} is the maximum static friction coefficient;

- m is the mass of the part;

- B_1, B_2, C_1, C_2 are coefficients derived in eq. (7).

f_U given in eq. (8) depends on grinding wheel properties, blade friction properties and grinding gap angles. Following to the definition of f_U, Hashimoto identified for any specific combination of whole frictional behaviours and grinding gap angles the existence of "safe operation zone", i.e. a zone in which the occurrence of spinning is avoided for any practical value of grinding force. Hence, based on this zones, the use of "Safe operation charts" was defined. One example is shown in figure 1-15.

[9] Requiring a minimum torque to starts the rotation, the workpiece roundness can be harmed because of the formation of a flat band. So, e.g. for heavy workpieces or low regulating wheel friction, an excessive value of the lower critical force may result in unsatisfactory final roundness.

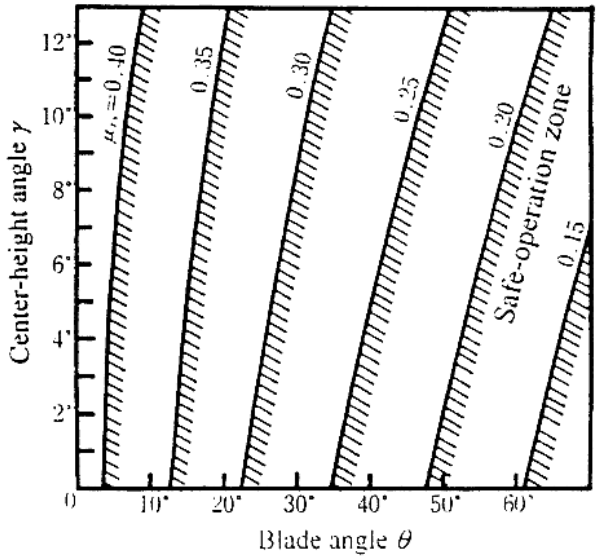

Figure 1-15 Example of safe operation chart (λ=0.5, μ_b=0.15) [Hashimoto, 1998]

Hence, friction properties may have a huge impact on working stability and on safety of grinding operations. Further properties and consideration on the rotational stability analysis are reported in chapter 2 and 3.

1.4.8 Geometrical and dynamical stability

The complete analysis of the rounding loop leads to the study of deviation from a perfectly round shape during the grinding process. In fact, considerations based on geometrical assumptions may underline how a deviation from the perfectly round shape on the holding points (i.e. the contacting point between blade and piece or between control wheel and piece) (figure 1-16) result in a deviation in the contact point between the grinding wheel and the workpiece.
Further, grinding point deviations from theoretical ones occur because of regenerative effect and dynamic deflections.

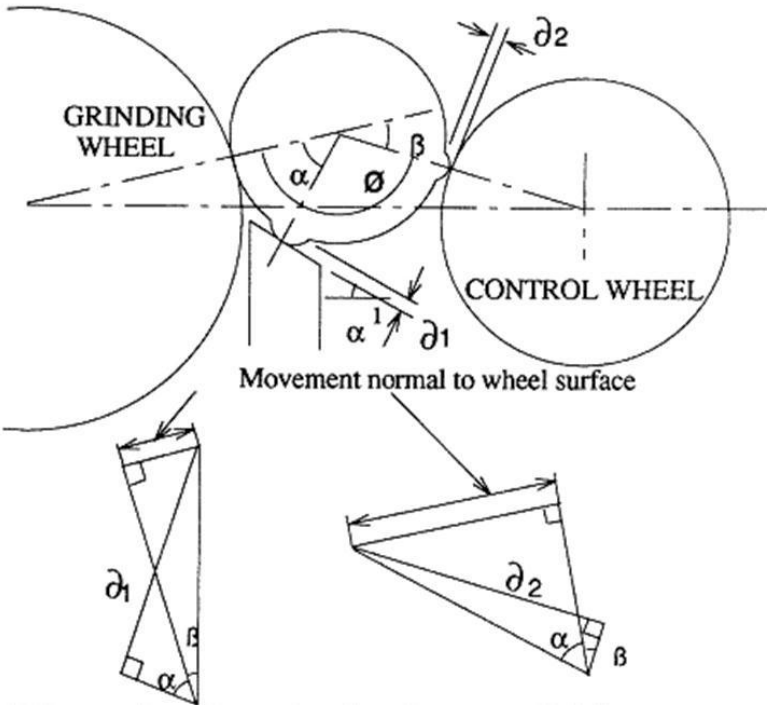

Figure 1-16 Transferring of imperfections in contacting points with blade and control wheel to the grinding point [Rowe, 1989]

The governing equations [Rowe, 1989] for the rounding up process is:

$$r(\phi) = X(\phi) - x(\phi) + k_1 * r(\phi - \alpha) - k_2 * r(\phi - \pi + \beta) \qquad (9)$$

where:

- $\emptyset$ is the workpiece angular coordinate;
- $r(\phi)$ is the reduction in radius;
- $X(\phi)$ is the infeed at the grinding contact;
- $x(\phi)$ is the machine deflection;
- k_1 and k_2 are geometrical coefficients defined based on figure 1-16:

$$k_1 = \frac{\sin\beta}{\sin(\alpha+\beta)} \qquad k_2 = \frac{\sin\alpha}{\sin(\alpha+\beta)} \qquad (10)$$

- $r(\phi - \alpha)$ is the radius error at the blade contacting point.

- $r(\phi - \pi + \beta)$ is the radius error at the control wheel contacting point.

Since the rotation of the workpiece is in counter-clockwise direction, the points in contact with the blade and with the control wheel are points previously ground, respectively with spanned angles of α and π-β radians. Considering the time domain:

$$T_1 = \frac{\alpha}{\Omega}$$
$$T_2 = \frac{(\pi - \beta)}{\Omega} \quad (11)$$

Rearranging the above equations in the time domain:

$$r(t) = X(t) - x(t) + K_1 * r(t - T_1) - K_2 * r(t - T_2) \quad (12)$$

The machine deflection has to be considered as the sum of the compliance effect of the whole centerless system. According to available literature [Rowe, 2009] [Jameson, 2008] [Furukawa, 1970] the latter can be considered as the uni-dimensional sum of the compliances of control wheel and grinding wheel heads with the contact compliances.
The grinding force exciting the cited compliances, is expressed traditionally as the force acting based on the actual depth of cut[10], and hence:

$$F_n = K_s * a_e \quad (13)$$

where:

- K_s is the cutting stiffness[11];

- $a_e = (r(t) - r(t - T))$ (14)

  is the actual depth of cut;

- $T = {}^{2\pi}/_{\Omega}$ is the workpiece rotation period.

The complete loop (described in figure 1-17) can be subdivided in two different configurations according to the size of the problem involved: the geometric (not considering machine deflections) [Rowe, 1972] and the dynamic complete loop

[10] The actual depth of cut is the real depth of cut machined. It differs from the controlled depth of cut due to machine and tool compliances.
[11] The cutting stiffness is defined as the ratio between the grinding force and the instantaneous real depth of cut [Snoeys, 1969]. In detail, grinding force and grinding stiffness are both proportional to the width of contact between part and grinding wheel [Snoeys, 1968] and, hence, specific cutting stiffness may be defined as the cutting stiffness per unit of width of cut; further, the specific cutting stiffness was shown to be proportional to the ratio between the cutting speed and the workpiece speed.

(considering grinding and control wheel wear and external disturbances) [Furukawa, 1970].
The geometric instability pertains to the work holding configuration typical of centerless grinding.
This had been investigated, first, by Dall (as reported by Rowe [Rowe, 1964]) who reported the effects on roundness errors due to the included tangent angle β and the top blade angle. Yonetsu[12] (as reported by Rowe [Rowe, 1964]) reported three main conclusions:

- lobed shapes related to odd harmonics of order below 11th are better removed with large included angles β;
- lobed shapes related to even harmonics of order below the 10th are better removed with small angles β;
- other lobed-shape errors (even and odd harmonics) vary with β and depends on the magnitude of the infeed motion;

Rowe [Rowe, 1964] investigated the problem through the use of simulations and, later, through the use of grinding charts [Rowe, 1972]. He came to the definition of charts to avoid geometric instabilities trough the study of the geometrical rounding loop.
Similarly, it is well-known the importance of Reeka's work, in determining stabilities charts.
The determination of configuration stability proneness is given by the open loop transfer function for the geometrical loop, which is [Rowe, 1972]:

$$\frac{-R(s)}{X(s)} = \frac{1}{1 - k_1 * e^{-sT_1} + k_2 * e^{-sT_2}} \quad (15)$$

From the above equation, solving the real part of the poles results to be:

$$Re_P(\omega) = k_2 * \cos \omega T_2 - k_1 * \cos \omega T_1 \quad (16)$$

Since:

$$\omega = N * \Omega \quad (17)$$

Then:

$$Re_P(N) = k_2 * \cos[(\pi - \beta) * N] - k_1 * \cos[\alpha * N] \quad (18)$$

The stability index (S.I.) is so defined [Kranijl, 2008] as:

[12] Theoretical observations were obtained for the case of sudden infeed and compared with experimental results made over an infeed 0.5 sec. long [Rowe, 1964]

$$SI_N = 1 + Re_P\,(N) = \; 1 + \; k_2 * \cos[(\pi - \beta) * N] - k_1 * \cos[\alpha * N] \qquad (19)$$

1.4.9 Dynamic instability

The dynamic instability is an aspect whose study concerns the application of compliance system characteristics involved in the centerless grinding loop. Because of the latter, grinding wheel spindle, control wheel spindle and blade compliances should be considered.
Further, control wheel contact compliance and grinding wheel contact compliance have to be considered too [Miyashita, 1982]. Other aspects that can be taken in consideration are control wheel and grinding wheel wear (an example of block diagram analysis are shown in fig. 1.17).
In order to include the cited aspects, different approaches had been taken in consideration over the past decades. Those approaches were mostly divided in two: frequency domain simulation, time domain simulation.
As above mentioned, the workpiece radius do not decrease steadily nor according to exact infeed law, but showing some radius defect (Δr_w). This is partly due to geometrical error, partly to dynamic deflections.

Hence, the radius defect Δr_w at time *t* is [Gallego, 2007]:

$$\Delta r_w(t) = \; \Delta r_{w_g}(t) + \Delta r_{w_k}(t) + \Delta r_{w_d}(t) \qquad (20)$$

where:

- $$\Delta r_{w_g}(t) = \; K_1 * r(t - T_1) - K_2 * r(t - T_2) \qquad (21)$$

  is the radius defect component due to geometrical issues (movement of the workpiece along the cutting direction due to errors in contact point with blade or control wheel);

- $$\Delta r_{w_k}(t) = \; {F_n(t)}\Big/{K_{eq}} \qquad (22)$$

  is the radius defect component due to time variation of system dynamic deflections; the system dynamic deflections are expressed in terms of an equivalent spring (K_{eq}), considering system compliances such as static stiffness and contact stiffness's;

$$K_{eq} = \left(K_m{}^{-1} + K_{cw}{}^{-1} + K_{gw}{}^{-1}\right)^{-1}{}_{13} \qquad (23)$$

- $\Delta r_{w_d}(t)$ is the radius defect component due to vibrations generated during the process and its analysis involves machining modal analysis (its contribution is inserted in eq. 24).

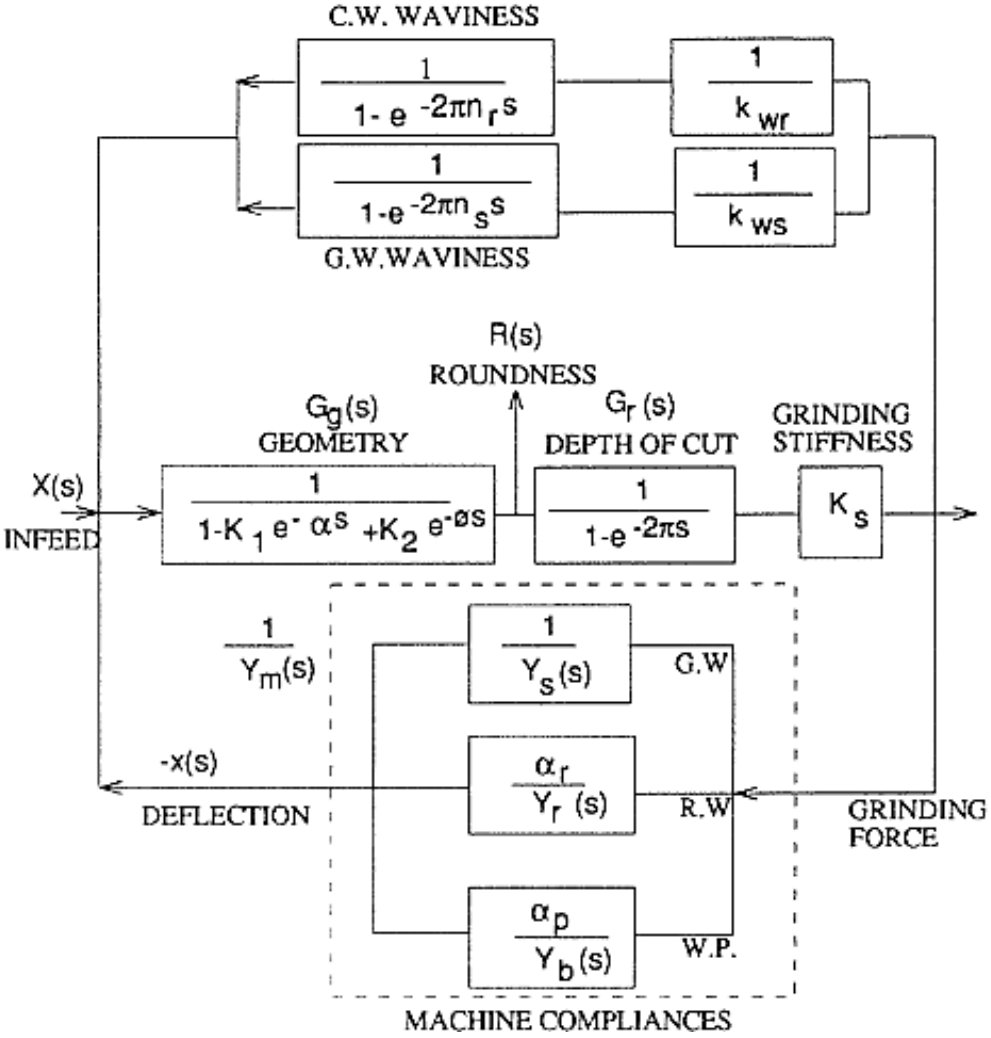

Figure 1-17 Representation of centerless system in frequency domain [Rowe, 1989]

$\Delta r_w \ (t)$ had been studied in two different domains: frequency and time.
In the frequency domain[14] the eq. 20 becomes [Gallego, 2007]:

[13] K_m , K_{cw} , K_{gw} are, respectively, the machine and blade stiffness, the contact stiffness between regulating wheel and workpiece and the contact stiffness between the grinding wheel and workpiece
[14] Laplace transformation is commonly applied.

$$0 = \Delta R_w(s) * \left[1 - k_1 e^{-sT_1} + k_2 e^{-sT_2} - K(1 - e^{-sT}) \right.$$
$$\left. - K_s \sum_{r=1}^{N_m} \left(\frac{V_r}{\omega_r^2 + s^2 + 2\, s\xi_r\omega_r} - \frac{V_r}{\omega_r^2} \right)(1 - e^{-sT}) \right] \qquad (24)$$

where:

- N_m is the number of considered machine vibration modes;
- $\omega_r,\ \xi_r$ the modal frequency and damping of r-mode;
- V_r is a parameter relating the cutting force to the displacement in the cutting point for the r- mode;
- $K = {K_s}/{K_{eq}}$ is a parameter relating the system compliance to depth of cut.

From the stability analysis, an example of chatter diagram [Miyashita, 1982] is shown in figure 1-18.
Aspects such as contact filtering and others may be included but with limited applications due to Laplace transformations properties.
The above aspects can be differently involved in time domain, where non-linear aspects can be considered separately with their effect on system stability and rounding action. Hence, interference (geometrical filtering), hertzian or non-hertzian contact, loss of contact during sparkout phase, temporal evolution of roundness and others had been studied in time domain.
An overview of approached problems available in literature is shown in table 1-3.
Generally speaking, time domain simulation result to have the capability of separately studying the varying influences of process/tool parameters on the cutting process.
Frequency domain simulation can give limited amount of information on root-causes requiring much smaller computational time.

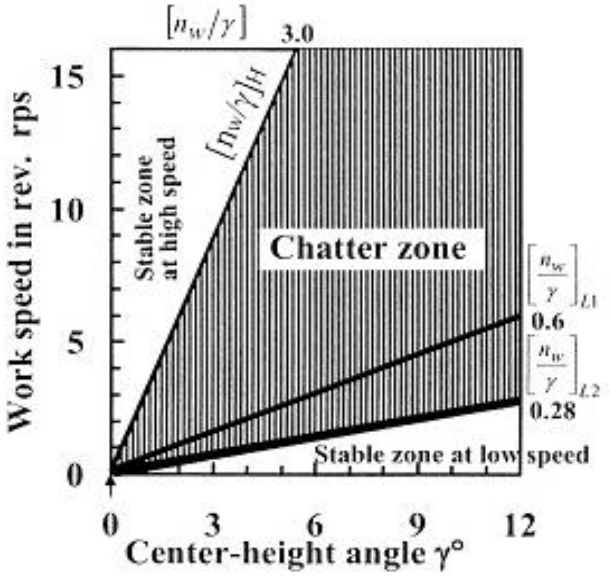

Figure 1-18 Example of chatter diagram resulting from dynamic analysis [Myiashita, 1982]

Despite the increased details and contributions in modelling in the time domain, literature review has highlighted a lack of numerical values for roundness prediction, putting in evidence the unavoidable need of an experimental approach for quantitative determination of best conditions to be applied in the design and set up of a centerless processes.

Anyway, from the literature analysis, different examined models, both in the frequency and in the time domain, showed good chatter predictability. From a practical point of view, chatter is indeed among the most important issues in centerless grinding, but also one of the less likely to occur and easy to avoid, if the machine is properly adjusted.

The roundness geometrical pattern formation and, in particular, the influence of single machining components on the machining loop, resulted of interest. Despite the multitude of aspects involved (grinding wheel cutting ability, regulating wheel compliance, dressing conditions, hardness, grit size and others) the examined models do not give an insight on aspects involved in the machining operation, often considering them as model constants in the dynamic loop; the determination of these constants seemed oversimplified too, apparently for the difficulties related to this machining type process.

Further, practical aspects involved in process quality (i.e. tri-lobed parts) are scarcely mentioned.

Hence, for qualitative analysis purpose, this thesis work deals with a detailed view of main dynamic models applied in grinding, focusing on tool properties and characteristics that may occur during the real process but that scarcely find approximations in the before-mentioned centerless models.

Secondly, a more detailed study on the geometric loop is considered inside the frequency domain analysis; this aspect, on the contrary of previously discussed dynamic characteristics, may be predicted easily and will be object of analysis in chapter 4.

Table 1-3 Main features studied on infeed centerless system stability

Year	Domain	Main features	Reference
1970	Frequency	Vibration analysis and rounding analysis in stable and unstable conditions	[Furukawa, 1970]
1973	Time	Sparking out characteristics and machine characteristics	[Rowe, 1973]
1980	Frequency	Importance of cutting stiffness related to workpiece rotation frequency	[Bueno, 1990]
1982	Frequency	Importance of contact stiffness and deformation of contact area; use of rounding effect criterion; diagrammatical coincidence method	[Miyashita, 1982]
1996	Frequency	Lobing behaviour as result of regenerative and geometric loop; determination of growth rate boundaries	[Zhou, 1996], [Zhou, 1997]
1998	Time	Prediction of spinning and workpiece shape evolution for above and below centerless configuration	[Guo, 1998]
2000	Frequency	Root distribution and chatter; contact filtering; diagrammatical approach	[Hashimoto, 2000]
2003	Time	Effect of threshold forces; cutting stiffness determination method	[Kim, 2003]
2005	Frequency; time	Deflections effects on roundness included; Time domain analysis included to consider non linearity	[Lizarralde, 2005]
2007	Frequency; time	Spinning; design of optimal grinding cycle	[Gallego, 2007]
2007	Time	Prediction of chatter and lobbing, use of distributed grinding force model and distributed contact pressures	[Li, 2007]
2008	Time	Workpiece forming mechanism and centre displacement influence	[Krajnik, 2008]
2008	Time	Out of roundness quantitative determination, waviness generation on the grinding wheel	[Brecher, 2008]
2008	Time	Use of hertzian contact deflections for worlpiece forming mechanism	[Jameson, 2008]
2009	Time	Continuous workpiece speed variation	[Barrenetexea, 2009]
2009	Frequency	Dynamic and geometric instability; cutting stiffness determination method	[Gatitaonandia, 2009]

1.5 Conclusions

The centerless infeed grinding system has been overviewed, with the aim of contextualize it among other abrasive processes, highlighting the main aspects and characteristics involved in it.
From this overview the major outcomes are:

- Grinding is a machining technology carried out by a number of geometrically undefined cutting edges, forced to follow a determined cutting path.

- The number of cutting edge is different from the number of protruding abrasive grits, based on the combination of kinematical parameters for the machining operation. The properties of the cutting edge may vary due to wearing out of grits.

- The centerless machining operation is an high precision, high production rate and highly prone to automation, used for mass production processes such as those typical of bearing industry and automotive components.

- In centerless grinding the datum of the machining operation is the machined diameter: the workpiece is held by a blade and by a regulating wheel, which puts the part in rotation while grinding wheel machines the part.

- Two are the main process variants: through-feed grinding, for single diameter machining, in which the workpiece feed movement is carried out parallel to the axis of the grinding wheel, and infeed grinding, in which the metal removal is carried out by the relative approach of workpiece to grinding wheel in radial direction.

- The process presents a number of instabilities bonded to different machining aspects: work holding (friction issues), geometrical (angles of the grinding gap) and dynamic (overall machining system).

- The process output depends on a number of machining parameters and characteristics needing further investigations: in particular contact stiffness's dependences, grinding force ratio and cutting stiffness.

- Literature review showed a lack of quantitative results for the roundess prediction but high chatter predictability.

2 Dynamic aspects of centerless grinding

2.1 Introduction

Since centerless grinding is an high production rate process, cycle time is essential.
Cycle time is a matter of loading systems, infeed rates, machining system stiffness and stability achievement. Only the latter three are considered to be technological issues. Loading system is mostly a technical issue.
The three technological issues are strictly bonded to grinding dynamics. The chapter will therefore focus on grinding dynamics and their relationships with tool characteristics, focused on the part concerning centerless grinding. In particular, after a generic overview of the main grinding dynamic models and features involved, the main tool features are considered with the aim of underlying their impact on the centerless loop dynamics.

2.2 Grinding dynamics overview

Grinding dynamics is a very complex subject because it can lead to a multitude of aspects including tribological aspects and others, which may greatly differ for each single specific applications.
Generally, dynamic models have been classified in two groups: empirical and analytical.
Empirical models deal mostly with a process of correlation between selected input and output parameters, based on objectives and with an integrated knowledge base. Then, empirical models concern a higher amount of qualitative information and need a long time to the knowledge base to be built [Lin, 2010].
Analytical models had a spread diffusion over the last 50 years and have the main advantage of permitting the understanding of the process through the main aspects influencing the process, avoiding the 'black art' of empirical modelling at selected parameter values.
In general two main types of analytical force models may be distinguished [Tonshoff, 1992]:

- the micro-based force model (or physics-based approach), starting from single grit tribology and grit distribution; it is mostly used to investigate how grit-level phenomena may affect grinding results (e.g. dressing conditions [Chen, 1996] [Badger, 2000] thermal and wear behaviour [Hou, 2003].

- the macro-based force model, based on kinematical grinding parameters and experimentally-determined coefficients.

The application of micro-based force models is considered hard to be applied for practical cases because of high amount of measuring efforts necessary [Tonshoff, 1992].
Macro-based force models can be distinguished in two [Lin, 2010]: the energy-approach models and statistical-approach models.

The energy approach model [Malkin, 1972]: consists in an energy breakdown of abrasive cutting behaviours. The power consumption during machining is considered as the sum of three components: cutting power (related to the material removal rate), plowing power (related to abrasive grit plowing action) and friction power (related to the friction effects of worn-out tips of abrasive grits rubbing the workpiece). Some authors extended this aspect using it as starting point for further analysis [Tang, 2009] [Durgumahanti, 2012].

The statistical approach regards grinding as a multi-edge cutting process such as milling ("micro-milling analogy").

Table 2-1 Bibliography review of some grinding dynamic models with main advantages and drawbacks

Year	Model	Advantages	Drawbacks	Model type	OP Type	Reference
1968	$F'_n = k' * (\frac{v_w}{v_s} * a_e)$	- application-oriented - use of h_{eq}	-Conformity not included	Experimental	OD	[Snoeys, 1968]
1971	$F'_n = const.' * \left(\frac{v_w}{v_s}\right)^{e1} * {a_e}^{e2} * D^{e3}$	-conformity -kinematical parameters	-Highly experimental	Experimental	S	[Shaw, 1971]
1978	$F'_n = const.' * \left(\frac{v_w}{v_s}\right)^{2\varepsilon-1} * {a_e}^{1-\varepsilon} * D^{\varepsilon}$	-material influence	-ploughing & rubbing not considered	Analytical	OD CF	[Werner, 1978]
1981	$F'_n = {F'_{n0}}' + \pi * D_w * v_{fr}/\Lambda_w$	- threshold force - metal removal parameter	-conformity not considered	Experimental	ID, OD, S	[Hahn, 1981]
1987	$F'_n(t) = F'_{np}(t) + F'_{cn}(t) + F'_{rn}(t)'$	- force components - loading considered	-heavy experimental procedure	Semi-analytical	OD	[Younis, 1987]
2007	$F'_t = F_0 * {a_d}^{f1} {s_d}^{f2} d^{f3} * (\frac{a * v_w}{v_s})^{f4}$	-dressing parameters included	- ploughing, rubbing, cutting not distinguished	Experimental	OD	[Choi, 2007]
2009	$F'_t = \left(c_1 + c_2 \, ln \frac{{v_s}^{1.5}}{a^{\,0.25} {v_w}^{0.5}}\right) * \frac{v_w * a}{v_s} + 4\left(\alpha + \frac{4\beta v_w}{d_e v_s}\right)(a d_e)^{0.5}$	-*Thermal softening* - energy-approach based	- complex - many approximations	Semi-analytical	S	[Tang, 2009]
2012	$F'_t = c_1 * \frac{v_w * a}{v_s} + \left(c_2 + c_3 \frac{v_w}{d_e v_s}\right)(a d_e)^{0.5} + c_4 * q^{-0.22} * D^{0.33} + a^{0.294} * c_5 * (a d_e)^{0.5}$	-ploughing, rubbing and cutting distinguished -time varying friction	-complex -many experimental coefficients - dressing not included	Semi analytical	S	[Durgumahanti, 2012]

One of the simplest models nowadays used is based on the concept of "Equivalent chip thickness": the applied grinding force is considered to be proportional to the equivalent thickness of chip removed [Snoeys, 1974]. The "equivalent chip thickness" (par. 2.2.1) permits to move among different grinding processes using a common dynamic parameter. This model re-arranges a previously proposed model (for OD grinding, [Snoeys, 1968]), including the effects of different grinding wheels, material and lubricants through the use of empirical exponents.
Werner [Werner, 1978] came to similar force equations using an analytical approach and explaining main material effects on forces; a distinction in easy-to-grind materials and difficult-to-grind materials[15] was firstly given. Difficult and easy-to-grind materials were distinguished also by Hahn and Lindsay due to their different behaviour concerning threshold forces [Hahn,1981][16]. The distinction between easy and difficult-to-grind materials was further improved by Lichun [Lichun,1980] starting from Malkin's work [Malkin, 1971], linking these aspect to two aspects of metal removal by abrasives: rubbing and chipping.
Another aspect of abrasive cutting, the ploughing action, had been considered, first in author's knowledge, in a work by Yuen [Younis, 1987] and thus included in dynamic analysis. Younis [Younis, 1987] considered time-dependent effects on grinding wheel behaviour in its model. The time-dependency of dynamics was reported in other models, as indicated by Tonshoff [Tonshoff, 1992], in terms of specific volumetric removal carried out by grinding wheel during one dressing stint.
Strain rate and thermal softening contributions in the energy needed for chip formation were included in a dynamic model by Tang [Tang, 2009], starting from energy considerations.
Recently, a work by Durgumahanti [Durgumahanti, 2012], included in modelled parameters the in-process varying friction.
Considering micro-scale-approach, indeed one of the most interesting investigation is the one by Badger and Torrance [Badger, 2000], who compared different force models starting from tribological approaches by Challen and Williams [Challen, 1978] [Williams, 1992], considering abrasive grain interactions, lubrication effects and workpiece hardness.
From a general point of view, it is clear that the more the model is rich of experimentally determined coefficients, the more it is time-expensive, risking to be application-customized and hardly to be used in different industrial situations.
Anyway, precision mechanics applications with conventional abrasives need for robust cutting conditions (e.g. process capabilities requests).
Bearing this idea in mind, a good trade-off between accuracy of the model and usability in practical applications seems to be Werner's model, eventually in Lichun's version. The robustness of their model to reported data has been shown by

[15] Easy to grind materials are the ones with a medium tensile stress strength, with a medium heat conductance and with a sufficiently low heat capacitance. On the opposite, hard to grind materials can be considered HS steels, due to an high amount of high hardness carbide resulting in high wear rates for grinding wheel. Similarly, ductile (higher elongation at break) or high thermal conductance and high thermal capacitance steels are difficult to grind due to difficulties in chip breakage (loading or clogging of the grinding wheel) [Spur, 1981].
[16] The threshold forces are the forces to be applied before metal removal begins [Hahn,1981]. This aspect may have a particular importance for high conformity between grinding wheel and machined surface (i.e. ID grinding).

Choi's work [Choi, 2007]. R^2 of latter models for specific normal grinding forces are reported to be equal to 0.9887 and 0.9969, respectively.
Hence, the use of Werner's model is simple and allows to include in one constant (to be determined for fixed combinations lubricant-wheel-workpiece) the influences of machining kinematical parameters.
The equivalent chip thickness approach proposed by Snoeys [Snoeys, 1974] is simple and effective too, especially for easy-to-grind, as reported by Lichun [Lichun, 1980].

2.2.1 Equivalent chip thickness model

One of the most important and easy-to-use grinding quantities is the one based on the equivalent chip thickness ("h_{eq}"). The model takes origin from the relationship between the grinding force and the volume of material removed, in an efficiently rough manner. Other approaches, such as uncut chip thickness, deal with edge distributions and are thus difficult to be applied in common practice [Marinescu, 2004].
The volume of metal removed (per unit of width of the workpiece due to a depth of cut a_e) is equal to the volume of metal removed by the grinding wheel action. Hence:

$$h_{eq} * v_s = v_w * a_e \Leftrightarrow h_{eq} = \frac{v_w}{v_s} * a_e \quad (25)$$

General model indicated by Snoeys ([Snoeys, 1974]) reported the following relation:

$$F_n' = c_1 * \left(\frac{v_w * a_e}{v_s}\right)^{c_2} = c_1 * \left(h_{eq}\right)^{c_2} \quad (26)$$

which is characterized by two constants specific for each combination of grinding wheel, workpiece material and lubricant properties.
For easy-to.grind materials, the exponential constant approaches the unity, letting, in first approximation, using a simpler version of eq. (28). The normal specific grinding force may therefore be defined as:

$$F_n' = k'_s * h_{eq} = k'_s * \frac{v_w * a_e}{v_s} = k'_s * \frac{1}{q} * a_e \quad (27)$$

where:

$$q = \frac{v_s}{v_w} \quad (28)$$

is defined as the speed ratio between workpiece speed and grinding speed;
Other parameters constant unvarying, this model permits to evaluate easily the impact of main kinematical parameter changes to grinding force. Anyway, due to oversimplifying, it is suggestible to be applied only in case of easy-to-grind materials.

2.2.2 Werner's Model

A refinement of equivalent chip thickness model proposed by Snoeys was developed, based on theoretical analysis, by Werner [Werner, 1978]. His model explains the main influences of working material on grinding operation: high speed grinding (used with easy-to-grind materials) and "medium"[17] speed machining (applied for difficult-to-grind materials).
This difference is expressed in terms of grinding behaviours due to different rates of frictional and formation forces. The rate of predominant cutting behaviour is expressed in terms of two coefficient, ε_1 and ε_2.
The number of dynamic active cutting edge is:

$$N_{dyn}(l) = N_{dyn} * (\frac{l}{l_g})^{\beta_2} \quad (29)$$

where:

$$N_{dyn} = const * {C_1}^{\beta_1} * \left(\frac{v_w}{v_s}\right)^{\beta_2} * (\frac{a}{D})^{\frac{\beta_2}{2}} \quad (30)$$

is the number of protruding cutting edges per unit of grinding wheel surface, depending on grit distribution[18].

$$l_g = (a * D)^{\frac{1}{2}} \quad (31)$$

is the contact length, approximated as geometrical contact length[19].

$$\bar{Q}(l) = \overline{Q_{max}} * (\frac{l}{l_g})^{1-\beta_2} \quad (32)$$

is the chip cross section (function of the contact length).
It can be demonstrated ([Werner, 1978]) that:

$$\bar{Q}_{max}(l) = {}^{2}/_{A_n} * {C_1}^{-\beta_1} * \left(\frac{v_w}{v_s}\right)^{1-\beta_2} * (\frac{a}{D})^{2-\frac{\beta_2}{2}} \quad (33)$$

For a single cutting edge in grinding, it is assumed that the cutting force is expressed ([Werner, 1978]) as:

[17] "Medium" stands for "not high", intended opposed to the research of increasing speeds. Here "high" speed is intended to be >45 m/s.
[18] C_1, β_1, β_2 are edge distribution characteristic values. Concerning exponentials, common values range: $1/3 < \beta_1 < 2/3$; $0 < \beta_2 < 2/3$. Further details available in [Werner, 1978]
[19] The contact length is approximated as geometrical contact length for sake of simplicity (details and references on differences between geometrical and real contact lengths are available in par. 2.5)

$$F_{grit} = const * \ Q^n; \quad 0 < n < 1 \tag{34}$$

Thus, for a number of cutting edge in contact along a contact length l_g, the resulting specific normal force will be:

$$F'_n = const * \int_0^{l_g} [\overline{Q}\ (l)]^n * \ \ N_{dyn}(l) * dl \tag{35}$$

Hence (from eq. 28, 29 30, 31):

$$F'_n = K * {C_1}^{\varepsilon_2} * \left(\frac{v_w}{v_s}\right)^{2\varepsilon_1 - 1} * a^{\varepsilon_1} * D^{1-\varepsilon_1} \tag{36}$$

With:

$$\varepsilon_1 = \frac{1}{2} * \ [(1+n) + \ \beta_2(1-n)]$$
$$\varepsilon_2 = \beta_1(1-n) \tag{37}$$

The practical range of ε_1 is 0.5-0.95; for ε_2, common values are 0.1-0.8.
Materials prone to high speed grinding (such as bearing material), typically have high ε_1 values and low ε_2. These are considered to have good "grindability". From these types of material it's possible to have significant advantages from high speed grinding, such as higher removal rate.
On the other side, austenitic steels, stainless steel, nickel based alloys, brittle hard materials, brittle hard materials are characterized by low ε_1 values and high ε_2. In this conditions, with increasing cutting speed the cutting force remains nearly constant: the increased input energy (result of increased cutting speed) result in an increase of cutting temperatures without any benefit from the machining operation.

2.3 Centerless loop and mutual influences

In the centerless grinding process the common practice is to reduce the grinding dynamic to a matter of "grinding stiffness". Based on the previously-shown influence of various kinematical parameters, it seems an over-simplification to consider grinding dynamics determined by the product of a constant (the grinding stiffness) with the actual depth of cut.
It is also to take in consideration a variation of kinematical parameters in the optimization of the cycle. The cutting stiffness will therefore considered as determined by selected kinematical parameters.
Further, it is to be noticed that dynamics are determined by the true depth of cut value, different from the machine-imposed depth of cut because of system stiffness. The imposed depth of cut can also be time varying, for example due to multi-stage process. Therefore, it is important to know and be aware of deflections occurring in the machining operation in order to understand how set-kinematical parameters affect the cutting behaviour.
Hence, it may be of relevance to include a deeper approach to dynamics in the centerless grinding loop, since dynamics have an influence on machine deflections, grinding and control wheel deflections, wave filtering (roundness) and others.

In figure 2-1it is possible to consider the relationships between different aspects related to grinding dynamic analysis, as reported in centerless plunge grinding operations.

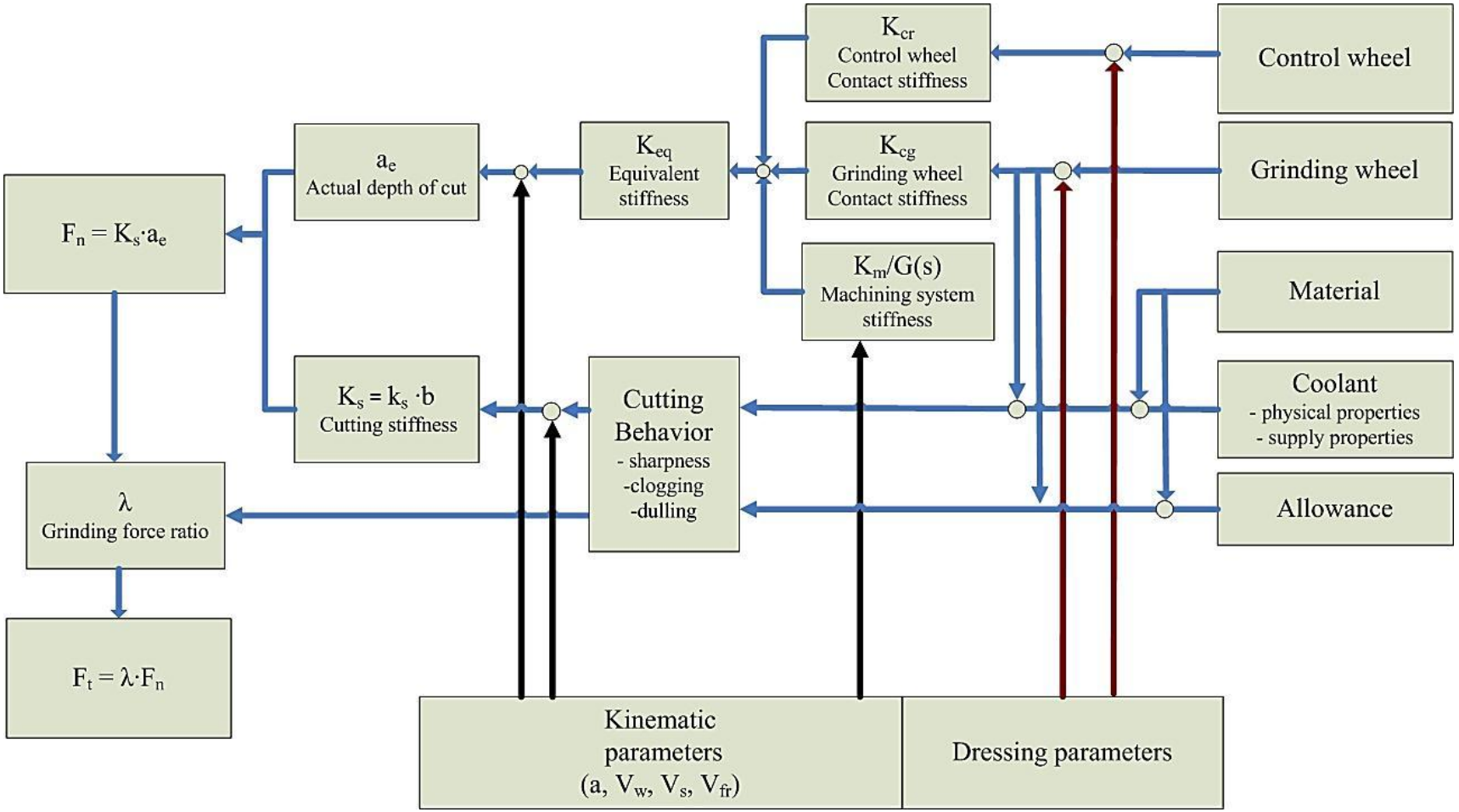

Figure 2-1 Aspects involved in centerless grinding dynamics

2.4 Tool influence

2.4.1 Grinding wheel properties

Grinding wheels can be thought as a three phase multicutter: abrasives (grits, cutters); bond (the holder); porosity (chip clearance and coolant inlet). In figure 2-2 a typical ternary diagram is reported [Malkin, 2008].

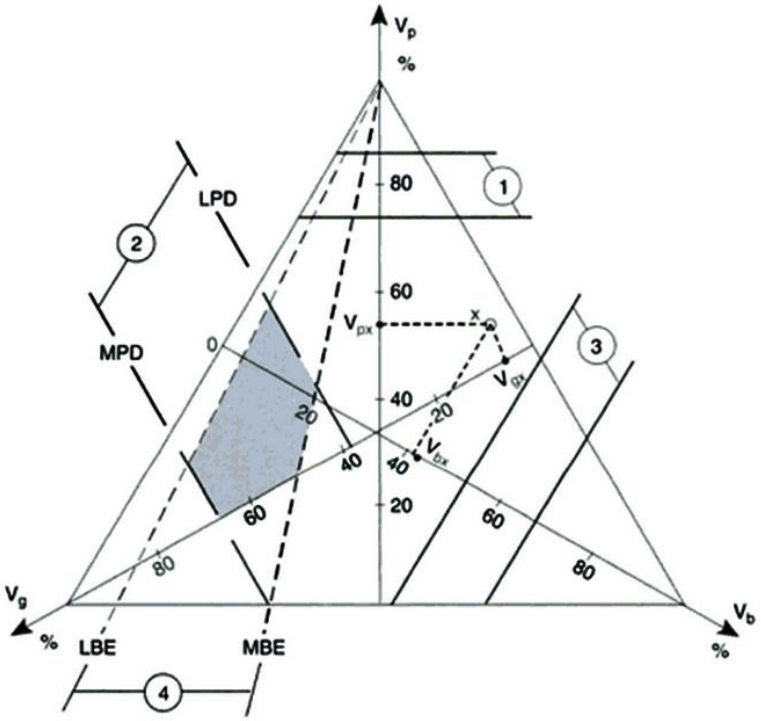

Figure 2-2 Example of ternary diagram for grinding wheel composition [Malkin 2008]

One of the most important characteristics of grinding wheels is the spread involved in their hardness and, consequently, their robustness considered on different batches [Shen, 1981]. By definition, the hardness of a grinding wheel concerns the capacity of an abrasive particle to be torn out of its bulk [Konig, 1987A] [Konig, 1987B]. Hence, the wheel hardness is related to long-process behaviour and to results such as burns, clogging, chatter and others.

Many methods have been applied by grinding wheel manufacturers (Zeiss-Mackensen, Grindosonic, Winterling and similars) [Klocke, 2009] [Shaw, 1996] to define wheel grade. The Young's modulus were recognized as a good indication of grinding wheel hardness, while other specification characteristics not varying [Konig, 1987A] [Konig, 1987B] [Rammerstorfer, 1974]. The most reliable way to investigate Young's modulus is the non destructive Grindosonic [Rammerstorfer, 1974] [Klocke, 2009]. This technique concerns the determination of the Young's modulus of a grinding wheel through its vibration analysis.

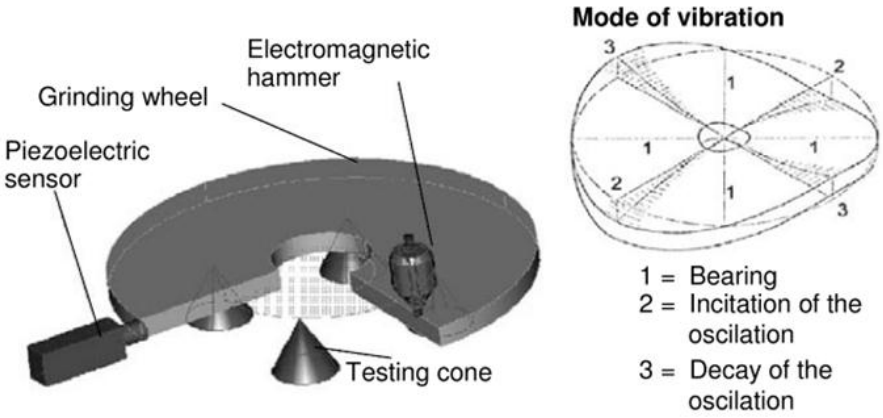

Figure 2-3 Grindosonic testing method [Klocke, 2009]

For example, this method permits to investigate the spread of Young's modulus in a same-specification batch of grinding wheels and permits to investigate the supplier's delivery quality [Shen, 1981].
Possible deviation in grinding wheel hardness have a double effect:

- varying Young's modulus;
- changing of the grinding force ratio [Takasu, 1988] (see par. 2.4.2).

The latter two may have an important effect on the grinding process stability [Snoeys, 1968], [Inasaki, 1977].
In mass production of precise parts, it is quite common to have long- terms behaviour differences with grinding wheels under the same specification (see figure 2-4 [Decneut, 1970]) The spread of wheel quality in a long term supply may be equal to one grade/two grades of wheels[20]. One hardness step, in terms of Young's modulus, is reported to be equal to 4,5 KN/mm^2 [21] [Klocke, 2009].
For the production of precision components in high volumes (such as automotive parts), it is important to keep wheel cutting behaviour as constant as possible. It is clear that, especially for intermittent dressing process (i.e. not dressing each cycle), constancy in cutting behaviour may be hard to be reached on the whole interval between dressings.
Another issue concerning cutting performance robustness may arise because of an high diameter difference during wheel life[22].
Therefore, a stable and robust process have to consider possible variations in grinding wheel conditions regarding:

- grinding wheel diameter;

[20] Informal info given by grinding wheel supplier.
[21] The amount of hardness grade step may vary for different grinding wheel producers. 4.5 KN/mm^2 is reported to be investigated for Norton company and for different bonding systems.
[22] High diameter difference may result in a difference of cutting grits. Less cutting grits result in higher wear-rate. Further, conformity (equivalent diameter) changes and affects the cutting forces.

- grinding wheel hardness (Young's modulus, cutting ratio).

In literature only few references give information about grinding wheel compositions and grade-Young's modulus relation, keeping other parameters constant.
Other grinding wheel properties may also impact on grinding wheel E module [Rammerstorfer, 1974], as shown in figure 2-5.

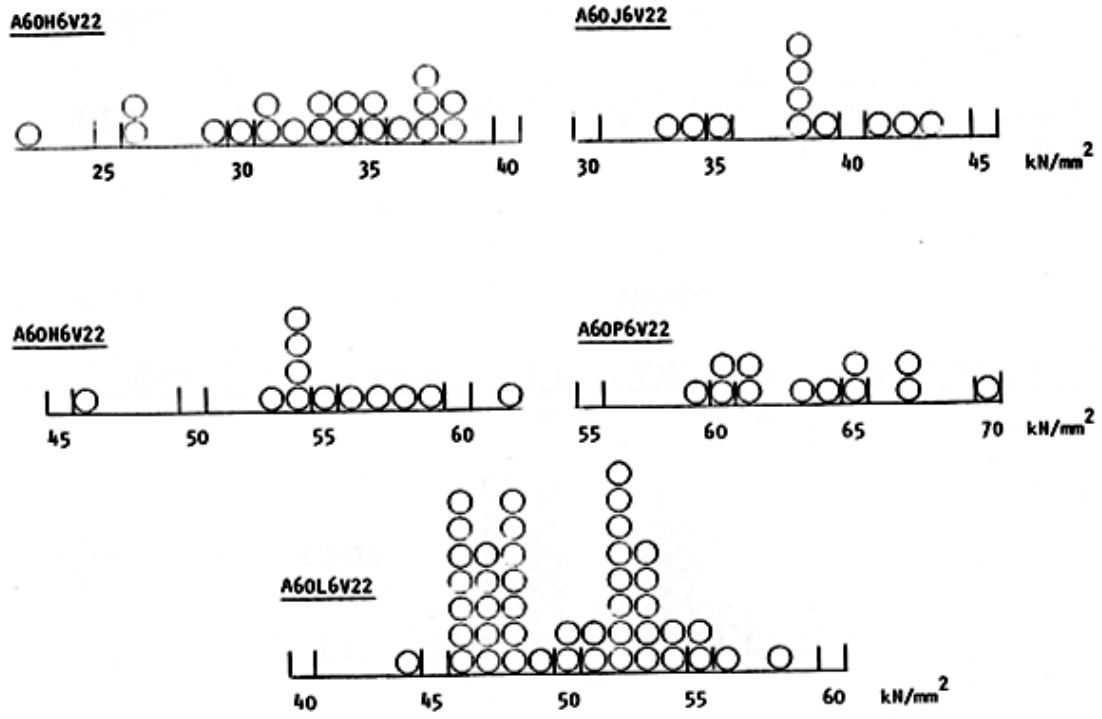

Figure 2-4 Example of elastic modulus distribution (C.H. Shen)

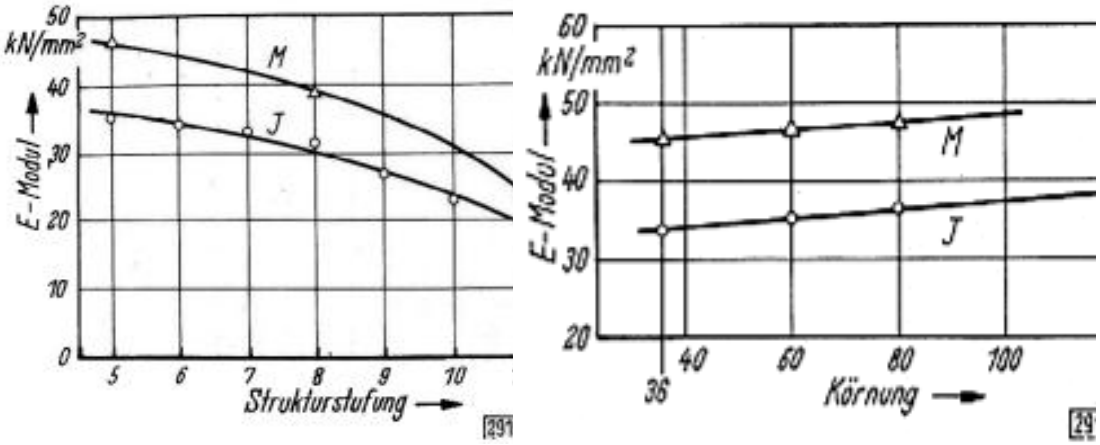

Figure 2-5 Example of influence of structure number (left) and grit size (right) on Young's module [Rammerstorfer, 1974]

Another possible heterogeneity of the grinding wheels may result in a diameter-stripe behaviour (i.e. different hardness at different wheel diameters). This phenomena, well-known in production, it is hard to be found until grinding wheel is not mounted on machine.

2.4.2 The grinding force ratio parameter

Friction has a double importance in centerless grinding:

- regarding control wheel and blade, is the ratio between applied normal forces and the tangential ones, with the aim of controlling the workpiece rotation.

- regarding grinding wheel, is the ratio between normal force and tangent cutting force ("grinding force ratio")

The grinding force ratio is defined by:

$$\lambda = \frac{F'_t}{F'_n} \tag{38}$$

This ratio is not usually involved in chatter problems study but can have strong impact for spinning issues and rotational stability analysis. Some values form literature are reported in the following table 2-2.

Table 2-2 Examples of grinding force ratios available in literature

λ	GW	Workpiece	Technical features	Reference
0.25/0.6	-	-	-	[Winterthur. 2005]
0.3	-	-	Typical value for centerless grinding and rotational stability evaluation	[Marinescu, 2008]
0.3-1	-	-	Ratio higher for sharp wheels, lower for blunt	[Zakharov, 2008]
0.55/0.63	-	0.45% C steel, 45 HRC	-	[Chen, 1996]
0.2/0.3	Various	AISI 1095 35 HRc	High value dispersion/ SG	[Kanappan, 1972]
0.35/0.48/0.55	EK80J7VX	316	SB-C 3%	[Snoeys, 1974]
0.54/0.75	6A54LSVA2	4615	SB-C 3%	[Snoeys, 1974]
0.36	EK60L7VX	100Cr6	SB-C 3%	[Snoeys, 1974]
0.32	EK80J7VX	100Cr6	SB-C 3%	[Snoeys, 1974]
0.35	P100, P60	100Cr6	SB-C 3%	[Snoeys, 1974]
0.37/0.39	1A60I	100Cr6	SB-C 3%	[Snoeys, 1974]
0.38/0.39/0.41	EK60L7VX	100Cr6	SB-C 3%	[Snoeys, 1974]
0.3	EK60L7VX	100Cr6	EPS 12 100%	[Snoeys, 1974]
0.22/0.35	EK60L7VX	X210CrW12	SB-C 3%	[Snoeys, 1974]
0.27	P60	X210CrW12	SB-C 3%	[Snoeys, 1974]
0.3/0.4	Various grades of RA80 (K, L, M)	S35C hardened	Tested apart	[Takasu, 1988]
0.3	B126VSS2804J…	100Cr6 62-64 HRc	-	[Kranjik, 2008]
0.15	SN70 M8 V 35	SAE 4820 60-62 HRc	Tested apart	[Li, 2008]

2.4.3 Control wheel properties

Control wheel properties may incur in problems of quality repeatability. They may be considered as grinding wheels, under this aspect. Their characteristic robustness may have primary importance for roundness issues. The latter is true also for dimensional capabilities, especially in plunge grinding of different diameters with tight tolerances: in this cases the wear resistance is critical (figure 2-6).

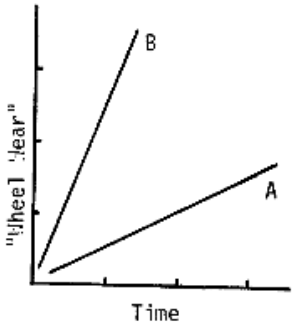

Curve	E mod. kN/mm^2	Whl.Wear Rate µm/minute
A	27.93	0.5
B	19.96	2.5

Machine: #2 Centerless Grinding Machine
Wheel : 300 mm x 200 mm x 125 mm
Part : 2.5 mm dia. x 12.5 mm long
Metal Removal Rate : 3.13 cm^3/min.

Figure 2-6 Control wheel hardness effect on wheel wear rate [Bhateja, 1981]

The variance in control wheel hardness occurring in medium-term term supply of control wheels was shown in Bhateja's paper [Bhateja, 1981], reported the following table 2-3.

Table 2-3 Example of static bulk hardness variation in control wheels batches [Bhateja, 1981]

Wheel	N° of wheels	Size [mm]	E modulus range		Density g/cm^3	
			KN/mm^2	%	Range	%
A80S2R	35	300x150x125	16.67-26.04	45	2.80-3.03	7.9
A80S2R	15	200x200x125	18.69-27.93	38	2.72-2.93	7.4
A120S2R	12	350x250x150	19.05-20.62	8.2	2.77-2.82	1.6

The variance of control wheel is known to be particularly relevant for rubber wheel due to their production cycle; the use of resinoid control wheel (epoxy) should overcome this problem, guaranteeing a more stable production cycle, thus increasing characteristics robustness [Atlantic Gmbh, 2009].

2.4.4 Control wheel frictional behaviour

The control wheel (or regulating wheel) has to control the speed of the workpiece through its frictional action.

An in-depth analysis of frictional behaviour of control wheels has been given by Hashimoto [Hashimoto, 1998]. Frictional characteristics may vary based on:

- bond (steel, vitrified, resinoid, rubber)
- dressing parameters
- grit size
- control blade angle [Winterthur, 2005]

Major results available in literature have been reported in table 2-4.
Particularly noticeable is the fricition-hysteresis effect reported by Hashimoto [Hashimoto, 1998]; there may be some slip between control wheel: this phenomenon results in an hysteresis effect on friction value and eventually in a loss of contact between workpiece and control wheel.

Table 2-4 Examples of control wheel friction values available in literature

Frictional coefficient μ_R	CW	Workpiece	Technical notes	Ref.
0.14-0.45	-	-	The friction coefficient depends on the blade angle: the steeper the blade angle, the smaller the friction coefficient	[Winterthur, 2005]
0.34	Vulcanite binder	-	300 mm/min dressing speed	[Zakharov, 2008]
0.17	Steel	-	-	[Zakharov, 2008]
0.24-0.25	A80 Rubber bonded	F522 hardened steel	Rough dressing; various contact pressures (45-86 MPa)	[Gallego, 2007]
0.20	A80 Rubber bonded	F522 hardened steel	Fine dressing; various contact pressures tested (52-85 MPa)	[Gallego, 2007]
0.45 (0.3 - slip condition)	A150RR (rubber bonded)	S35C hardened	Different values for static and slipping coefficients	[Takasu, 1988]
0.4 [23]	(Vitrified bonded) A150 RV	52100 hardened and green	Wet 1% soluble oil	[Hashimoto, 1998]
0.34	(Rubber bonded) A150RR	52100 hardened	Wet 1% soluble oil	[Hashimoto, 1998]
0.25	(Resin bonded) A150RB	52100 hardened	Wet 1% soluble oil	[Hashimoto, 1998]
0.21	(Poliurethane bonded) A150RKM	52100 hardened and green	Wet 1% soluble oil. Relevant effects of workpiece hardening on mu. Small effect due to grit size of rubber wheel.	[Hashimoto, 1998]
0.17	Steel	52100 hardned	No hysteresis	[Hashimoto, 1998]
1	Rubber	100Cr6 62-64 HRc	-	[Krajnik, 2008]

2.4.5 Blade

Blade concurs in rotational stability of centerless machining process. Hence, friction characteristics of blade have to be examined for holding stability (i.e. spinners). Anyway, it is usually not extensively analysed in literature; in table 2-5 some values of frictional characteristics are reported.

[23] In Hashimoto's work the concept of friction hysteresis has been shown, underlying the difference between rolling friction coefficient (traditional concept) and the "slipping-rolling contact" friction. In table 2-5, the traditional pure rolling friction is reported.

Table 2-5 Examples of blade friction coefficient available in literature

Blade kinetic friction coefficient μ_b	Blade material	Workpiece	Technical notes	Reference
0.1	-	S32C		[Takasu, 1988]
0.3	-	-	-	[Kim, 2003]
0.15-0.17			Used for rotational stability purposes	[Zakharov, 2008]
0.15	-	-	Typical applications	[Marinescu, 2008]
0.1-0.15	-	-	-	[Winterthur, 2005]
0.3	"standard"	100Cr6		[Krajinik, 2008]

Another distinctive feature of blade, is its material or, better, the material of the brazed plate on the top of it (holding the workpiece). Mostly known materials are [Cincinnati, 1988] [Klocke, 2004]

- copper/bronze
- cast iron
- hard metal (mostly used)
- policristalline diamond (PCD)
- tungsten carbide
- cBN disperged carbide
- alumina

It has to be noted that the wearing behaviour may be relevant for very low roundness needs, in which the blade consumption may result in disturbances affecting the rounding phenomenon [Klocke, 2004].

2.5 Contact behaviour

2.5.1 Contact effects in centerless grinding

Contact stiffness is a complex matter and it has a strong impact on the grinding process for phenomena ranging from chatter avoidance to thermal effects.

The complexity is basically due to the number of characteristics that its study has to deal with. Mainly, it is possible to group these characteristics in the following three aspects[24]:

- grinding wheel stiffness;
- workpiece stiffness;
- size of deformations compared to depth of cut.

Traditionally, there are two main aspects of investigation in literature concerning the finite stiffness of grinding wheel, control wheel and workpiece: the contact length and the contact deflections, l_c and δ_c.
In centerless grinding these two issues have to be considered of interest in order to simulate machining system deflections and to investigate the filtering effect on the lobing behaviour.
Deflections are to be considered with the aim of knowing the actual values of kinematical parameters, thus determining the real state of the machining operations. The knowledge of deflections concerns the possibility to optimize the cycle time (e.g. reduction of spark-out time, increase of infeed speed).
Contact lengths are traditionally more interesting for thermal aspects or for waviness filtering properties (as in the case of centerless grinding [Hashimoto, 2000]).
In literature traditionally two kind of approaches are applied for the grinding wheel-workpiece contact (similarly for the control wheel-workpiece): "traditional" hertzian approach and the modified hertzian approach.
The traditional hertzian approach lacks of precision because of its smooth-surfaces-in-contact hypotesis. Furthermore the application of pure hertzian analysis is not allowed because of the following:

- the bodies in contact are not smooth [Qi, 1997]
- the deflection process involves elastic and plastic deflection (just elastic for control wheel deflections);
- the contact curve is far from being a continuous smooth curve (unground surface plus "under-grinding" surface plus ground surface) [Qi, 1997];
- the transmitted force is far from being purely normal, especially in the grinding process.

Further, the contact pressure distribution is strongly influenced by rough contact (at low loads, as in the grinding case, as reported by Rowe [Rowe, 1993]). Hence, the roughness of contacting surfaces involves deflections and the number of contacting points (i.e. the cutting edges for the grinding wheel, in the machining process) [Rowe, 1993].

[24] In considering the contact compliances, particular attention has to be given to machine and holding devices.

Other models have been adopted in the past: Snoeys and Wang's model was based on grains mounted on springs [Snoeys, 1968]; Brown et al [Brown, 1971] used a composed hertzian model to investigate deflections superimposing two contact behaviours: bulk grinding wheel-grits and grit-workpiece. Other approaches consisted in studying single grain deflections to understand the decrease in depth of cut [Qi, 1997]. Despite the fact that this approach analyses the single grit behaviour in cutting, (while bulk approaches concern static measurement results), the most used analysis seems to be the "hertzian corrected approach" [Rowe, 1993]..

2.5.2 Corrected hertzian problem

This approach is consistent with an high number of previously reported studies concerning the between the geometrical and the real length of contact, as shown by [Qi, 1997]
The wheel-workpiece contact length is expressed as a sum: contact length due to force related deflections and contact length due to the geometry of depth of cut.
Hence,

$$l_c{}^2 = l_{fr}{}^2 + l_g{}^2$$

$$l_c = \sqrt{R_r{}^2 * l_f{}^2 + l_g{}^2} \qquad (39)$$

where:

- l_c is the real contact length
- l_{fr} is the contact length due to the normal force between the surfaces, corrected to consider the rough contact characteristic ($l_{fr} = R_r \cdot l_f$)
- R_r is the ratio of the contact lengths of rough contacting surfaces on smooth contacting surfaces and it has to be applied at low loads. At low loads, effective pressure is distributed on a significantly higher contact area, reducing the maximum average contact pressure [Rowe, 1993]
- l_g is the geometrical contact length (commonly considered to be $\sim a_e{}^{0.5}$)

The R_r ratio is given by [Johnson, 1985] for normal contact between cylinders, in terms of a parameter linked to surfaces roughnesses.
A numerical approach ("Matrix inversion") has been applied by Li [Li, 2007] [Johnson, 1985]. This permits to consider surface deviations from geometrical case studies (e.g. roundness errors in a cylindrical body), giving a realistic deformation and contact gap between contacting bodies. Anyway, this approach does not consider in pressure distribution correction due to rough bodies in contact.

2.5.3 Contact stiffness

The contact stiffness has been recognized as an important factor for the stability study in grinding as reported by Inasaki [Inasaki, 1977] and Snoeys [Snoeys, 1969]. The contact behaviour was shown to be an hard-spring type, as shown in figure 2-7.

Hence there is a need for contact stiffness updating during a typical multi-stage in feed process.

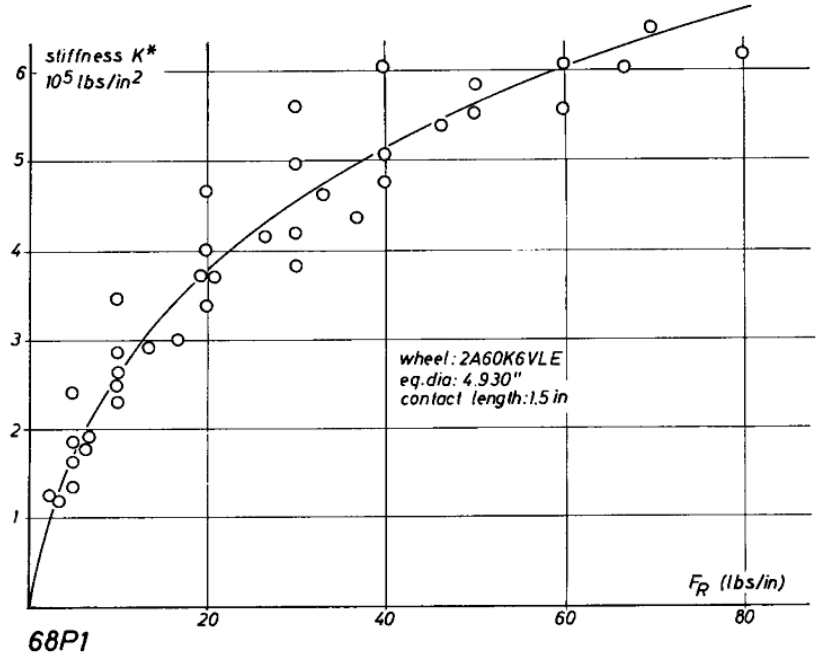

Figure 2-7 Example of contact stiffness [Snoeys, 1969]

The contact stiffness is defined as the ratio:

$$k_c = \frac{\partial F'_n}{\partial \delta} \tag{40}$$

Therefore, the theoretical analysis of the contact stiffness depends on the correct analysis of contact displacements. Brown [Brown, 1971] proposed a "corrected" hertzian approach. The deflection of contacting bodies has been considered as the sum of mutual approach grits-workpiece (modelled as sphere-plane contact) and wheel(bulk)-workpiece (modelled cylinder-plane contact). This sum of effects-approach has been used also for cylindrical plunge grinding approach.
Here in table 2-6, few applications for the calculation of contact stiffness are displayed.

Table 2-6 Examples of contact stiffness calculation available in literature

Year	Contact stiffness	Notes	Ref
1968	$k_c = 3.72 * \left(\frac{k}{a}\right)^{0.25} * {D_{eq}}^{-0.25} * {F_n}^{0.75}$ k = grit spring characteristic a =distance between grits	Wheel surface = system of individual springs	[Snoeys, 1968]
1968	$K_c = 2 * p_s * ln\left[\left[\left(\frac{D_s}{2 * F_n * p_s * D_{eq}}\right)^{1/2} + - \frac{{c_s}/{2}}{(1 - c_s)}\right]\right] + 4 * \frac{p_s * {F_n}^{\frac{2}{3}}}{D_s}$ p_s, c_s = physical parameters (depending on Young's and Poisson's modulus)	Rearranged from elastic theory, smooth bodies	[Snoeys, 1968]
1968	$k_c = const * freq^2$ *freq*= contact resonant frequency investigated by V clamping device	Contact stiffness proportional to contact resonance frequency	[Hahn, 1968]
1971	$k_c = \frac{\partial {F'}_n}{\partial \delta} = \frac{\partial {F'}_n}{\partial(\delta' + \delta'')}$	Composition of effects: grit-piece contact and bulk wheel-workpiece	[Brown, 1971]
1977	$K_c = C * \left(\frac{v}{V} * h_0\right)^p$	-	[Shimizu, 1977]
1987	$k_c = cost * e^{(-cost * d_g)} * E^{cost}$	Local Young's modulus and grit size related to contact stiffness	[Tooe, 1987]

2.5.4 Experimental values

Few contact stiffnesses values taken from literature have been reported in the table 2-7. Since regulating wheel can be considered as a grinding wheel too, the previous considerations can be applied too. Hence, regulating wheel contact stiffness has to be considered for stability considerations.

Table 2-7 Examples of contact stiffness values available in literature

Contact type	Tool-materials in contact	K_c [N/mm*mm]	Reference
OD, GW-piece	SN70M8V35 – SAE 42100 60-62 HRC	1000(=70*10^3/70)	[Li, 2007]
SURFACE, GW-piece		0.8*10^3 ;1.1*10^3	[Yamada, 2006]
GW-piece	-	3.4*10^3	[Snoeys, 1968]
GW-piece	-	15-20*10^3	[Tooe, 1987]
OD,GW-piece	WA60J8V – piece	1.14*10^3/	[Miyashita, 1982]
OD,CW	A60V5L6 – EN8 60-62 HRC	620(=3.1*10^4/50)	[Rowe, 1973]
OD, CW-piece	Rubber - SAE 42100 60-62 HRC	300 (=21*10^3/70)	[Li, 2007]
OD, CW-piece	Rubber 80 RR – EN8 60-62 HRC	540(=270*10^4/50)	[Rowe, 1973]
OD, CW-piece	A150RR	0.6*10^3	[Miyashita, 1982]
OD, CW-piece	A100RR	0.3*10^3	[Miyashita, 1982]

2.6 Conclusions

In the present chapter the different aspects involved in centerless grinding dynamics are presented:

- An huge number of cutting model is available in literature. These models may explain main trends and influences of several grinding operations (workpiece speed, grinding wheel speed, machined materials, dressing operations, coolant and others). The model currently used in centerless grinding seems over-simplified.

- An analysis is carried out on main frictional characteristics of centerless grinding system: grinding wheel, blade and control wheel, reporting data available in literature. Whilst blade friction characteristics are almost the same throughout the literature, grinding and control wheel friction may incur in high differences based on their specifications.

- Based on their manufacturing technology, grinding wheels and control wheels may have an influent variations in physical properties and, hence, on

their manufacturing performances. In particular, vitrified grinding wheels hardness can span two grade of hardness. In some cases, rubber bonded control wheels may change their elasticity module up to 45%. A literature review with major friction- related issues is carried out.

- Contact compliances show an hard-spring-type behaviour, thus varying based on applied load.

- The contact compliance between wheels and workpiece consists of two aspects: the contact length has a significant component due to the rough nature of the contact between the wheels in abrasive and the workpiece; further, the contact stiffness are relevant for stability analysis and comparable with machine stiffness. A review of contact stiffness models and values available in literature is reported.

3 Practical aspects of centerless grinding (plunge)

3.1 Introduction

Plunge centerless grinding is mostly used for machining multidiameter part. Otherwise troughfeed method is preferably used, due to its possibility of reaching high accuracies through its slower cutting action (i.e. lower Q_w') with high throughput.
Centerless grinding is a very high production rate process but it is time expensive in tooling up. In this chapter the biggest issues about plunge centerless grinding have been reported from the setting up to the final acceptance of the machine performances, based on author's experience.
It has to be reminded that, due to the particular holding of the workpiece, it is always worth to spend some time in order to check all the set up and the loading device: in fact, once the machining cycle has started, there is not a big chance to avoid damages to tools and, in the worst cases, to the machine (guides, bearings).
Despite the fact that some little adjustment and problem-fixing may be however necessary, the most of the problems can be avoided trough a careful process and tooling design, avoiding setting up waste of time.
Based on author's experience, this chapter gathers the main hints concurring for a correct machine setup. The main issues are organized as in following:

- Analysis of machine configuration type (par. 3.2).
- Analysis of wheel and blade positioning (par. 3.3).
- Study of cycle configuration (par. 3.4):
  - stock allowance;
  - dressing systems and tools;
  - blade analysis;
  - dressing templates;
  - loading of workpieces;
  - dressing depth and federates.
- Cycle time calculations (par. 3.5):
  - cycle time composition;
  - loading and unloading time;
  - grinding time;
  - dressing time.
- Prevision of possible inconveniences (par. 3.6).
- Troubleshooting (par 3.7).

3.2 Machine configuration analysis

A correct analysis of workpiece feasibility has to start from machine analysis. The machining may require different types of tools and, more important, may require different ways to solve the same tasks.
Despite different types of machine set-ups are possible (horizontal, vertical, angular [Klocke, 2009]) and a big number of part-customized solutions (suitable for highest volumes of few parts), author differentiated machines based on their distribution of the technologically-involved axes.
Three main types of machines for multi-diameter plunge grinding have been identified based on axes configuration, as in figure 3-1:

- moving control wheel axis and blade axis, with grinding wheel CN dressed (eventually template dressed), called "machine configuration A";

- moving grinding wheel axes and control wheel axes, with both grinding and control wheel CNC dressed (steady dressers and blade), called "machine configuration B";

- moving grinding wheel, CN dressed; steady control wheel and blade, called "machine configuration C".

Despite some general aspect involved such as compact design and access comfort, in order to machine multidiameter workpieces the following aspects should be considered:

- machine configuration A (e.g 4 axes Ghiringhelli M200 series, Cincinnati 2-250 series) may require additional dressing template and an additional infeed movement for dressing the control wheel. The dressing template keeps the shape and has to be customized for the part. This configuration allows for "under the blade" unloading.

- machine configuration B (e.g. Modler MC85 series) requires customized control wheel. Control wheel doesn't wear out such as conventional ones[25] since manufactured in steel (eventually cBN reported); the loading system has to be accurately adjusted.

- machine configuration C (e.g. Mikrosa) permits high flexibility without additional tools. No workpiece-dedicated templates are needed. Theoretically, it permits under the blade unloading but no applications are known. Thanks to its axes configurations gives the possibility to work angled part as well.

[25] The wearing out of control wheel can be particularly tedious for high precision multidiameter parts with high cilindricity requirements or narrow dimensional tolerances. Whilst regulating wheel and driven-workpiece diameter have the same peripheral speed, due to peripheral speed difference at different diameters, slipping frictions are applied. These actions result in quicker wearing out of control wheel holding diameters with corresponding increase of dimensions. To avoid the latter, a keen adjustment of control wheel recesses to find a slipping compromise between different diameters may be done.

3.3 Analysis of wheel and blade positioning

Wheel and blade positioning is commonly not considered to be a big issue but in some cases problems may occur, especially in case of wheel shapes matching with workpiece reliefs or in case of double-piece grinding.
Special care has to be put in having a good axial alignment between grinding wheel shoulder and workpiece. According to this principle, an accurate choice of the workpiece stop position may be necessary to limit the impact of size variation in the supply of grinding wheels. An example of tooling up drawing is given in figure 3-2.

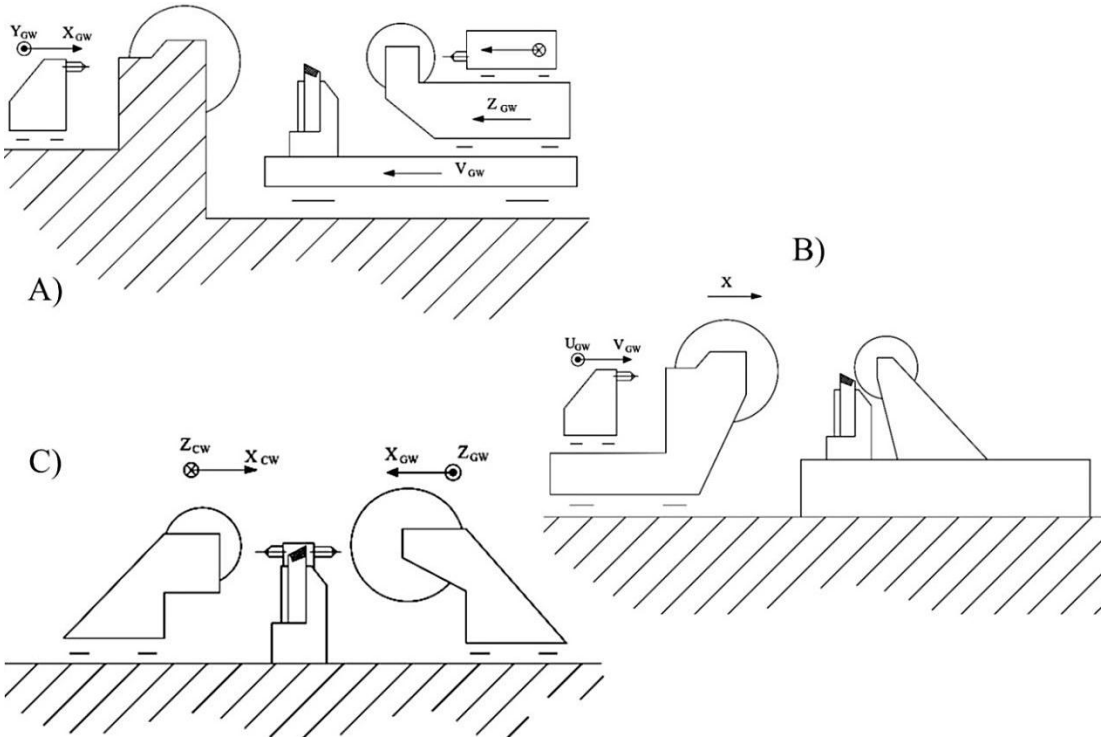

Figure 3-1 Examples of different axes configuration

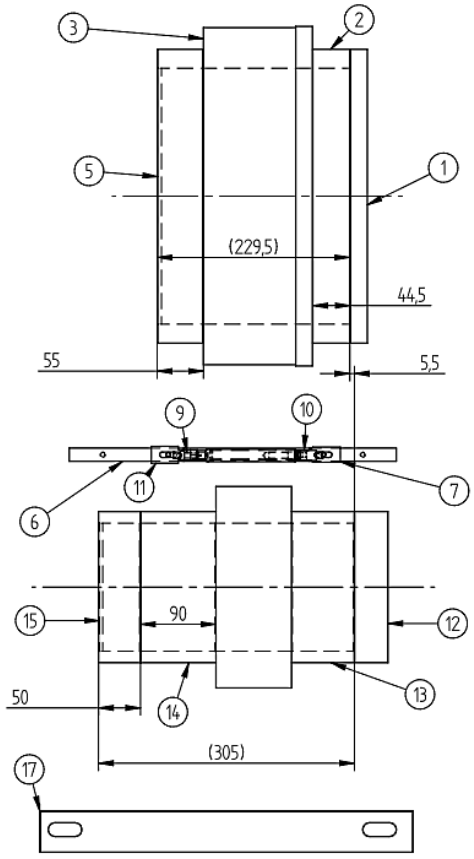

POS.	DENOMINAZIONE	Q.TA
20*	Camp. albero fresato GM 1.6	1
17	DIMA RULLO	1
16*	MOLA CONDUTTRICE 305x90x152,4	1
15	DISTANZIALE MOLA CONDUTTRICE 180x50x152,4	1
14	DISTANZIALE MOLA CONDUTTRICE 180X90X152,4	1
13	DISTANZIALE MOLA CONDUTTRICE 180x45x152,4	1
12	PORTA MOLA CONDUTTRICE	1
11	FERMO PEZZO DX	1
10	BICCHIERE PORTA PEZZO	1
9	PERNO PRESA PEZZO	1
7	FERMO PEZZO SIN	1
6	LAMA SOSTEGNO PEZZO	1
5	DISTANZIALE 350x55x304,8	1
3	MOLA OPERATRICE	1
2	DISTANZIALE 350x45x304,8	1
1	PORTA MOLA OPERATRICE	1

Figure 3-2 Example of alignment among blade, wheels and dressing template

In case of double-piece grinding other problems may occur due to the combination of side-runout tolerances (applied according to ISO 13942, former DIN 69107), and to width tolerance (up to +/-1,6 mm), particularly.

Therefore, for optimal study of grinding wheel positioning, both the tolerance on double runout achievable on wheel shoulders and the thickness tolerance have to be considered. Hence, a previous verification of wheel supplier's achievable quality (mostly based on its machining finishing production process) has to be considered and verified.

Another point (often underestimated) concerns the minimum allowed radius to be ground on the part. Despite the fact that the latter is limited by dressing device (type and size of diamond and its holding matrix), the accuracy guaranteed by the CN profile may be harmed by the grit size. An example of achievable radius accuracy based on grit size is shown in figure 3-3 [Hermes Schleifkoerper Gmbh, 2010].

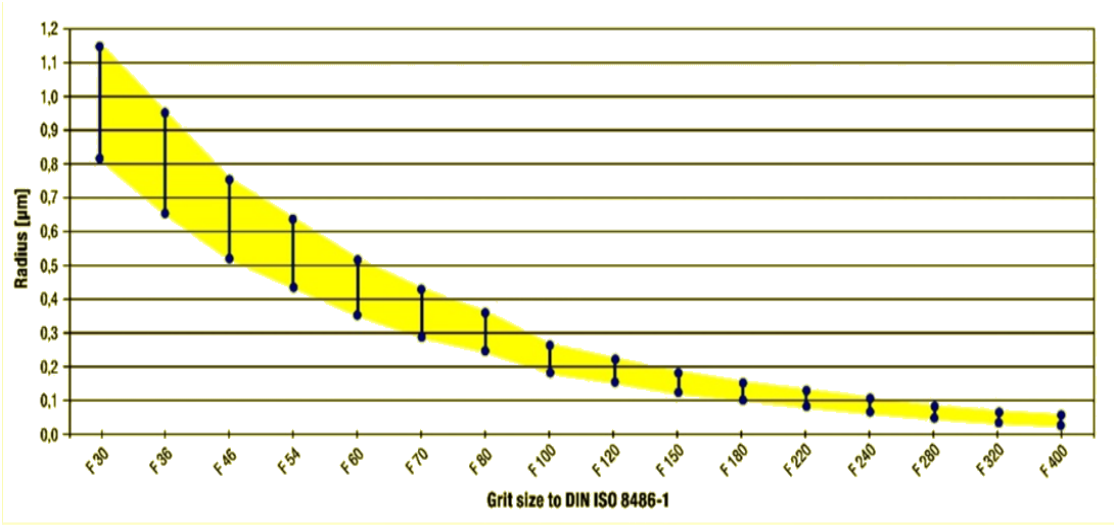

Figure 3-3 Achievable radius for grit size adopted [Hermes Schleifkoerper Gmbh, 2010]

3.4 Study of cycle configuration

3.4.1 Allowance

The incoming part quality has to be a strong concern for the centerless grinding process.

Previous problems (e.g. chips, burrs, excessive runout or excessive roundness) on holding surfaces (especially those in contact with axial stop) may result in holding or quality problems.

Generically speaking, if possible, blade and control wheel design should consider the possible arise of the cited problems (e.g. through the use of grooves and reliefs).

Another point to be considered is the amount of stock removal. This is indeed affected by the quality of incoming raw part, but a good example of thumb of rule is indicated in table 1-2 [Tsasch, 2009].

The stock amount has a huge influence on grinding wheel choice (see table 3-1) [Klocke, 2009] (i.e. grit size, hardness, structure) and can therefore be a limit to the achievable quality in terms of roughness and size holding capability (i.e. diameter tolerance and cilindricity) and roundness (related to cycle time availability). It has to be reminded that in case of heat treatment, machining dimensions and tolerances from previous phases (e.g. length) may vary. If dimensions shortening/increase cannot be forecasted based on experiences or (roughly) trough theoretical models [Cibaldi, 2006], tolerance variations has to be evaluated by trials and may ask for feedback correction to previous phases drawings (an example of variation due to induction hardening is reported in figure 3-4).

Table 3-1 Guidelines for grain size selection [Klocke, 2009]

Grain size		Obtainable surface roughness	Maximum allowance	Machining stage
mesh	µm	µm	µm	
46	320	5.0 to 2.4	Practically unlimited	Pre-grinding
80	200	2.5 to 1.5	1 % of the d_w, not ≤ 300	Finish-grinding
120	120	2.0 to 1.0	150 to 200	Fine grinding
200	80	1.6 to 0.7	50 to 100	Finest grinding
320	46	1.2 to 0.4	20	Finest grinding

Others heat treatment effects may be related to workpiece bending; this can be particularly strong for stressed part from previous phases; since it is not always possible to reduce machining stresses, an increase in stock amount may be considered.

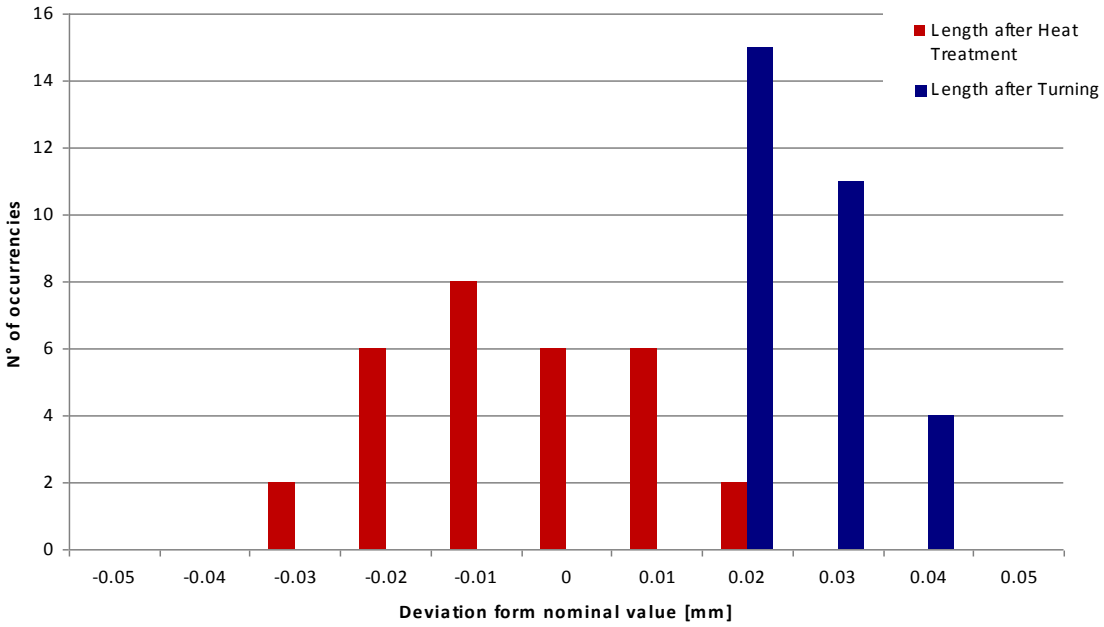

Figure 3-4 Shortening of shaft due to induction heating treatment (C53 Ti)

3.4.2 Dressing systems and tools

3.4.2.1 Dressing system

Dressing system type may have a strong impact on product feasibility. Three main types may be distinguished: ultrasonic assisted dressing, NC dressing, form dressing.
Author's experience do not include ultrasonic assisted dressing, used for metallic bonding grinding wheels. For machining with standard abrasives, profile dressing and form dressing are mostly used.
Profile dressing can be carried out through the use of a shaped dressing template or two NC-driven axes. These axes can be the same used for machining (as used by Mikrosa) or can be just dedicated to dressing (e.g. Ghiringhelli).
Concerning dressing template, due to their tolerances[26], it is always better to be aware of their manufacturing limits, delivery time and costs when planning a production changeover. Machining precision limit may deeply affect the possibility to reach desired part shape and/or tolerances.
Often a good trade-off between costs and precision consists in using one dressing template (for the control wheel) and 2 NC axis dressing system to overcome machining errors.

3.4.2.2 Dressing tools

Available dressing system can be distinguished in 2 main types:

- dressing plates
- dressing rolls

Further, dressing plates may be distinguished in three main types:

- dispersed diamonds (powder)
- positioned diamonds (spheres or rice-grain shaped)
- positioned diamond sticks (various dimensions, e.g. figure 3-5)

Figure 3-5 Example of positioned diamond stick dresser

[26] Common tolerances for height differences in template profiles are in the order of few µm.

Two are the sub categories of dressing rolls:

- form rolls (e.g. figure 3-6)
- shape rolls (for CN profiling)

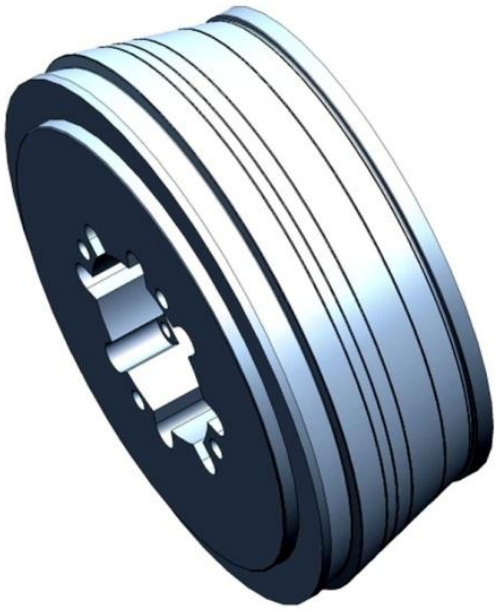

Figure 3-6 Example of 3D model of dressing form roll

One of the biggest problems related to the dressing systems is the shaping of angular sides in the grinding wheel and, in particular, of radii.
The possibility of machining radii correctly depends on:

- Type of dressing system used (dressing template, NC form dressing, dressing roll):
  smaller radii (typically in the order some tenth of mm) are feasible through dressing roll only. The use of dressing templates is limited by machining tolerances and, in particular, by feeler tip dimensions. Often the easiest way to machine smaller radii is through the use of a dressing roll. In this case radius magnitude affects strongly the life of the dressing roll (and its cost). This is due to the size of diamonds to be used (the smaller, the weaker) and depends strongly on the orientation of the radius (i.e. convex or concave), because of stress concentration and the coolant delivery.

- Dressing device (i.e. diamond type): dispersed diamond dressing plates cannot be used for accurately shaped profiles due to possible misalignment of cutting diamonds inside the matrix. The only choice to do this is through blades with diamond sticks (Fliesen type): because of their fixed cutting position they can perform reliable cut, i.e. reliable profiles on the grinding wheel. Their drawback is the proper choice of the sticks dimensions (e.g. 0.6x0.6, 0.8x08) and orientation and their sensitivity to coolant delivery which may be a cause of premature graphitization and loss of cutting ability.

- Grinding wheel properties(previously examined 2.4.1)

3.4.2.3 Blade analysis

Blade height is well known for its impact on roundness error.
In order to choose correct height above the centres, in literature several suggestions are available:

- use 20° blade in case of heavy load shaft in order to avoid spinning or flat bands [Takasu, 1988];
- set height so that blade tangent angles are equal to 6° or 8°, depending on grinding wheel hardness [Monzesi, 2000], with 30° blade;
- use tangent angles equal to 6° 30', 8° 30', 9° 15', 12°50' 13°30' [Mikrosa, 2005] with 30° blade;
- use 30° blade, with 12° tangent angle or for workpiece diameters less than 20 mm $h = d/2$ and for bigger than 20 mm use $h = \sqrt{1.6 * d}$ [Tsasch, 2009];
- use tangent angle equal to 7°, with 30° blades [Furukawa, 1970]
- avoid of the following combinations: $\alpha \Big/ \left(\frac{2*\pi}{UPR}\right) = N$; $(\pi - \beta) \Big/ \left(\frac{2*\pi}{UPR}\right) = N + 0.5$

  being N a natural number[27] [Rowe, 2009].

Technical notes are also furnished by machine suppliers' (see figure 3-7) in order to determine the "best height above centres" value. Based on machine manufacturer's experience, some tangent angle combinations are particularly favorable. These combinations (as in figure 3-7) are, in any case, defined for a particular blade angles. Different possible tangent angle suggestions are given based on machine size (i.e. grinding wheel, regulating wheel and workpiece diameters) and blade constrictions (e.g. small diameters cannot be machined with excessive center heights due to workblade production limitations).
Other indications (less diffused on the workshop) are stability charts, introduced in the late 60s (see figure 3-8). This chart, through the calculus of grinding gap angles and the stability index, permits to identify geometrically stable combinations of blade and tangent angle. In the chart is further reported the number of lobes geometrically most likely to occur (i.e. with lowest negative stability index).
From practical point of view, the above indications can be considered as a good starting point but cannot predict all the production behaviour of grinding wheels. For instance, it is clear that since grinding wheels and control wheels have different wear rates (e.g. 0.1 µm/part on radius for grinding wheels, 0.01 µm/part on radius for control wheels), it is possible to work with new control wheels and end-of-life grinding wheels (and vice versa).

[27] With UPR is intended the number of lobes characterizing the workpiece OD.

Based on a constant height above the centres, the variance of wheel diameters results in varying tangent angles throughout the production. Further, for longer parts, another significant deviation from an ideal constant tangent angle occurs because of regulating wheel tilt inclination (up to 2°).
Another variation source can be represented by wearing out of blade [Klocke, 2009]. In order to reduce the two latter variation, steel control wheel and PCD blade may be adopted.
Since the high number of variables involved in the proper determination of workpiece height, it appears important to consider them all, aiming to shorten setup times, limiting them to the selection of fine adjustments for machining parameters and tool testing.

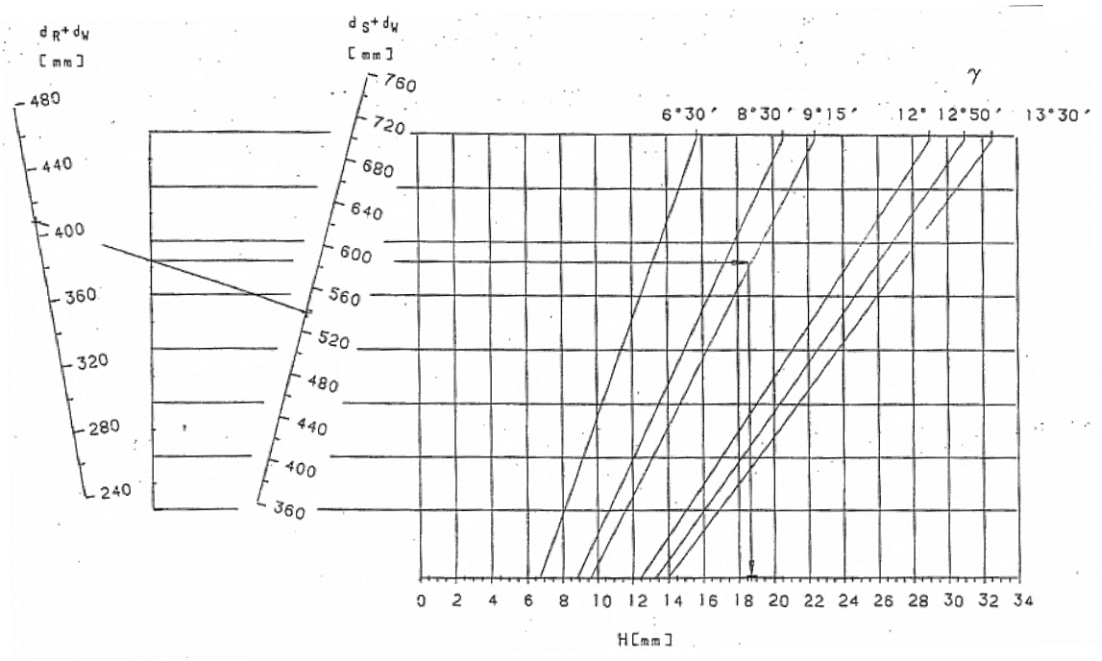

Figure 3-7 Normogram for the choice of grinding gap geometry [Mikrosa, 2005]

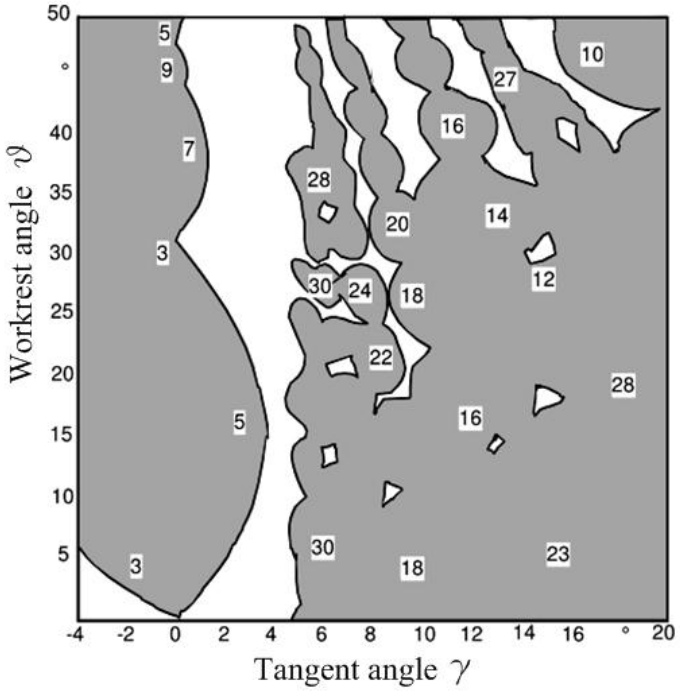

Figure 3-8 Example of Reeka's stability diagram for D_R/D_S=0.6 [Klocke, 2009]

3.4.2.4 Dressing templates

The dressing template has the function of shape reference for control wheel/grinding wheel dressing, in order to reduce the number of axis needed for wheel dressing. A feeler, held in contact with the template, gives the path to be followed by the dressing diamond.

Dressing template is the reference for the diamond slide and the precision of the contact path[28] with the dressing feeler is fundamental. In order not to have wearing out problems it has to be heat-treated, and then accurately[29] finished. Template hardness should be lower than feeler hardness in order not to damage it with a resultant deviation in the shape of the dressed wheel.

There are two main finishing systems for template manufacturing: wire-EDM and grinding. Wire-EDM is very accurate and normally can cut the whole profile in one step. Grinding finishing is more common but, for profiled shape, it is less accurate since it is usually more difficult to complete the manufacturing of the whole profile in one step only.

In figure 3-9, an example of dressing template for control wheel dressing is shown with the correspondent part to be ground and the grinding gap configuration.

[28] Parallelism and squareness between machine holding surfaces and feeler path, i.e. template profile, has to be assured

[29] Commonly tolerances are in the order of +/-0.002 mm

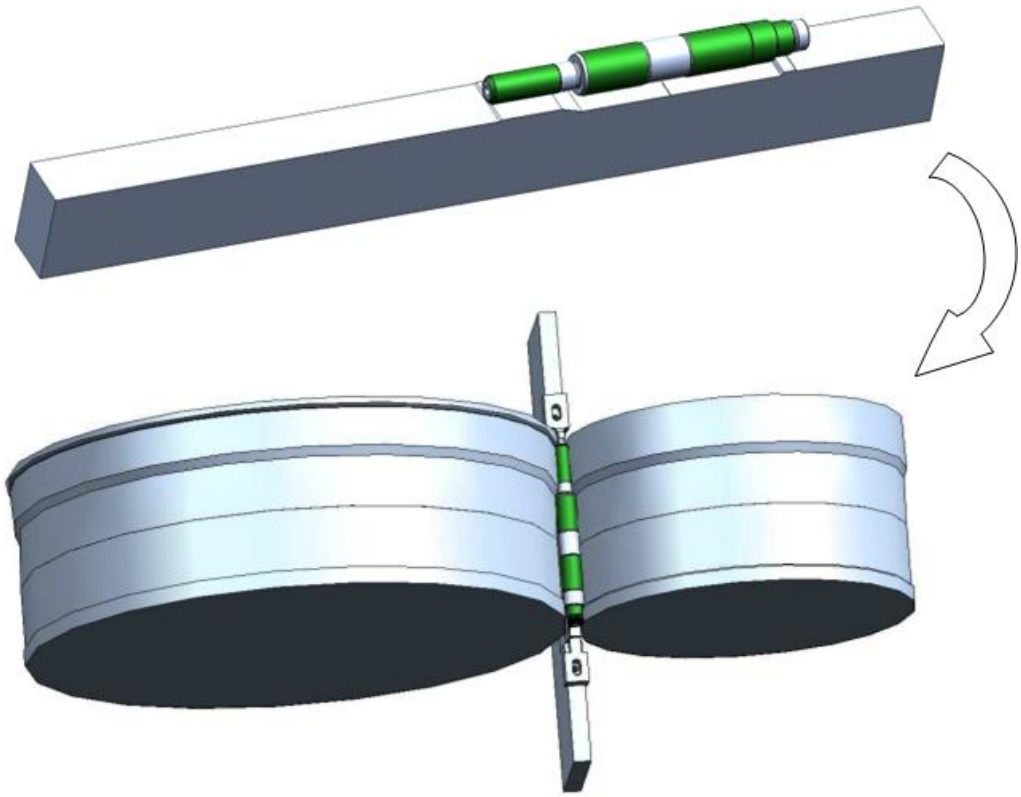

Figure 3-9 Dressing template and corresponding shape wheel in machining position

3.4.2.5 Loading of workpieces

Despite the difference in mechanical devices, the loading systems has to be strictly related to part geometry and part-holding configuration.
It has to be reminded that a bad loading or a bad loading set-up often results in workpiece loss while machining. This commonly results in blade breakage, wheels damage, axial stop breakage and, possibly, in loading devices damages. Overall costs may thus result in a cost of few thousands euro, depending on materials involved.
Hence, few good set – up rules should be, when possible, followed:

- load the part as close as possible to machining position (typically, some tenth of mm);
- avoid any possible interferences between loading and unloading movements and machining tools (provide for eventual reliefs at change-diameter shoulders);
- in case of loading with jaws, avoid excessive tightening on the part (sticking of the part to the opening jaws may occur in positioning errors);
- if possible, ease the positioning of the part through chamfers in tooling.

3.4.2.6 Dressing depth and feedrates

The dressing parameters are indeed one of the most underestimated and tricky aspects of grinding. They are commonly related just to the roughness obtained on the part, but they have strong effects on:

- cycle time
- grinding cost
- machining stability

Commonly the used parameter to determine the correctness of the infeed rate is the dressing overlap parameter U_d [Winter, 2012] [Marinescu, 2004]:

$$U_d = \frac{b_d}{f_{ad}} = \frac{b_d * n_{sd}}{v_{fad}} \quad (41)$$

where:

- b_d = diamond dresser cutting width [mm]
- f_{ad} = helix step grooved by the transverse movement of diamond on the revolving wheel [mm]
- n_{sd} = grinding wheel speed during dressing [rpm]
- v_{ad} = dressing speed [mm/min].

U_d is considered as the overlap ratio between the dresser and the grinding wheel surface; it is therefore considered as a smoothing factor of the rough grinding wheel surface.
A roughly dressed grinding wheel would give high cutting ability but worse surface roughness, a finely dressed one would give good surface characteristics but with reduced cutting action. A very smooth grinding wheel could come from worn grits, thus undergoing to higher friction action; higher friction result in higher forces on wheel bond and hence to less lasting grits (release) and lower infeed rates achievable. Indicative values for U_d parameter reported in literature [Winter, 2012] are shown in table 3-2.

Table 3-2 Suggested values for dressing overlap [Winter, 2012]

Wheel grain size	Suggested U_d max
60	4
80	6
120	8

Different overlap values may be applied in practice, depending on dressing strategy (dressing interval) and machining operation (fine finishing, finishing or roughing). In any case, the choice of low dressing speed is limited since the influence of U_d on workpiece roughness was shown to be asymptotic (figure 3-10).

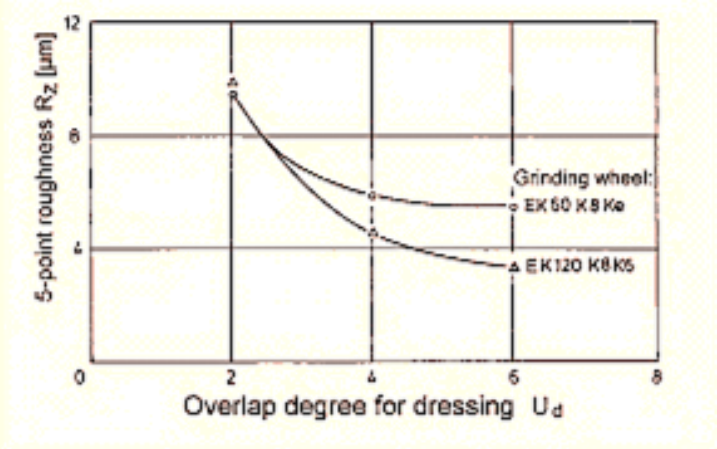

Figure 3-10 Roughness decrease against dressing overlap U_d [Winter, 2012]

Concerning the dressing depth, three main indications are usually given:

- obtaining a clean wheel surface after dressing (this is hard to be achieved, especially for long time between dressing without high pressure cleaning nozzles[30] on the grinding wheel cuff)
- setting the dressing depth according to "10 % rule" (i.e. set the dressing depth to 0.1 times the grit size in µm);
- setting the dressing depth according to indications of grinding wheel supplier (table 3-3)

Table 3-3 Example of recommended infeed [Winter, 2012]

Grit size	Recommended infeed
> 100	0.01 mm
60 →100	0.02 mm
< 60	0.03 mm

[30] The more constant the grinding wheel surface is, the stiffer the grinding process is. Very high process accuracies can be kept through the use of high-pressure cleaning of the grinding wheels and through dressing every cycle with very low dress depths.

3.5 Cycle time calculations

3.5.1 Cycle time composition

In order to reach a given cycle time the following operations have to be considered:

- loading and unloading time;
- grinding time;
- dressing time per grinding wheel;
- dressing time per control wheel

3.5.1.1 Loading and unloading time

The loading and unloading time depends upon loading system and loading cycle. Usually, the axial movement from the working position to the loading chain/belt (and way-back) are done during the machining operation (ghost time).
The loading time consists in the time between the start of unloading movement and the start of infeed cycle.
The unloading movement can be performed in two ways:

- under-the-blade unloading configuration (mostly used for heat-treated part, not with high surface quality demands);
- clamping device unloading configuration.

The unload of the part under the blade requires an additional movement of the control wheel respect to the blade position (figure 3-11). This movement has to be big enough to let the part fall.
If the control wheel is moved in a controlled manner (e.g. the control wheel is controlled by NC axis) then this movement will have a very limited time expense.
Unloading the part through a clamping device requires a precise set up in order to take the machined part correctly out of the machining zone. Further, this unloading configurations needs two additional movements compared to under-the-blade unloading: additional vertical and additional horizontal movements. The impact of latter may be different based on the loading system configuration (CN controlled, pneumatic) but can roughly be evaluated in additional 1'' cycle time.

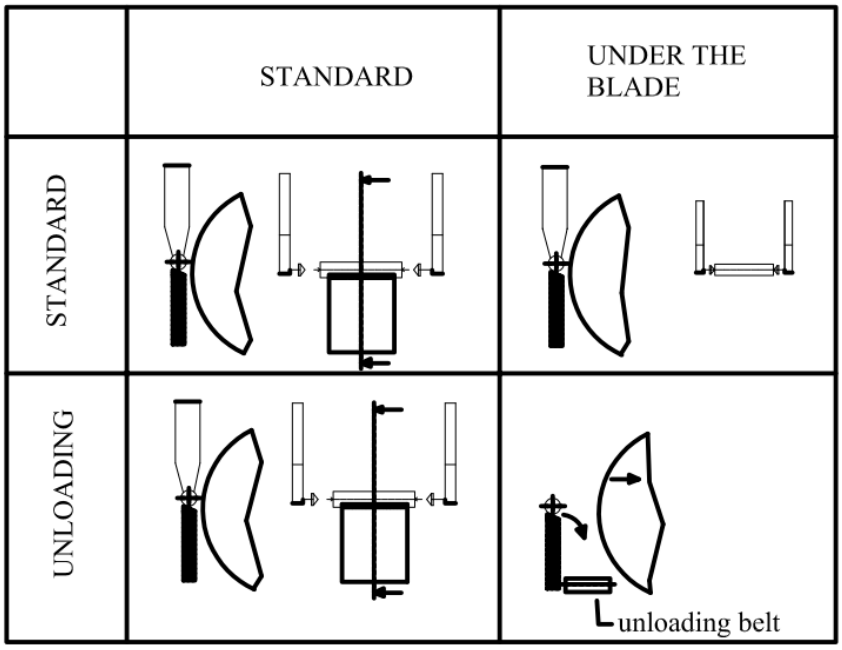

Figure 3-11 Loading and unloading configuration

3.5.1.2 Grinding time

The grinding time is the machining time, highly determined by machining parameters and by quality requirements on the part.
Since the cost and long setup times, as in most of machining processes, cycle time is an essential target of centerless grinding process.
The infeed rates can be particularly critical in case of precision grinding when narrow tolerances may be compromised by wearing out of grinding wheel and control wheel (if organic bonded).
Since forces are not only due to infeed rates but also to other kinematical variables (cutting speed, control wheel speed, lubricant, coolant rate, wheel sharpness), a used practice is to fix a cycle time as reference for experimental investigation.
Hence, cycle time has to be analysed in order to spread it in dressing time (estimating roughly part per dress and dressing speed), loading and unloading time (if known) and, finally, in grinding cycle. Ghost times (considered as time not involved in continuous production[31]) are hard to be estimated before the start of grinding test and are not commonly included in a first cycle time analysis.
The selection of infeed rates also depends on machine size (i.e. grinding a D20 with grinding wheel D400 would be harder than machining it with D600 grinding wheel) and stiffness.
The latter point should always be kept in mind in order to have better accuracy with lower cycle times.
An example of different sizes of machines are shown in table 3-4 [Bocca Malandrone].
An important parameters to be evaluate the correctness of infeed movement, is the Q_w', i.e. the rate of metal removed for linear mm of width, reported for centerless infeed grinding from table 1-1.

[31] e.g.: movement to load the first part in blade; time before the dressing starts;

$$Q_w{}' = \frac{\frac{1}{2}\,\pi\, D_w\, v_{fr}}{60000}\ \text{[mm}^3\text{/mm/s]}$$

Common Q_w'values are reported in tabel 3-5 for centerless plunge grinding [Winterthur, 2005]

Table 3-4 Typical value of $Q_w{}'$ for different machining operations [Winterthur, 2005]

Process	$Q_w{}'$ [mm^3/mm/min]
Roughing	3.5 →8
Standard	1.0 →1.5
Finishing	0.2→1.0

Other aspects concerning the centerless processes are:

- the multi stage infeed process
- the grinding wheel

In table 3-6 indications for assessing the infeed rates (through the depth of cut) are reported for steel and grey cast iron.
In centerless plunge grinding (according to table 1-1):

$$a = \frac{v_{fr}}{2 * n_w}\ \text{[mm].}$$

Table 3-5 Example of different size of machines with according tool dimensions and machinable workpieces [Bocca Malandrone]

MODELS	R 50/CF	R 90/CF		R 130/CF	
Work Diameter Range (mm)	gen-80	1-150	1-100	3-400	3-250
GRINDING WHEEL DIMENSIONS					
Max. ext. diameter (mm)	508	610	660	610	660
Min. external diameter (mm)	380	420	510	440	440
Internal Diameter (mm)	254-305	305		305	
Width (mm)	250	350		508-600	
CONTROL WHEEL DIMENSIONS					
Max. external diameter (mm))	305	305	355	355	
Min. external diameter (mm)	230	230	240	240	
Internal Diameter (mm)	152,4	152,4		127-152,4	
Width (mm)	250	350		508-600	
GENERAL FEATURES					
Cutting Speed (m/s)	33-60	33-60		33-60	
C.W.speed [rpm] (Variable)	0-300	0-300		0-300	
C.W. speed [rpm] (in dressing)	300	300		300	
G.W. Drive Motor (kW)	15-18	45-55		45-75-90-110	
C.W. Drive Motor (Nm)	10	22		42-58	
Machine Dimension (mm)	2150x3400xH2200	2200x4070xH2260		2200x4500xH2425	
Weight (kg)	8000	13000		17000	

An example of literature indicated values for different machining processes is reported in table 3-6

Table 3-6 Suggested infeed depth a (in mm) for different machining applications [Tsasch, 2009]

Machining type	Material	Cylindrical grinding			Flat grinding
		External	Internal	Recessing	
Roughing	Steel	0.02-0.04	0.01-0.03	0.002-0.02	0.03-0.1
	Grey cast iron (GG)	0.04-0.08	0.02-0.06	0.006-0.03	0.06-0.2
Finishing	Steel	0.002-0.01	0.002-0.05	0.0004-0.005	0.002-0.01
	Grey cast iron (GG)	0.004-0.02	0.004-0.01	0.001-0.006	0.004-0.02

The above values are merely indicative. A good reference is reported in [Metcut R.A., 1981].
The infeed cycle is commonly divided in different infeed steps with a final sparkout phase (figure 3-12).

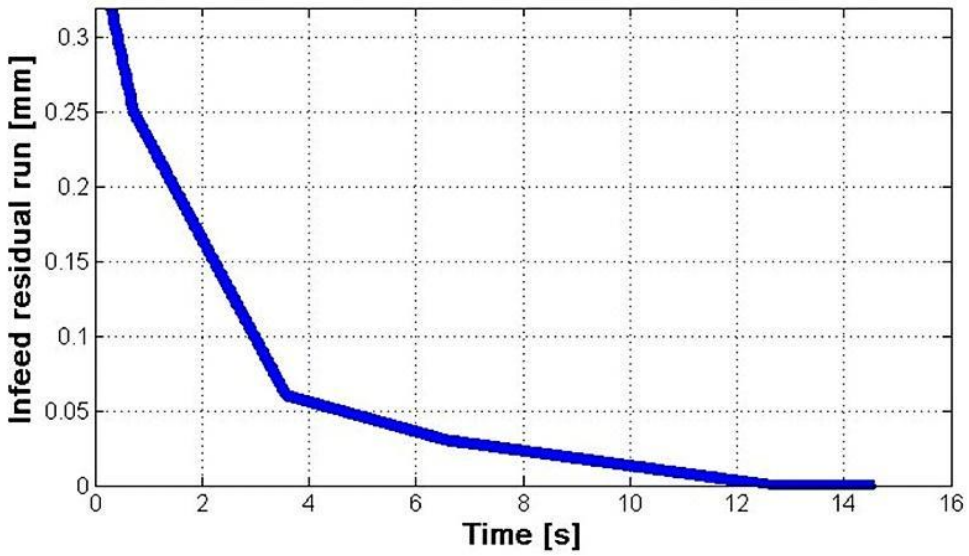

Figure 3-12 Example of infeed run

The sparkout phase is defined as a zero-infeed rate phase, aimed to recover deflections occurred during the grinding cycle. These deflections have different origin, as explained in par. 1.4
The infeed rate differences permit to have contained deflection during the whole cycle thus permitting to reduce the sparkout phase.
Theoretically speaking, the more the sparkout phase lasts the more possibilities to have blade and control wheel errors on the part. A rule of thumb from literature [Wintherthur, 2004] to calculate the sparkout phase duration is based on the number of turns the workpiece has to incur in: 4 to 5; anyway, based on author's experience, most common values of sparkout turns range between 15 to 25.

Another reason to use multistep infeed is related to incoming workpiece quality: higher depth of cut in first phases permits to reduce incoming part deviations (roundness and cilindricity) while last phases, with reduced depth of cut, give the possibility to reduce further the final error (figure 3-13)[32].
Indeed, it is important to notice that above considerations give another result: if the raw part quality is unsatisfactory, the stock removal has to be big enough to guarantee rounding and error-recovering action.

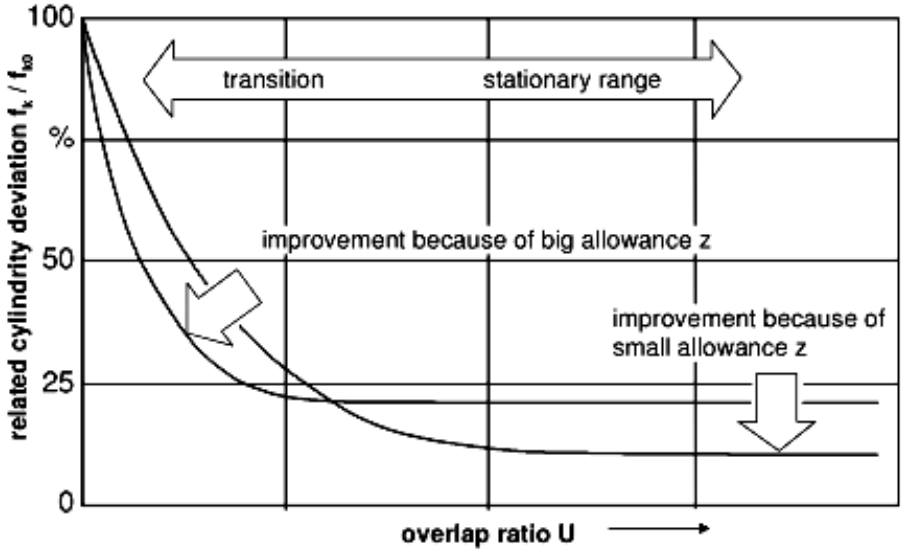

Figure 3-13 Principles of choice of multistep infeed process [Klocke, 2009]

3.5.1.3 Dressing time

Dressing is needed since the properties of the wheels (both grinding wheel and control wheel) vary as the number of cycles executed passes by.
For machining with common abrasives in standard conditions in plunge centerless grinding we may have the following phenomena:

- control wheel anomalous wearing out (shape deviation)
- grinding wheel (shape deviation)
- grinding wheel cutting ability (chatter, friction, heat)

Grinding wheel dressing time can generally be distinguished in two types, based on available configurations:

- Form roller (shaped dressing wheel), requiring just a radial plunge movement.
- CN profiling (profile disc or dressing plate) requiring higher dressing times if not done very quickly in ghost time.

[32] In figure 3-13 the overlap ratio U is a measure of the infeed rate: $U = \Omega \cdot \text{allowance}/v_{fr}$ [Klocke, 2009]

The use of a form roller have two main advantages:

- Possibility to dress in ghost time with resultant gain in cycle time;
- Robustness of grinding wheel condition.

Whilst the dressing time for the grinding wheel depends on the feed rates determined according to table 3-2, commonly used dressing speeds for control wheel are in the range of 60 to 80 mm/min.

3.6 Prevision of possible inconveniences

The loading system is crucial for the avoidance of crashes and for the correct unloading of the shape (flat planes during unloading).
Usually, not hardened parts or parts with highest quality requirements are preferred to be unloaded trough clamping devices. This can increase the floor-to-floor time due to the loading device additional movements to remove the part from the blade.
Furthermore, unloading by clamping devices has a great impact on the design of the axial stop: the latter has to allow for the raw part loading, for the finished workpiece unloading (axially positioned in a different point from the loading) and for an easy regulation in order to match possible general inaccuracies/misalignment among tools (an example of recessed axial stop mounted on blade with one loading harm in loading/unloading position is shown in figure 3-14).
It has to be reminded that jaws should clamp the part in the most reliable way: to do this, if possible, it is better to design the clamping system based on the highest accuracies given in the raw part (e.g center-hole or chamfer).

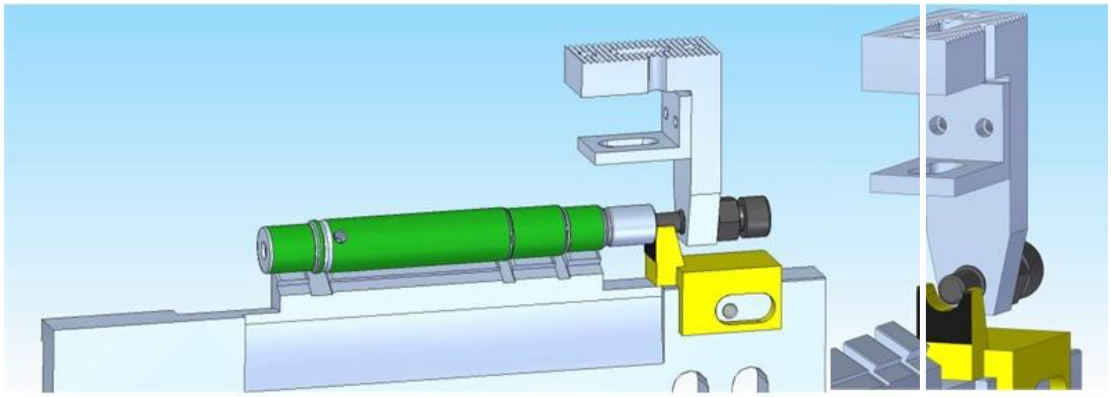

Figure 3-14 Example of jaw in loading position and workpiece stop (detail on the right)

3.7 Troubleshooting

It is often useful to have main troubleshooting principles ready to solve possible inconveniences occurring in common practice, both in case of new process development and in case of an unexpected change in ongoing process (e.g. due, for example, to a changed behaviour after a new grinding wheel mounting).
Most useful suggestions (independent of possible workpiece particularities) are reported in table 3-7.

Table 3-7 Troubleshooting table

What	Why (possible causes)?	What to do:
Wheel is not cutting properly	Abrasive unsuitable to the working material	Change the wheel to a softer and coarser one and eventually change abrasive to a sharper one
	Wheel too hard	Increase workpiece speed, if possible
	Wheel too fine	
	Pheripheral speed too low	Increasse cutting speed
Burns or warming up of the workpiece	Unsuitable feed	Reduce feed
	Too large contact area with inadeguate coolant	Check oil ratio, direction and flow rate of coolant
	Unproper diamond dressing	Check infeed,transeverse, size and diamond quality
Quick wearing out of grinding wheel	Wheel too soft	Change wheel to an harder or denser one
	Pheripheral speed too low	Increase cutting speed
	Diamond infeed too high or too slow	Reduce dressing infeed
Wheel loading and glazing	Wheel too hard or not open enough	Change wheel spec to wider and softer one
	Unsuitable abrasive type	Change wheel spec to a sharper abrasive
	Not enough cooling action	Increase cooling and check oil-water ratio
Roughness too high	Too soft wheel	Increase cutting speed
Profile variability	Wheel too soft	Change the wheel to an harder one or to a finer or to a denser one
	Infeed too high	
	Unsuitable bond	
Irregular surfaces (comma-like scratches)	Abrasive grains in the coolant	Check coolant filtration and change it, if needed
		Clean wheel guard
		Clean the machine
Chatter marks	Wheel not balanced	Rebalance the wheel and pay attention to drying it; use a steady rest
	Outside source of vibration	Remove source of vibration or move the machine
	"q value" too low	Check the "*q*" ratio according to best practice values
Burning marks (overheating)	Insufficient or incorrect coolant supply	Increase dressing speed
	Wheel too finely dressed	Increase coolant supply (or speed)

	Wheel too hard	Use softer grinding wheel
		Reduce removal rate
Grinding with angular marks (spiral marks)	Marks due to excessive dressing speed transferred to the part	Reduce the dressing speed
		Always dress the wheel from one direction
Poor size holding	Conicity of the part	Not parallell axes
		Control wheel too soft
		Control wheel diamond not cutting
		Grinding wheel diamond not cutting
Bad roundness quality	Raw part quality	Excessive roundness or runout on raw part
		Non uniform stock allowance on raw part
	Infeed speed	Eccessive infeed speed
	Tooling/set up	Blade too thin
		Wrong blade position
		Grinding wheel too soft/too hard
Spinning	Excessively low friction of the regulating wheel	Increase control wheel holding surfaces
		Change grinding wheel to a sharper one
		Increase control wheel dressing speed
		Increase blade angle

3.8 Conclusions

In this chapter the main issues about practical plunge centerless grinding are critically analyzed, based on author's workshop experience, highlighting the following:

- Different machine design concepts have an impact on workpiece feasibility and on process source of variance. Tool tolerance may influence machining process feasibility too.

- The relationship between workpiece features (radii), workpiece roughness and allowance is given through the use data available in literature. Proper removal rate, depth of cut and dressing thumb rules are reported.

- The main aspects of blade and template design are given with suggestions for avoidance of inconveniences. Practical rules for the set-up of workpiece height from machine builder's and scientific literature are reported.

- The analysis of cycle time components (machining cycle time, loading, dressing time) is carried out with attention on available technologies.

- Main tips and troubleshooting for grinding and centerless grinding are reported.

4 Process analysis tool

4.1 Premises

After having examined the characteristic of the main features entering the centerless loop and grinding dynamics, it is necessary to consider the system possibilities of variation from a possible steady situation.
In order to assess the latter, a review of different aspects involved in the centerless process should be carried out. Anyway, in terms of quality issues, only few of the system characteristics are critical and the necessity of monitoring them will be dependent on their possibility to affect workpiece quality.
The main features commonly desired from a centerless grinding production process are:

- Roundness and cilindricity (taper).
- Roughness.
- Size holding characteristics.

Mass production processes have narrow requirements in terms of process performance, usually expressed in terms of C_p and P_p[33]. These requirements concern the process capacity of giving a good and stable results during a production stint long enough[34] to be considered representative of the production processes and, hence, to be representative of its outputs variances.
The built-up of a mass production process includes five main levels:

- Process and tool design.
- Tool gathering.
- Setting up of the machine, production of parts and meet of capabilities requirements.
- Serial production with reinforced process control.
- Serial production, process control and further process optimization.

Based on project requirements, the process and tool design is the sum of practical and theoretical aspects reported in chapter 2 and 3.
From the raw part to one single finished product conforming the required quality standards, a number of process features have to be satisfied. These include proper grinding and regulating wheel selection, proper coolant flow rate, proper wheel speed and others. The main steps of process design development and involved variables are

[33] C_p = Process Capability; Pp = Process Performance.
[34] The length of the investigation stint is usually determined based on defined standards.

shown in figure 4-1. In the first phase of production process ("ramp-up phase"), there is the need of testing the reliability of the process to overcome production issues such, for instance, a grinding wheel change. In conclusion, a process optimization phase aims to reduce costs and solve minor issues arisen during the ramp-up phase.
The present chapter deals with the following:

- over the whole process, from the process and tool design to the process optimization, there is a need of comparing different parameter selections with the aim of evaluating different process solutions in a quick and handle manner, avoiding the commonly adopted trial-and-error approach ("Cycle design").

- over the whole process life, tool wear occurs and, hence, the grinding gap angles are subjected to variations; consequently, also UPR stability indexes vary (see eq. (9)): there is a need of evaluating the amplitude of this change, considering this as an inherent variation of centerless grinding geometrical stability and modifying existent tools to consider this aspect (Geometrical uncertainty))

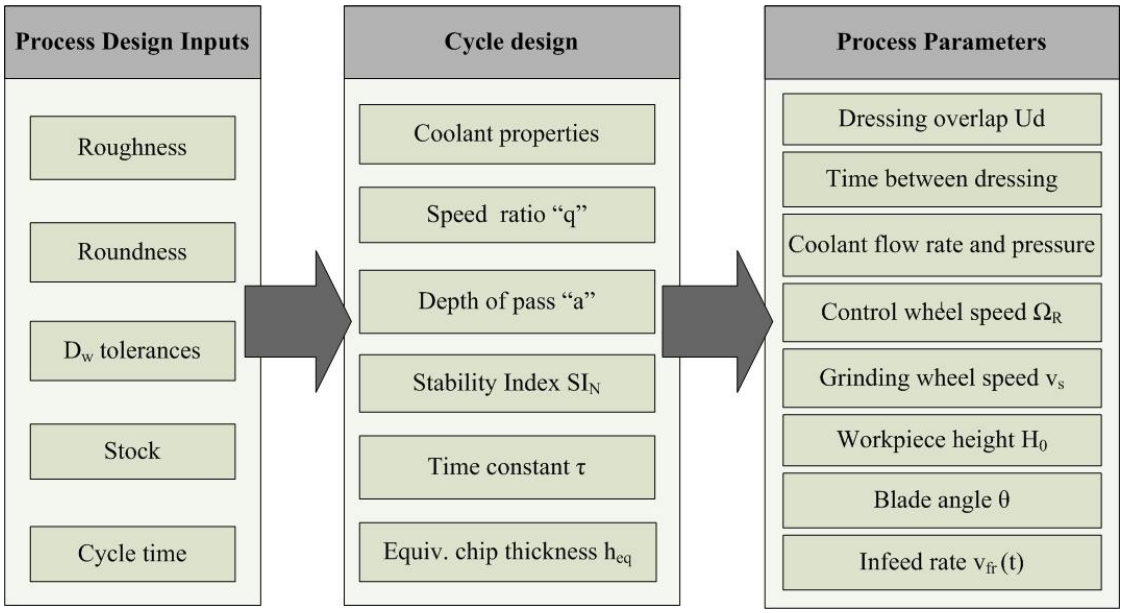

Figure 4-1 Process development phases

4.2 Geometrical uncertainty

The centerless grinding process and its stability analysis are based on angles. The whole stability of the centerless loop do include geometrical and dynamic effects. As seen in par. 1.4.9, the dynamic effects study include modal analysis and contact stiffness's study. These aspects are not easy to be evaluated precisely without a deep and time-consuming experimental analysis and, in any case, cannot be considered before the start of grinding trials. Hence, dynamic evaluations do not match the quickness and ease of use required in first process building-up steps. The focus of this paragraph concerns the possibility of avoiding geometrical stability issues due to predictable geometrical variations.
Considering the common grinding applications, conventional abrasives grinding wheel and organic bonded control wheels will wear significantly and, hence,

dimensional change during the whole grinding process will occurr. For instance, one new grinding wheel may be used roughly down to 70% of its starting diameter.
Another fact to be considered is the regulating wheel tilting angle α_r. This inclination, necessary to guarantee the correct axial positioning of the workpiece, results in a difference of control wheel diameter along the control wheel length. Hence, based on the amplitude of control wheel active length and of the value of α_r, geometric variations can be significant or neglect able.
The impact of the cited uncertainties is illustrated on the base of a normogram for the selection of proper workpiece centre height (figure 4-3, [Monzesi,2000])

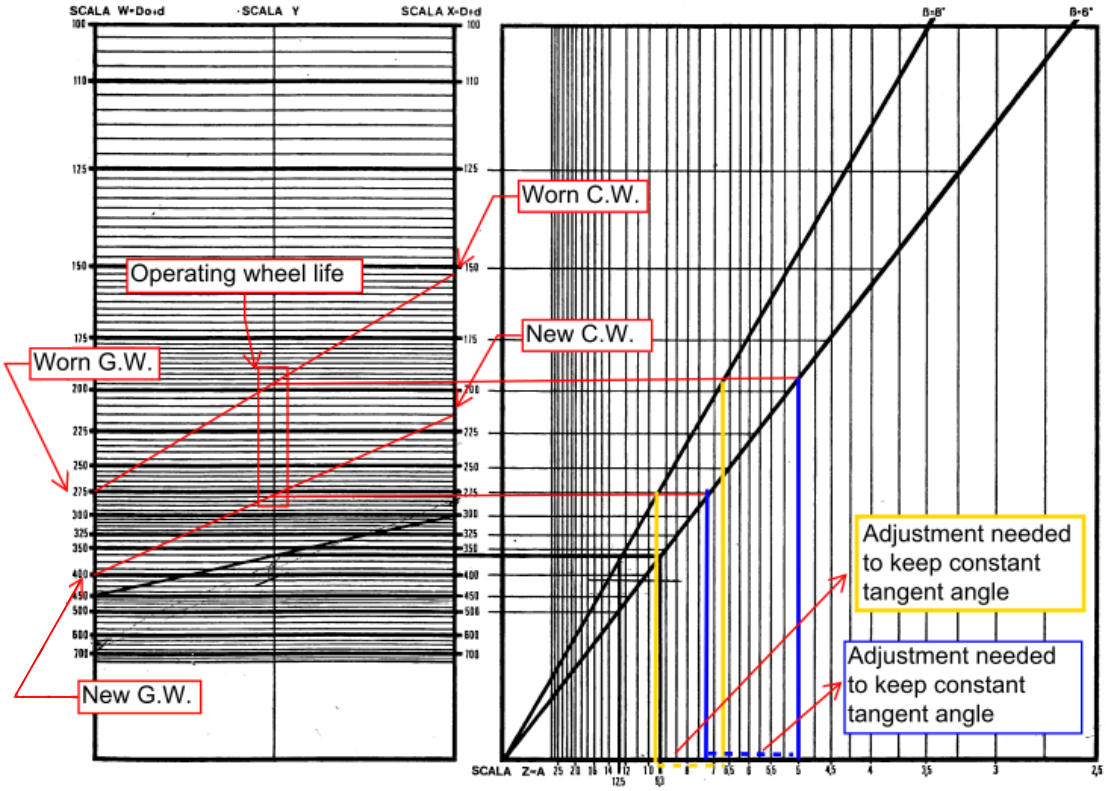

Figure 4-2 Example of uncertainties in blade height setting due to geometrical variations[35]

Briefly, when setting up the process, the geometrical analysis has to consider the following aspects:

- Control wheel wear.
- Grinding wheel wear.

[35] Applying the normogram, from the use of the left input line (titled "SCALA W =D_0+d", where "D_0" is the grinding wheel diameter and "d" is the workpiece diameter) and of the right input line (titled "SCALA X =D+d", where "D" is the control wheel diameter and "d" is the workpiece diameter), it is clearly understandable, from the range resulting in "SCALA Y" – line, the uncertainty in the choice of the best workpiece center height caused by the varying dimensions of control and grinding wheel. Similarly, in order to keep the tangent angle constant over the whole consumption of the wheels, a constant height adjustment should be needed. For example, for a GW diameter varying between 390 e 265 mm, a CW diameter between 205 e 140, in order to grind a 10 mm part at a constant β= 6° tangent angle, roughly 3.5 mm height should be carried out.

- Control wheel tilting angle (especially relevant for long parts).

4.2.1 Geometrical analysis charts

Geometrical stability study details are reported in par. 1.4.8.
Commonly, the use of geometrical stability charts gives information about lobing stability. The use of these charts aims at the proper selection of grinding gap configuration. This configuration consists in selecting the blade angle θ and center height angle γ.
These charts may provide qualitative indications about the stability index of a grinding gap geometry (see figure 4-3) and/or the lobing order more prone to occur in the roundness error, based on geometrical considerations. Qualitative accordance between stability index (par. 1.4.8) has been shown in literature and the order of lobes investigated is commonly limited for practical reasons to 30 lobes [Krajnik, 2008]. Theoretically speaking, the maximum lobe order should be determined by the filtering effect due to contact widths. In author's experience, with conventional abrasives, the lobing interest is limited up to 16 lobes. Hence, the interest in knowing stability attitude for each lobe finds its reason in the awareness of which instabilities will be more likely to occurr. For particular cases with several machining phases carried by centerless grinding, it may be of interest to tune the machine on different lobing orders, in order to facilitate the removal of the roundness error.

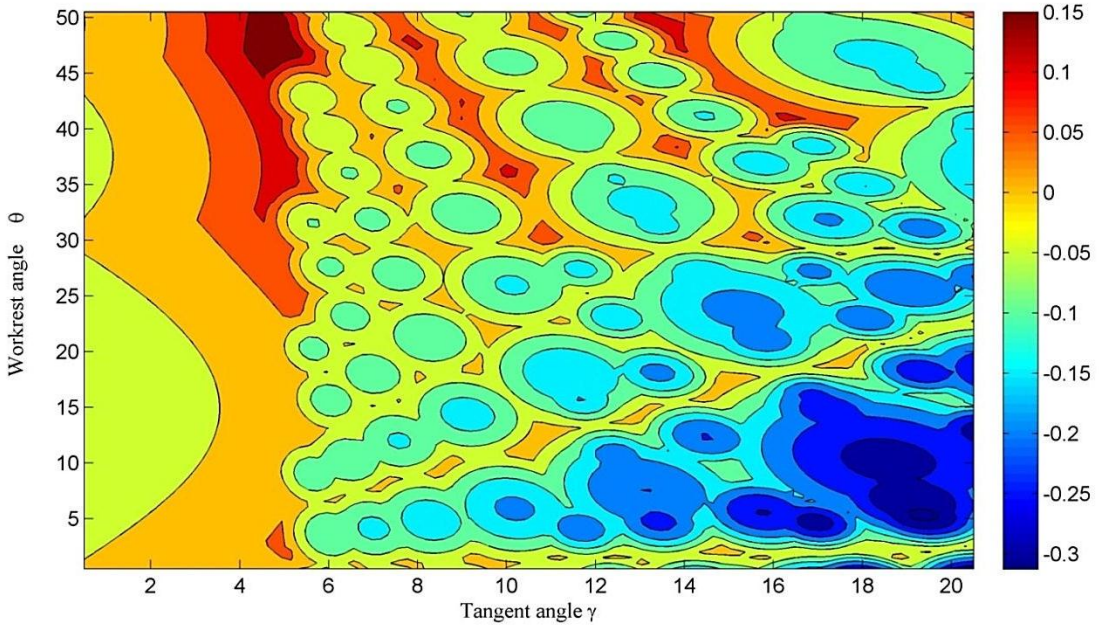

Figure 4-3 Example of Stability chart for Dr/Ds=0.6, blade angle =30 deg., N_{max}=30 lobes[36].

The task of the chapter analysis concerns the determination of stiff stability charts, thus finding set-up condition to keep the process geometrically stable without any

[36] This stability charts explains, for a determined set of geometrical feature of the grinding gap (i.e. ratio D_r/D_s , blade angle θ) which is the minimum of the geometrical stability indexes for the number of lobes investigated in centerless grinding a small amount of geometrical instability can be admitted, due to limited growth possibility (short machining times); hence, it is indeed of interest to investigate the amplitude of the instability.

care of tool consumption. The wrong choice of grinding gap configuration may be due to the variance in stability charts: different diameters move stability charts contours in a relevant manner. An example of overlapping of different stability charts considering the maximum and minimum grinding and control wheel diameters is shown in figure 4-4.
In any case, for short processes (i.e. small wheel consumption between set-up and end of production typical of small production campaign) an optimal set of stability indexes could be effective whilst another one for product dedicated machines is needed (long term campaigns involving end of life diameters for both control and grinding wheels).
The other aspects involved in determination of possible variations in geometrical stability due to geometrical issues concern the tilting angle α_r contribution. The control wheel tilt produces a variation in the center heigth of the control wheel and a concurrent variation of the cylindrical shape of the regulating wheel[37]. This tilting angle effect, considered in throughfeed processes[38], is usually neglected in infeed processes. Anyway, for long shaft or multistepped shaft, the tilting angle has to be considered[39], due to its contribution.

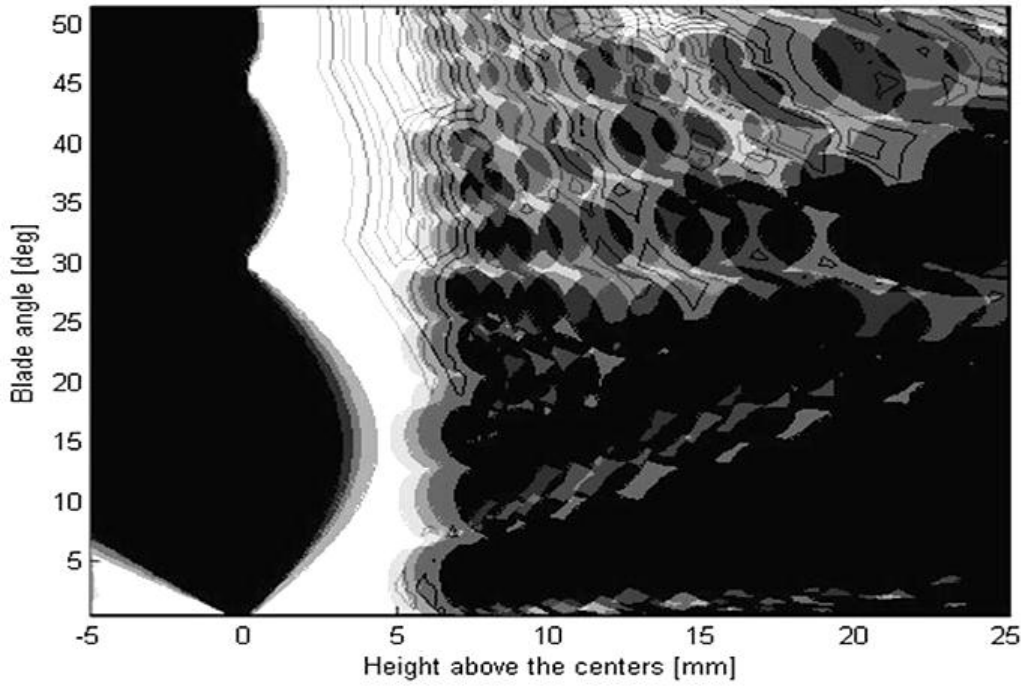

Figure 4-4 Example of overlapping stability charts for D_w=10 mm, $D_{s\ max}$=410 mm, $D_{s\ min}$= 350 mm, $D_{r\ max}$= 203 mm, $D_{r\ min}$=170 mm; maximum number of lobe analyzed =30[40].

[37] This regulating wheel shape variation is normally carried out by proper dressing adjustments (for instance [Cincinnati ,1981] or may result by the independence of regulating wheel dressing slide and the dressing slide.
[38] Through feed process common tilt angles range from 2° to 4°.
[39] In an infeed operation of a straight 100 mm-long shaft, with a 0.8° tilting angle, the height difference between the two control wheel ends is about 1.4 mm.
[40] The present chart shows the geometrical stability boundaries, with physical accordance to process behavior (i.e. with constant center height and blade angle but with varying combinations of wheel diameters): for 4 given combinations of control and grinding wheel diameters ($D_{s\ max}$- $D_{r\ min}$, $D_{s\ min}$- D_r

Hence a tool has been developed to overcome these aspects giving robust geometrical stability indications.
The effect of tilting the control wheel by an angle α_R on β_R and D_r , is analyzed according to figure 4-5 and figure 4-6.
The analysis is carried out considering the control wheel section, normal to the contact line, as a circle (i.e. the difference between circle and ellipse was neglected). This was done in order to find the contact point between the control wheel and the part along the connecting line between their centers, thus allowing for an easy calculus of the correct tilted control wheel radii.
Let z_w be the axial workpiece coordinate, with its origin in one of the workpiece end faces. The control wheel is tilted by an angle α_R about a focus located at an axial length $z_w = L_{center}$. This tilt causes the locus of RW centers along the workpiece axis to shift up or down, of an amplitude proportional to the axial position ($z_w - L_{center}$) respect to the rotation pivot.

$_{min}$, $D_{s\,max}$- $D_{r\,max}$, $D_{s\,min}$- $D_{r\,max}$) the obtained stability charts are obtained and overlapped in terms of geometrical stability boundaries. It is evident the reduction in the stability boundary due to variations in GW and CW diameters.

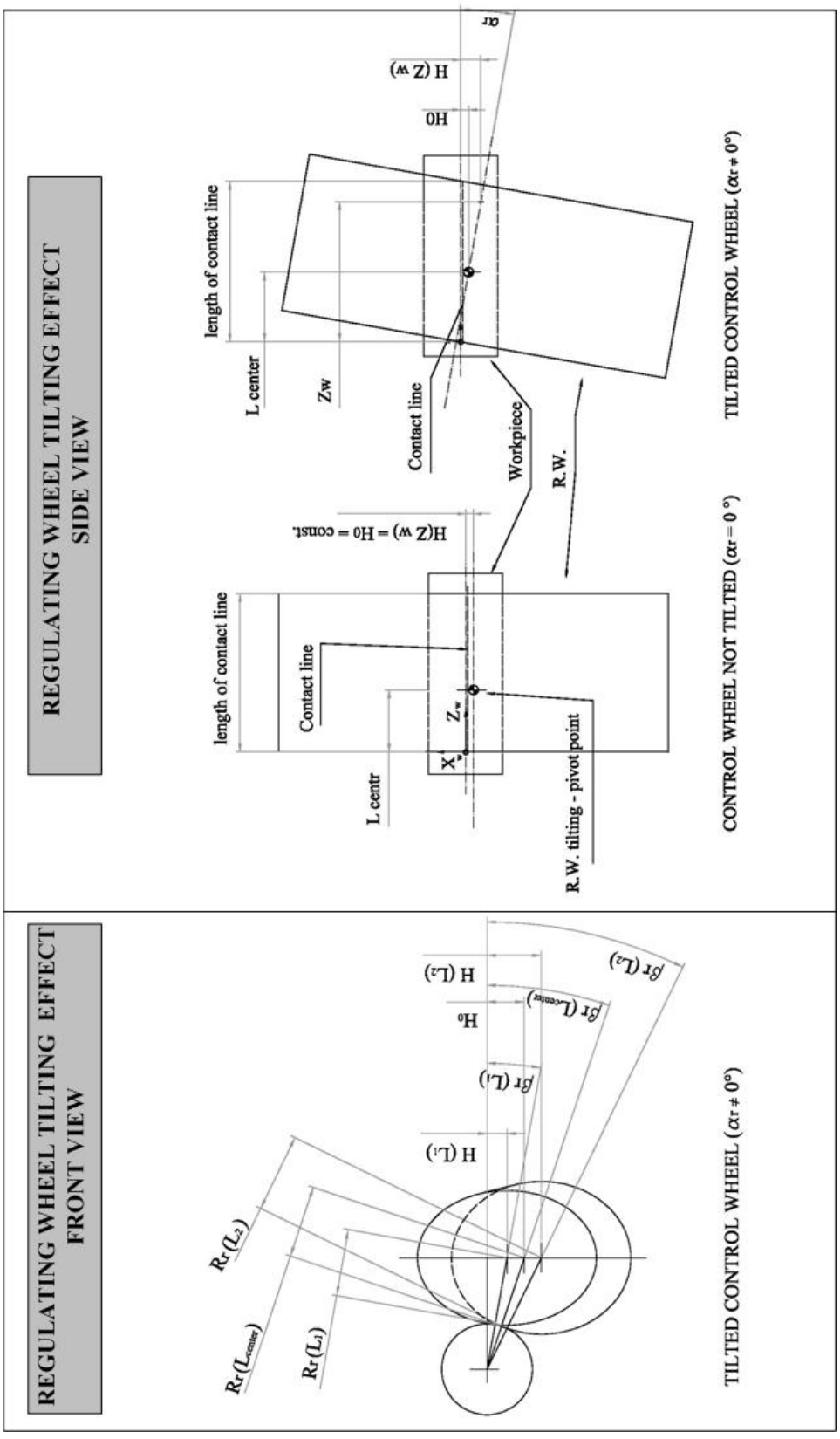

Figure 4-5 Deviation in contact geometries (H, β) along the workpiece axial coordinate z_w due to the tilt angle α_r of the control wheel in $z_w = L_{center}$ (not in scale)

Because of this shift, the RW centers at each workpiece axial section are updated ($O_r(z_w)$) and, consequently, the new RW radii ($R_r(z_w)$) are calculated. Finally, new characteristic angles are assessed, varying over the whole workpiece axial length.
The updated radius for the control wheel due to the control wheel incliunation is given by the following equation:

$$R_R(z_w) = \left\{[-H_0 + (L(z_w) - L_{center}) \cdot \tan\alpha_r]^2 + \left(-H_0/\tan\beta_{R_{@\ Zw=L\ center}}\right)^2\right\}^{0.5} - R_w \quad (42)$$

Form the assessed radius, it is trivial to calculate the updated grinding gap angles as a function of the axial coordinate and the
The analysis is repeated for all the possible combinations of grinding wheel and control wheel diameter, varying based on wear, in different rates.
The structure for the robust analysis of geometrical stability, considering tilting angle as well as the wear of the tool diameters, is shown in figure 4-6.

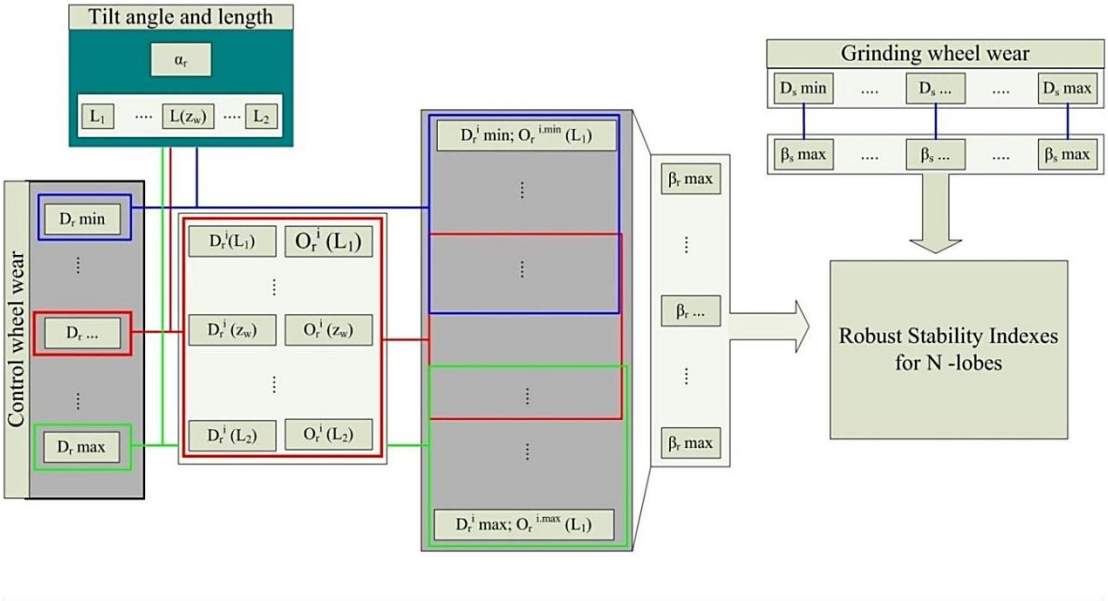

Figure 4-6 Structure for the determination of robust stability index

After having assessed the corrections to control wheel diameters and angles, with corrections given to grinding wheel angles as well, and after having considered the full life of control and grinding wheel as well, stability indexes have been calculated for each workpiece section, for each UPR.
Hence, stability indexes are evaluated and their range expressed in a robust geometrical stability chart, as shown in figure 4-7.

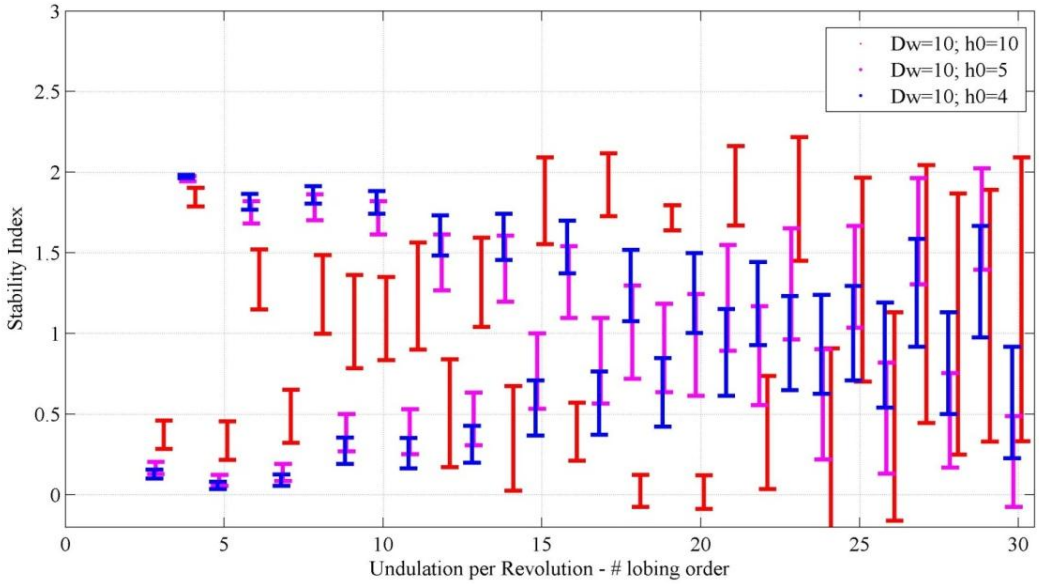

Figure 4-7 Example of output of robust geometrical analysis tool, α_r=0.8 deg, L_{center} =65, L_{min} =10; L_{max}=35 mm with different set heights upon the centers for a D_w = 10 mm.

From comparison of robust stability charts, the evaluation of stability indexes over the whole grinding wheel lifecycle can be assessed for different workpiece height at the same time.
The example in figure 4-7 shows a typical example of centerless grinding process, known to be particularly tedious for low order odd lobes (3, 5, 7, 9, 11, 12).
The tool results show accordance with the main set up trends of centre height adjustment based on lobes order resulting on the machined workpiece.
From the analysis, it is possible to come to the following conclusions:

- The effect of geometrical variations due to gap and grinding angels has to be considered over the whole wheel life

- Higher order lobes are sensitive to geometric set up angle variation and, hence, to tool variation processes.

4.3 Infeed rate evaluation

Infeed rate selection is a process based on project cycle time. As written in par. 3.5, cycle time is sum of machining time and auxiliary time, including dressing and loading. After a first estimate of fixed auxiliary and dressing time impacts on single cycle time, it is possible to have a first estimate of cycle infeed time.
Once the cycle time is fixed, the infeed rate can be evaluated.
The infeed rate $v_{fr}(t)$ is roughly divided in three parts: spark-in, grinding cycle, sparkout.

4.3.1 Spark-in phase

The spark-in feed rate[41] may be limited by the following:

- Upper critical tangential force f_U (eq. (8), par. 1.4.7).
- Available spindle power.
- Flat bands (par. 1.4.7).

Commonly the spark-in time is fixed to cover the 50% of the infeed cycle plus a safety gap (to overcome the possibility of incurring in defective raw parts).

4.3.2 Spark-out phase

The spark-out phase is governed by a system time constant, i.e. the time constant describing the system compliance and its capacity of recover deflections trough machining action. During this phase the actual depth of cut, defined in eq.(14) par. 1.4.6, diminishes at every j^{th} half-revolution turn according to a geometrical progression, as [Rowe, 1973]:

$$a_{e_j} = \frac{a_{e_{j-1}}}{1 + \frac{K_{eq}}{K_s}} = \frac{a_{e_p}}{\left(1 + \frac{K_{eq}}{K_s}\right)^p} \qquad (43)$$

where K_s and K_{eq} are stiffness properties of the machining system (par. 1.4.8).
Since the difficulties in the determination of correct system stiffness (par. 2.5) and the need of precise values for the characterization of the sparkout duration, it is necessary to characterize the system behaviour experimentally (par. 5.4.2), in two possible ways:

- Measurement of the stiffness ratio K_{eq}/K_s [Gallego, 2007] [Rowe, 1973].
- Measurement of the system time constant τ.

The measurement of the stiffness ratio K_{eq}/K_s can be carried out in a rough way, measuring two workpieces, produced with and without the spark-out phase. Known the number of spark-out revolutions, from eq. (43) the evaluation will be feasible. During the sparkout, the system power[42] (in first approximation proportional to

[41] The spark-in is not a proper cycle phase. The spark-in is the first phase of machining, in which the workpice begins to be machined. Since centerless grinding is a space-defined process, the spark-in phase is here considered as the first machining step after high speed loading movements, i.e. the first in which it is possible to have the beginning of the stock removal action.
[42] Theoretically, any other physical quantity proportional to the real depth of cut could match the task. Anyway, grinding wheel spindle power measurement is particularly prone due to its ease of application.

cutting power) can be approximated by the following [Allanson, 1997][Cheng, 2009]:

$$P(t) = P_o * e^{-(t-t_0)/\tau} \quad (44)$$

where:

- P_0 is the power at the beginning of the sparkout phase.
- t_0 is the time coordinate at the beginning of the sparkout phase.
- τ is the system time constant.

The sparkout is commonly determined to be 3 τ long [Cheng, 2009]. This length is based on measured system constants; other suggested rules of thumb from literature ask for 4 to 5 sparkout workpiece turns (par. 3.5.1.2). The correct length of the sparkout phase is fundamental in order to have stable diameters; otherwise, the final part dimensions result to be determined by the equilibrium of machining and system deflections, dependent on the precision of the raw part (i.e. of the built up of deflections in the grinding system).

4.3.3 Grinding cycle

Keeping constant cycle time, there may be different ways to adjust multi-infeed processes and to adjust infeed rates. The main issues about a multi-infeed-rate cycle are reported in par. 3.5.1. The choice of infeed rate (and eventually the comparison between different alternatives) has to consider the effects on system forces and, hence, deflections. Further, infeed forces are responsible for the wearing out of tools (i.e. grinding wheel and control wheel).
Indeed the reduction of cycle time is a primary task for the process; anyway, it has to be remembered that cycle time should not harm production efficiency and capabilities.
With the aim of comparing different cycle designs and their effects on system properties, a tool has been developed.

4.3.4 Cycle evaluation tool

A tool has been developed in order to consider all the possible parameters, starting from cycle time typical parameters and kinematical parameter.
First, from machine parameters it is verified the correctness of phase values, based on commonly accepted values for the amount of specific stock removal per unit of time Q'_w (par. 1.3), the equivalent chip thickness h_{eq} (par. 2.2.1), speed ratio q (par. 2.2.1), the sparkout revolutions and percentage of machining time given to all the sub-phases.
Lately, based on system time constant (in case of data unavailability, a rough value can be considered) the reduction of real workpiece diameter is plotted against the residual infeed run, in order to evaluate if proposed infeed rates fit the machining system resulting in a stiff process. The process stiffness, here intended as a process dimensionally stable on diameter, is arbitrary considered to be reached once the

actual diameter reduction has entered by two thirds the upper limit tolerance line (UTL) (figure 4-8).

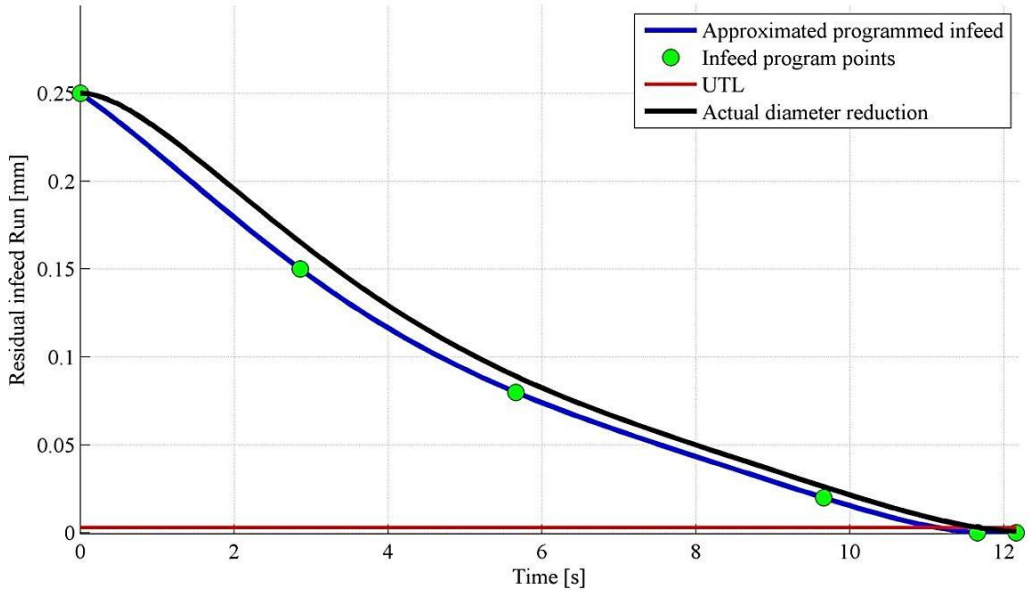

Figure 4-8 Example of machining infeed programmed rates and calculated actual diameter reduction

This tool permits, further, to consider possible variations in the system stability ratio due, for instance, to uncertainty in the time constant[43] (figure 4.9).
The following equations are applied, in similar manner to cylindrical plunge grinding [Malkin, 2008] [Cheng, 2009]:

$$V_f(t) + \frac{\partial D_w(t)}{\partial t} = \frac{\partial \Delta_{r_w}(t)}{\partial t} \qquad (45)$$

Where :

- $\Delta_{r_w}(t)$ is the machining system deflection (eq. 20 par. 1.4.9);
- $V_f(t)$ is the infeed rate.
- K_{eq} is the system equivalent stiffness (eq. 29 par. 1.4.9);

[43] Time constant variations may occur due to short term variance (few parts repetition analysis) and long term variance (time between dressing). This is done in order to evaluate cutting behavior variation due to cutting edge wear. For further detail, refer to par. 5.4.2.

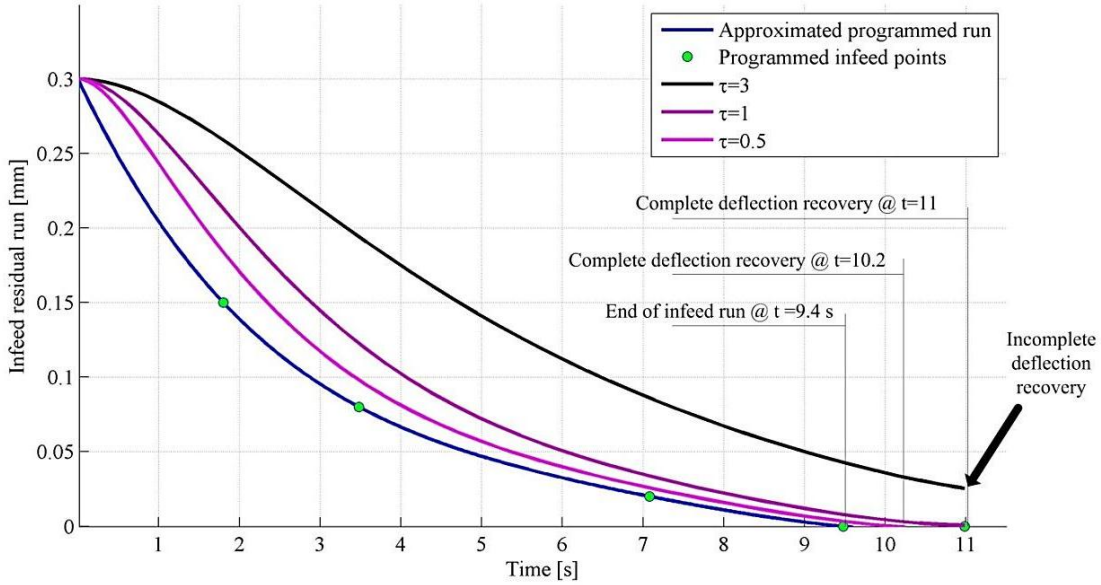

Figure 4-9 Effects of different system time constants on workpiece diameter

Applying the equivalent chip thickness definition for the evaluation of F_n , using the a_e for the centerless infeed machining (table 1-1) and re-arranging[44]:

$$\frac{d\left(\frac{F_n(t)}{K_{eq}}\right)}{dt} = \frac{1}{K_{eq}} * \frac{\partial(k_s * \frac{v_w}{v_s} * a_e(t))}{\partial t} = \frac{k_s}{K_{eq}} * \frac{v_w}{v_s} * \frac{1}{2 * n_w}\left(-\frac{\partial^2 D_w(t)}{\partial t^2}\right) \quad (46)$$

Hence, eq. (45) can be rearranged to:

$$V_f(t) = -\frac{\partial D_w(t)}{\partial t} - \tau\left(-\frac{\partial^2 D_w(t)}{\partial t^2}\right) \quad (47)$$

Equation (47) describes the evolution of the real diameter during the machining process and, hence, its behaviour during the sparkout phase.
The system time constant τ is expressed as:

$$\tau = \frac{k_s{}'}{K_{eq}} * \frac{\pi * D_w}{2 * v_s} \quad (48)$$

Hence, based on equivalent chip thickness force model, system time constant results to be not depending on workpiece speed.
The working environment for the analysis of diameter development was Mathworks Matlab.

[44] For the sake of simplicity the v_w has been considered to be constant (e.g. in common machining processes the variation of the v_w associated with the reduction in D_w is considered to be around 1%).

Based on machine programmed infeed rate, a Lagrange polynominal approximation method had been applied to have a 2nd grade-continuous infeed rate law.
The solver used was the Matlab built-in ode45 solver, based on Runge Kutta method.

4.3.4.1 Tool validation

In order to verify the predictability of the system model and of the time system expression, two experimental campaign had been carried out:

- Application to a system with two different time constant with low sparkout duration.
- Measurement of system time constant.

Concerning the first point, measurement variability found a good qualitatively result with predictions, finding a correspondence between the lack of dimensional stability and the lack of sparkout time, related to the particular system time constant. This phenomenon, well known on the production lines with short cycle time machining operations, is shown in figure 4-9, i.e. systems with longer cycle time constant cannot cope with small tolerances and short sparkouts.
In this case, workpieces from the same batch (plungers, 100Cr6, hardened) were machined with two different grinding wheels, whose system time constants had previously been measured.
The multistepped infeed cycle did not change nor other parameters changed, except the grinding wheel specification.
The difference in grinding wheel cutting behavior caused a difference in the system time constant. This difference in system time constant (likely to occur due a difference in grinding wheel cutting stiffness), did not allow one of the two grinding wheels to recover elastic deflections in a satisfying manner (insufficient sparkout duration).

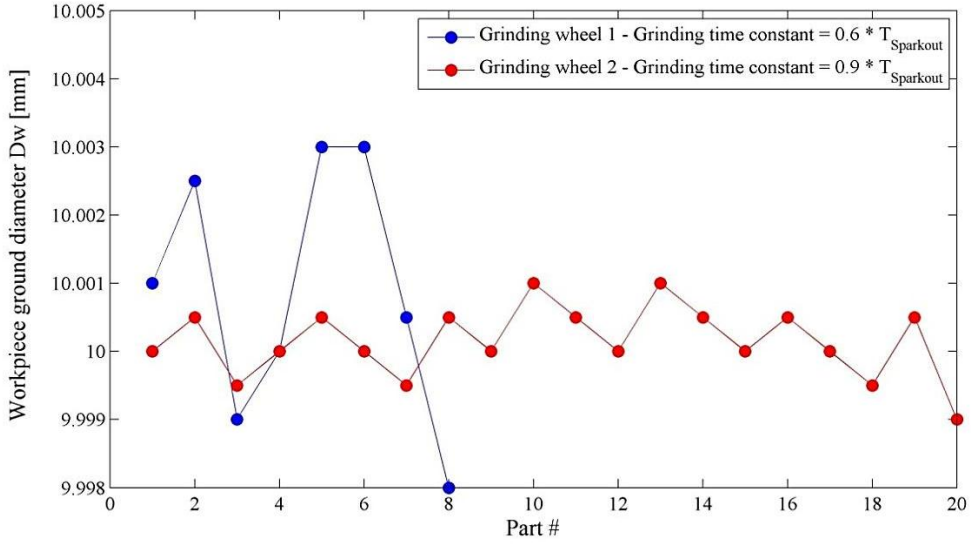

Figure 4-9 Ground diameter variances due to insufficient sparkout last[45]

[45] Grinding wheel specification: 1) SC 180 grit size; 2) SG Al_2O_3, 120 grit size. The infeed cycle is multistepped, so short sparkout could be used.

The measurement of system time constants dependency on kinematic parameters has been investigated in par. 5.4.2.

4.4 Conclusions

In the present chapter , a tool was developed in order to support kinematical parameter assessment and set up geometries for the complete design of new centerless grinding cycle, incorporating main features and practical rules given in previous chapters. The tool aims to be of help for the assessment of set up conditions and grinding cycle in an easy and handle way prior to the start of production. It consists of two innovative aspects:

- The development of a robust geometrical stability charts, taking in consideration the whole combinations of wheel dimensions and angle. This means considering the different wearing out rates of wheels and the variation of control wheel dimension along its axis length due to its tilting inclination.

- The cycle evaluation tool permits to compare different cycle infeeds, with a comparison in terms of main kinematical parameters. Further, it allows to investigate proper sparkout duration, aiming at the built up of stiffer cycles in terms of dimensional output.

Despite the possibility to simulate various aspect of centerless grinding operation, as previously stated, before the start of the production there is a need of experimental campaigns in order to evaluate the following:

- Roundness characteristics output.

- Time constant evaluation.

- Measurement stability.

5 Process monitoring in centerless grinding

5.1 Introduction and purposes

The present case study is taken from preliminary process tests for the infeed centerless grinding of a two diameter plunger.
The aim of the investigation concerns:

- the determination of main system properties and variation (DoE investigation).
- the study of the rounding action and its main variation sources (DoE investigation).
- the in-line monitoring of the process by means of AE sensor and power emission sensor.
- the use of in-line monitoring to control process characteristics.

5.2 Machined workpiece and tools

The machined workpiece (figure 5-1) is an 100Cr6 Hardened 62+0/+2 HRc component for gasoline high pressure pump with two diameters (∅10 and ∅6) to be ground at the same time.

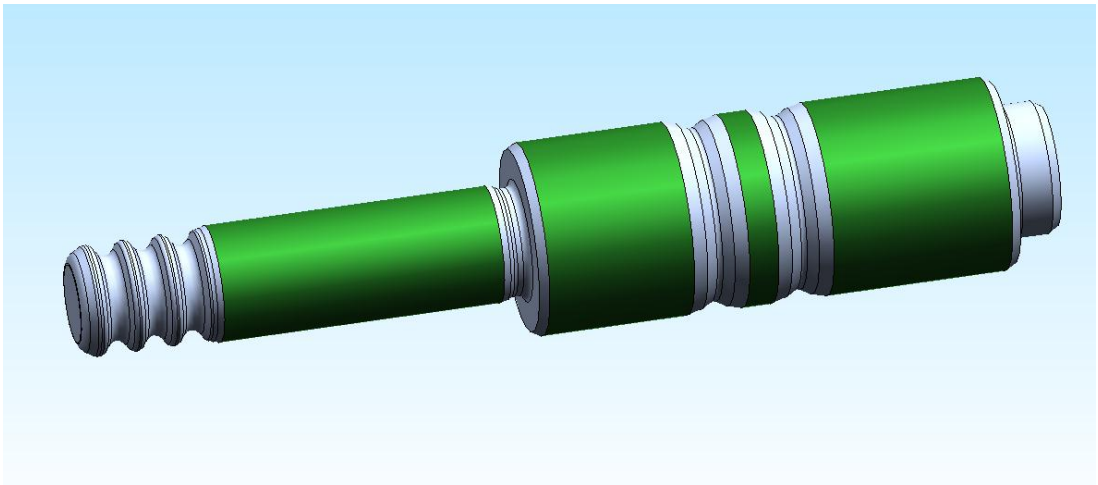

Figure 5-1 Ground component and ground surfaces

The blade (K10 hard metal at the top) holds the part on both the diameters.
The same is true for the organic bonded control wheel, 180 grit size.
Tested specifications of grinding wheels were selected based on different needs:

- Grinding wheel 1: SC, 180 grit size.
- Grinding wheel 2: SG Al_2O_3, 120 grit size.

The coolant is a 5% oil-in-water emulsion.
Grinding test were performed on a Ghiringhelli M100SP400 CNC4A.
For the purpose of the future illustrated results, the interest of the roundness analysis was focused on ∅10, whilst the roughness is intended investigated at ∅6[46].

5.3 Monitoring of the centerless grinding system

Prometec EPT20 electrical power sensor was applied at the grinding wheel spindle (figure 5-2). The acoustic emission root mean square signal (AE_{rms}) was measured by means of Kistler acoustic emission type 8152B (50-400kHz frequency range, integrating constant 0.12 ms); with the aim of having the best possible signal, it was applied at the side of the blade.
All sensor signals were sampled at a frequency of 20kHz by using a National Instruments data acquisition board and stored later for analysis. The integrated input data were stored and analysed on a common laptop.
The working environment for data elaboration and analysis was Mathworks Matlab.

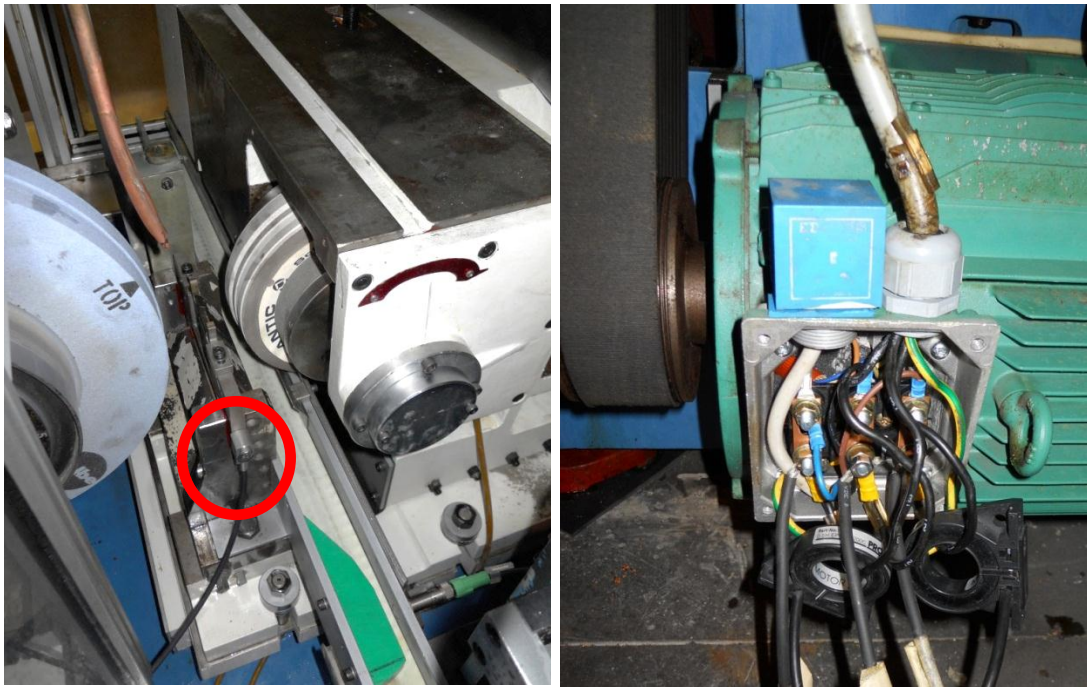

Figure 5-2 Centerless grinding gap with installed AE sensor (left) and power sensor installed on grinding wheel ferenmandrel (right)

An example of recorded power signal (constant infeed plus sparkout) and its subdivision in different cycle phases is shown in figure 5-3.

[46] Regarding roughness, once the coolant flow rate and nozzles had been properly adjusted, no significant difference wasw noticed between different diameters.

5.4 Time constant evaluation

5.4.1 Introduction

As reported in par. 4.3.2 one of the main characteristics of centerless grinding system is the parameter K, as defined in par. 1.4.9 and par. 4.3.2

The determination of this ratio may be done experimentally in a rough way through the study of the sparkout effects on workpiece diameter measurements [Gallego, 2007] [Zhou, 1996][Rowe, 1973][47].

Otherwise, this determination is possible through the study of the whole evolution of the diameter measurement. The diameter evolution cannot be in-line measured, but it is possible to know its variation. Its variation, as reported in par. 4.3.2, is equal to the real depth of cut (eq. (43)); hence, in order to have a reliable results for the K parameter it is crucial to have some experimental data linearly depending on the depth of pass a_e. Since, keeping other parameters constant, the power is only depending on the actual depth of cut, then, during the sparkout phase, the power variation is directly proportional to the depth of cut variation, i.e. to the machine capability of recovering elastic deflections.

A similar characterization of the sparkout period and, hence, of the machining system characteristics, is given by the study of the straight absorbed power at the grinding wheel spindle. According to eq. (44) in par. 4.3.2, during the sparkout period, the reduction in grinding power [48] is approximated by an exponential function.

In literature, the sparkout duration is suggested to last approximately 3 time constants τ [Cheng, 2009]. Further, overshooting is suggested [Malkin, 2008] and automatic dwell control strategies were implemented to cope with machine flexibility and to reduce cycle time [Allanson, 1997].

The time constant τ .is reported [Allanson, 1989] to be (for plunge grinding between the centres):

$$\tau = \frac{v_w * K_s}{\pi * d_w * K_{eq}} = \frac{v_w * K}{\pi * d_w} \qquad (49)$$

Based on the above equation, time constant variations should occur[49] due to:

- variation in v_w
- variation in K_s (i.e. cutting stiffness, depending on a wide number of conditions[50])

[47] The determination of K, is reported to be done based on the measurements of the workpiece machined with and without sparkout. Anyway, due to high experimental effort and data dispersion, the finding of reliable results is reported to be a long procedure [Zhou, 1996].

[48] During sparkout phase, no further infeed occurs; hence the diameter reduction process goes only based on the so-far grown deflections in the machining system due to the infeed grinding forces.

[49] For common application d_w variations are not considered to be significant.

[50] Commonly the cutting stiffness stands for the ratio between normal cutting specific force and the real depth of cut. Anyway, as seen in previous chapters, a wide number of parameters may have an

- variation in K_{eq} (i.e. machine and contact compliances)

Hence a number of test was carried out based on DoE approach.
The main aim of this investigation deals with process kinematical parameter influences (eventually considering dynamic effects through K_{eq}) on system time constant τ.
If the above model was confirmed then, from time constant, it would be possible to have a straight indication for the centerless loop parameter K.

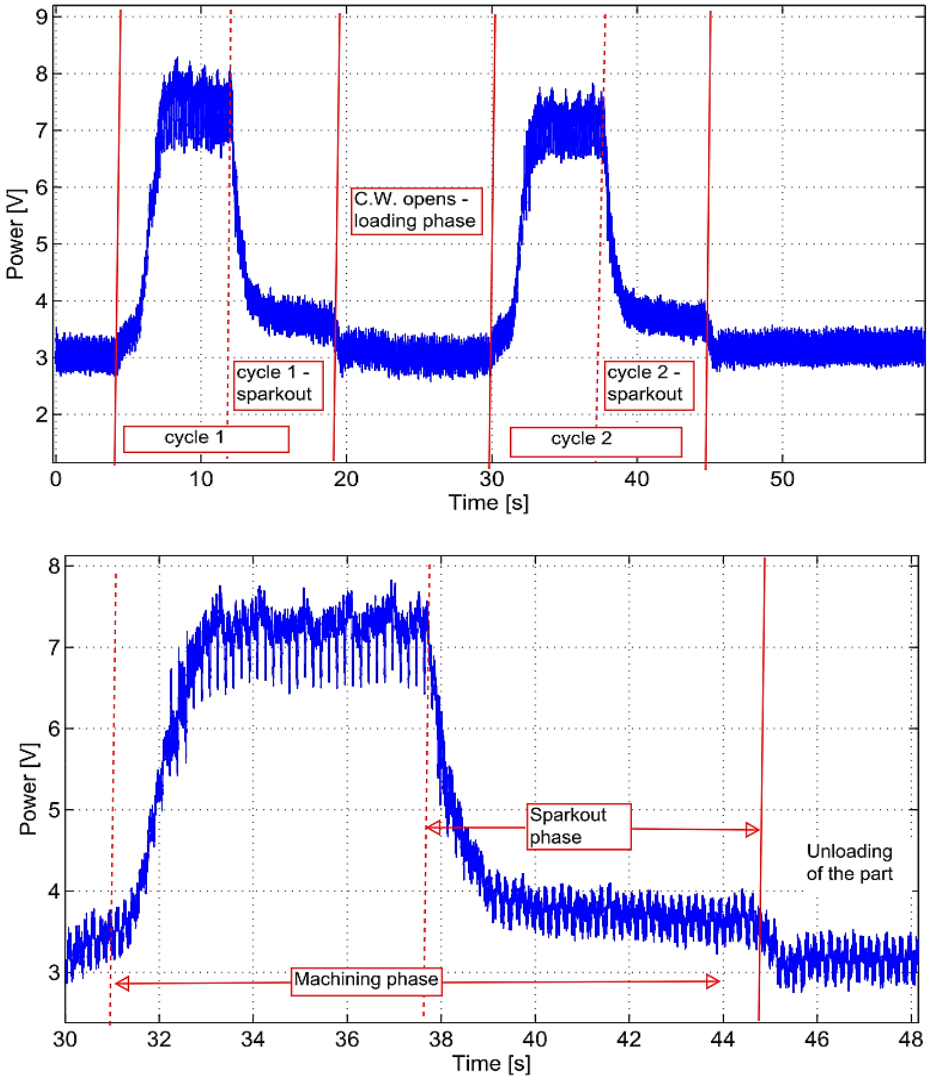

Figure 5-3 Example of recorded power signal (up) and single cycle power record (bottom)

For this purpose, the test infeed cycle was a constant infeed rate, followed by a 7 second sparkout.
According to commonly adjustment parameters, the investigated influencing parameters were:

---

influence on this parameter such as: grinding wheel specification, coolant, speed ratio, dressing conditions.

- Workpiece speed v_w (i.e. control wheel Ω_r, on three levels)
- Cutting speed v_s (on two levels)
- Dressing speed (i.e. the dressing overlap parameter U_d, on two levels)
- Grinding wheel specification[51] (on two levels).

Further, a long term test (relevant number of ground parts) was carried out in order to determine if the time constant is subjected to variations during the time between dressing. This, in fact, would require further preventive measures during the in-process design, i.e. the time between dressing estimation.
The working environment for the evaluation of time constant was the Curve Fitting Tool, provided in Mathworks Matlab (figure 5-4).

5.4.2 Evaluation of time constant τ

5.4.2.1 Short term study

The investigation of the time constant parameters was carried out according to table 5-1.

Table 5-1 Investigated DoE parameters for

Grinding wheel specification		**Grinding wheel speed v_s[m/s]**		**Control wheel speed Ω_r[rpm]**			**Grinding wheel dressing overlap U_d**	
1	2	35	45	25	45	65	6.3	12.6

The curve fitting results were considered to be satisfying since R^2 values from the interpolation ranged between 0.78 and 0.975 [52].

[51] From now on, the acronym GW stands for "grinding wheel specification".
[52] The R^2 deviation was not considered to be significant

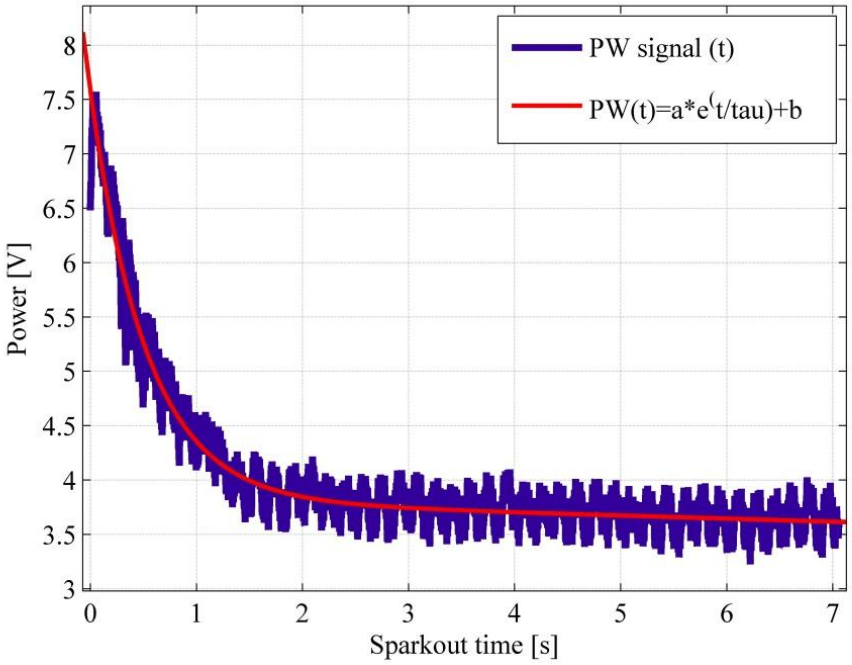

Figure 5-4 Example of sparkout power signal interpolation

The main results are reported in terms of scatter plots in figure 5-5, figure 5-6 and figure 5-7.

5.4.2.2 Short term study: analysis of results

From the results of the above analysis, the following conclusions may be outlined:

- time constant τ values significantly vary based on grinding wheel specification, up to 60%;

- there is an influence of wheel specification on other machining parameters: a grinding speed increase lifts the time constants τ (up to roughly 20%) for GW 2 but seems to decrease for GW 1 (10%). Further, dressing parameter seems to have an influence on time constant for GW 2: anyway the analysis of variance did not confirm this consideration and further data acquisition may be needed for statistical significance to be confirmed.

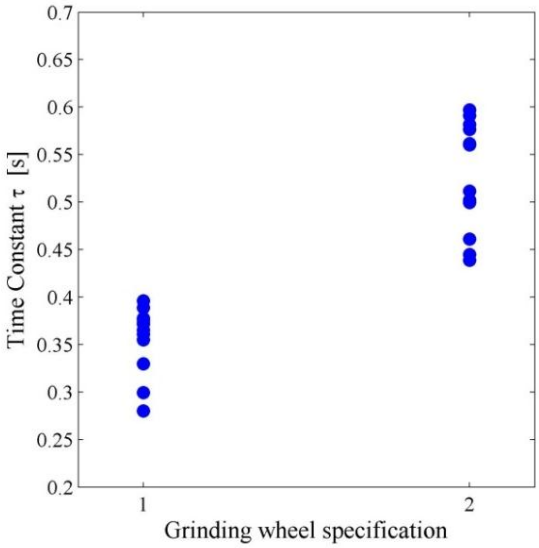

Figure 5-5 Time constant versus grinding wheel specifications

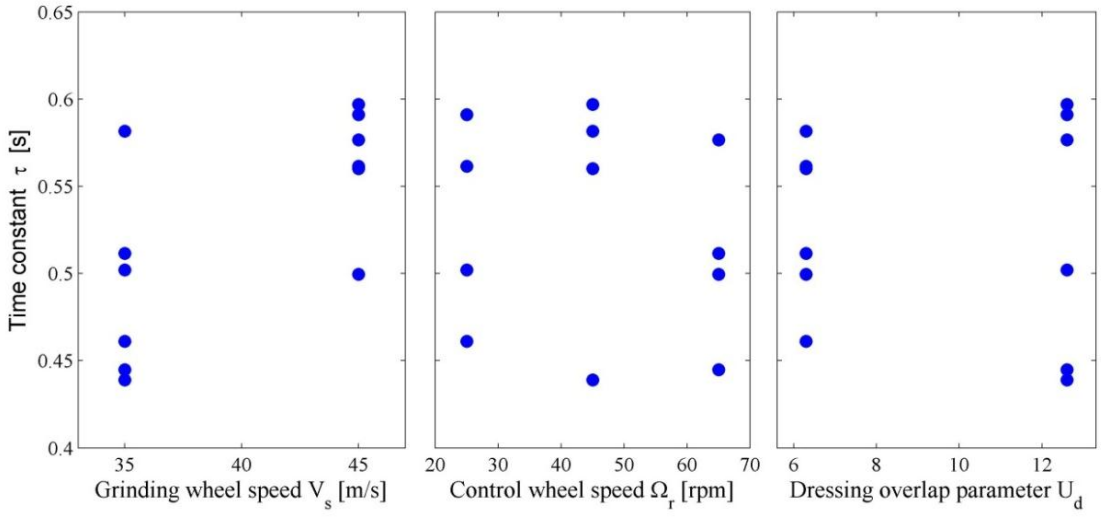

Figure 5-6 Grinding wheel spec. 2: Time constant τ against v_S, Ω_R, U_d

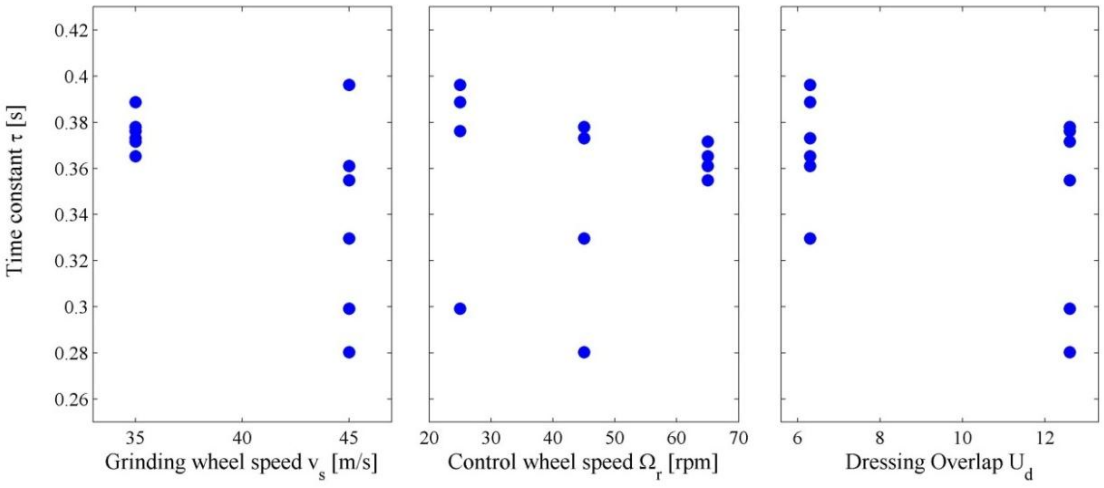

Figure 5-7 Grinding wheel spec. 1: Time constant against τ against v_S, Ω_R, U_d

- There is not any marked influence of the workpiece speed[53] on the τ value: this is likely to be due to the cutting stiffness K_s dependency on the speed ratio q, as indicated in par. 4.3.4. Hence, the τ analysis proposed in literature seems over-simplified in its dependencies, requiring further application customized studies to be carried out.

5.4.2.3 Long term study

Due to wear, cutting behaviour is known to vary. Since the time constant takes in consideration the cutting capacity by means of the cutting stiffness K_s (in fact, $K = K_s/K_{eq}$), it may be of help to evaluate the variation in τ during the time between dressing.
An example of τ plotted against the number of ground parts is shown in figure 5-8[54].

[53] For present analysis pure static contact has been considered between control wheel and workpiece, i.e. no slipping occurs.
[54] 80-part-lenght test was considered since it is was a reasonable time between dressing, based on workshop considerations. While machining last parts, noticeable noise occurred due to excessive wearing of the grinding wheel, resulting in poor surface quality. Despite this fact, only a small increase of the τ over the whole interval occurred.

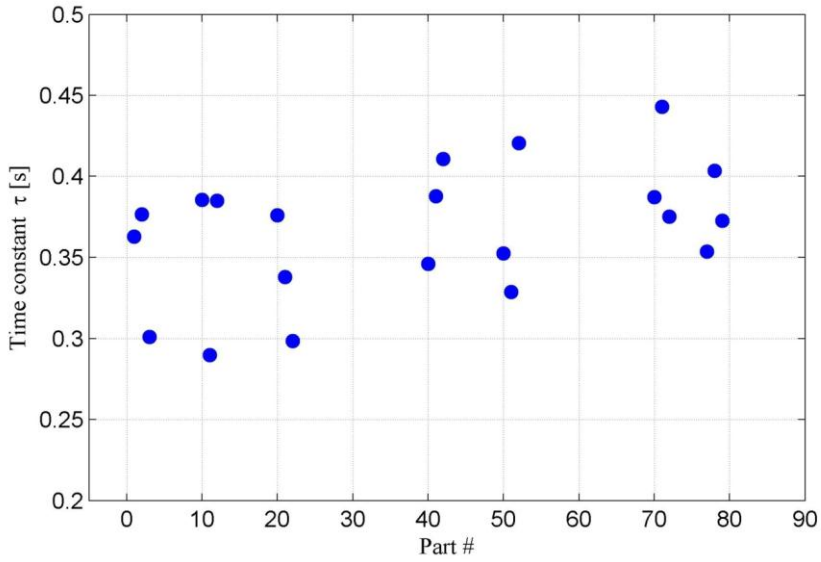

Figure 5-8 Time constant variation over time between dressing interval (GW specification n°1)

5.4.2.4 Long term study: analysis of results

A spread in very short term (few parts sample) shows that time constant determination may vary up in relevant manner from part to part (up to 20%).
Further, there is a trend, showing an increase in τ on the whole time between dressing. The deviation of local maxima of τ [55] [56] resulted to be evaluated in 18% over 80 parts interval.
In practical terms, if the sparkout duration was set to 0.9 seconds ($= 3\tau$) based on single cycle spark out analysis, problems would arise during the 70^{th} machining cycle, when the τ measured, due to change in cutting behaviour, resulted to be 0.45. Hence, particular care should be given to sparkout determination and its variance throughout the machining process.
The increase of time constant as the number of parts goes on, may find reason physically in the lack of cutting behaviour of the worn grits. These observation would be particularly of interest in order to understand what happens during the wearing out of the grinding wheel (i.e. less cutting grits). In some cases, according to the previous consideration, it is common to have diameters variation during the last useful mm of grinding wheel life.

5.5 Roughness monitoring through AE_{rms}

5.5.1 Premises

Surface quality requirements may be tedious to be monitored because ground part cannot be checked in a quick and accurate way in workshop floor. Often, less expensive roughness meter are used; for proper use, these devices should be used with special care and high zeroing frequency.
Hence, surface requirements are usually met in first process trials and seldom optimized as the process goes on.

[55] The maximum time constant was considered due to its impact on robust process design.
[56] With local maximum, the maximum value from three adjacent cycles is intended

In order to find proper time between dress, a common practice is to keep the process monitored with adequate surveillance plans (i.e. workforce cost) or to fix a safe-side number of parts between dress, usually determined by few long-term study during the process start-up trials.
This approach lacks precision concerning two issues:

- it does not consider long-term variances occurring during the production process (e.g. a difference in grinding wheel hardness or variation in coolant supply)

- the determination of the number of parts between dress can be excessively on the safe side, due to lack of data recovery, thus neglecting performance increase chances and resulting in worthless tool costs.

Therefore, for high surface quality requirements there is a need of on-line monitoring of grinding process behaviour.
From signal analysis, even if power emissions had been applied in order to estimate the flattening wear of cutting grits [Malkin, 1971], it was, in a preliminary phase, verified that this technique does not match high requirement application: this is possibly due to the low grinding wear rates involved in precision machining. Thus, power signal characteristics do not seem to be significantly helpful in roughness monitoring. For instance, in figure 5-9 after an almost linear increase of mean power (from dressing to part n°30), a sudden variation occurred. After that, a decrease in mean power content started[57]. This behavior is particularly hard to be connected to a worsening of the part surface characteristics.
Instead, acoustic emission signal showed an clear increasing trend as the production proceeded (figure 5-10). In particular, signal mean[58] has an almost linear behaviour while the signal standard deviation showed a second order behaviour. Despite the clearness of the latter, it does not find any clear meaning or correlation with investigated workpiece surface characteristics. Hence it is not considered an appropriate parameter for roughness monitoring.

[57] This inversion in mean power signal could be interpreted due to a sudden change in grinding wheel cutting behavior (loading and start of splintering behavior). Anyway, this variance did not result in any workpiece measured characteristic.
[58] In order to perform signal mean, the recorded signal is considered without spark-in and spark-out phase.

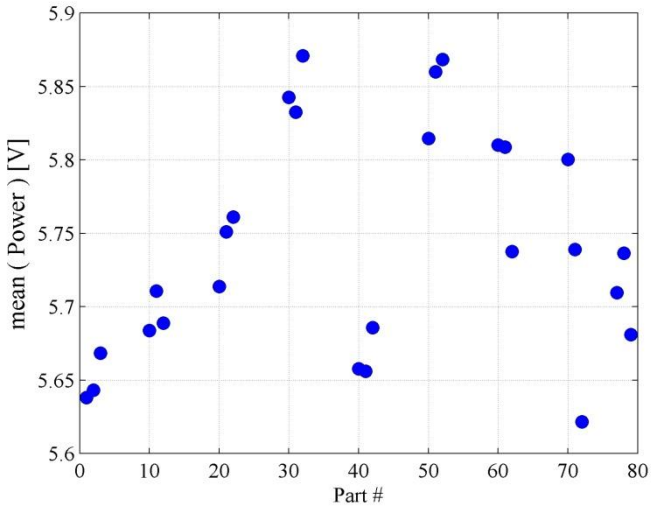

Figure 5-9 Mean and standard deviation of power signal against number of part

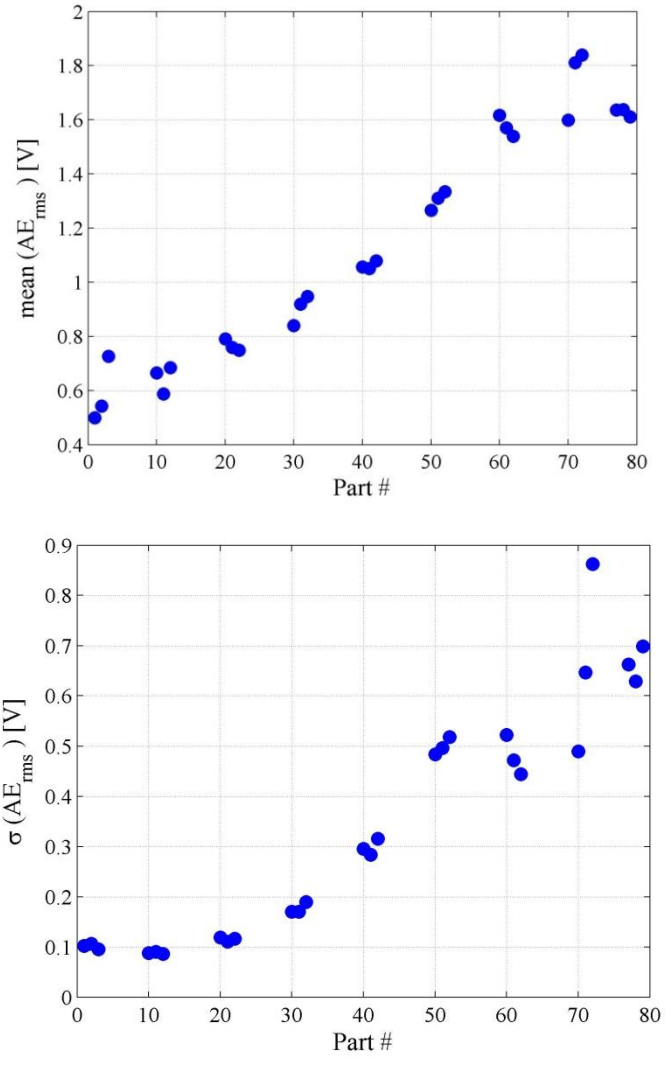

Figure 5-10 Mean and standard deviation of AE_{rms} signal

5.5.2 Analysis of results

The scatter plot of R_a and R_z versus mean is shown in figure 5-11.
R^2 values were found to be roughly 0.72 and 0.73. Despite the fact that these R^2 values do not seem to be very satisfying, it has to be reminded that roughness measurement is very tedious and prone to mis-measuring. Since the relationship found includes any possible roughness measurement uncertainty, the resulting R^2 values are considered promising.

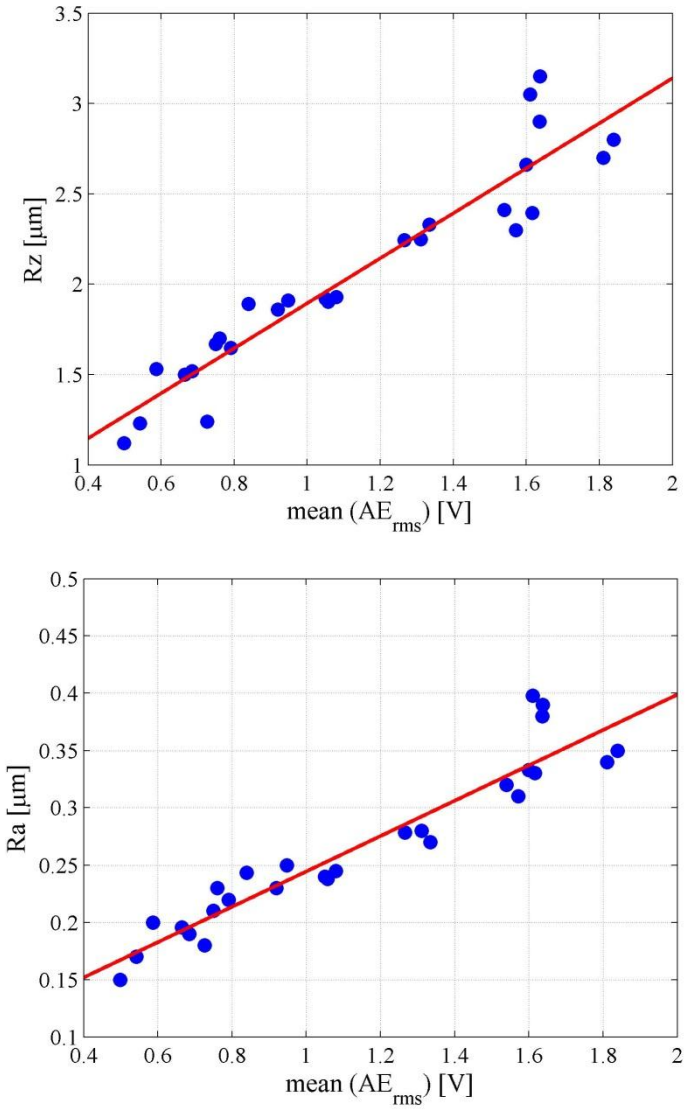

Figure 5-11 Mean (AE_{rms}) against Rz (top) and Ra (bottom)

5.6 Rounding action (roundness) and variation sources

5.6.1 Introduction

One of the main feature of the centerless grinding system relates to the possibility to have good shape characteristics (i.e. low cilindricity and low roundness) with high throughput and ease of automation.

Anyway, as seen in previous chapters, roundness and other quality issues are affected by quantitatively unpredictable issues. Whilst predictable aspects, such as grinding gap geometrical change, are qualitatively analysable prior to the start of machining, other issues have to be coped with during setting up phase. Roundness is one of the most tedious quality issues to be fronted.
Main kinematical parameters ($v_{s,}\, \Omega_{r,}\, v_{fr}$) not varying, in common practice roundness is known to be varying based on:

- height of the part (above/below the centres);
- control wheel wear;
- control wheel speed;
- grinding wheel specification/batch;
- dressing parameters.

Another aspect of interest is the shape of the roundness[59] error, i.e. how the error is composed. For instance, a roundness error of 3 µm may have different relevance whether a particular pattern (e.g. 4 lobe-part see figure 5-12) is recognized or not.

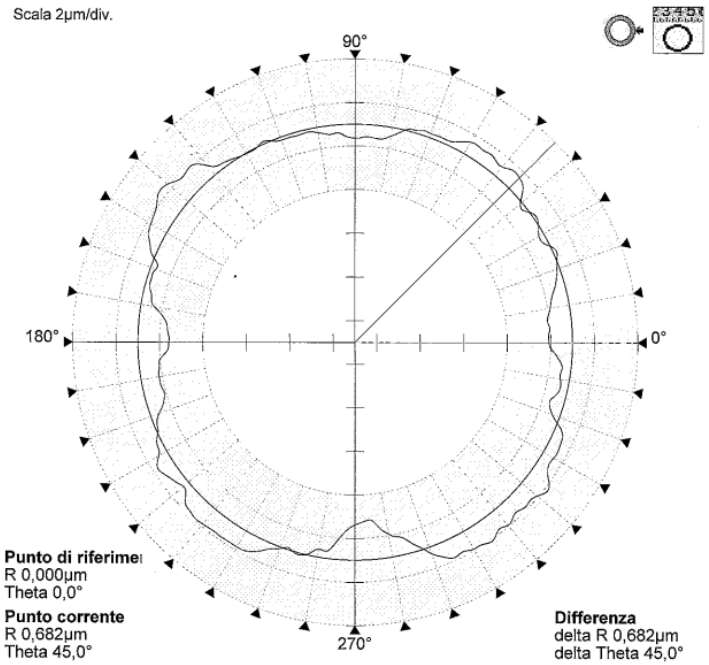

Figure 5-12 Example of 4-lobed part induced by kinematical coupling

To do this, roundness error is analysed trough Fourier analysis and expressed as a sum of varying-amplitude sinusoids of integer frequency. This aspect is named "waviness of the component", concerning the long-wavelength part of the deviation from the perfect round part, differentiated from short wave components ("high frequency hash" [Bhateja, 1984]) through the use of chosen filters.

[59] The roundness error is defined as per ISO/TS 12181-1/2:2003.

The error harmonic frequency is expressed in forms of UPR (undulations per round)[60].
For the analysed roundness pattern, measurement were carried out on a Taylor Hobson Talyrond 395, with a ø1 mm ruby feeler. Applied filter is Gaussian type, 50%, 1-50 UPR.
Error analysis and its spread in terms of UPR were carried out through the built in analysis software Ultra, given on the measuring machine.
An example of the measuring context and error analysis is given in figure 5-13.
The interest in the investigation of the UPR amplitude is due to two main issues:

- Ground components to be matched with roll/sphere bearing: in this case a particular interest periodic type roundness error (i.e. roundness error concentrated in one particular UPR) result in noise and reduced life.

- Ground components to be machined in a second centerless grinding phase: in this case, based on roundness pattern regeneration (mostly based on geometrical stability), some UPR are desirable to be avoided (e.g. if the investigated centerless grinding process produces 12 lobed parts may be acceptable because of 5 lobes regeneration tendency in the following machining operation).

In common practice, the most tedious UPR orders to be removed from a ground workpiece result to be the 3rd, the 5th and the 12th. Higher number of lobes may be present, but commonly with smaller amplitudes.
Another point to be reminded is the avoidance of kinematic coincidence between number of grinding wheel rpm (and multiples) and the number of workpiece rpm (a result of the kinematical coupling is reported previously in figure 5-12). In fact, this conditions may overcome geometrical stability resulting in severe lobing.

[60] From now on, the acronym UPR may be used instead of "undulation per second".

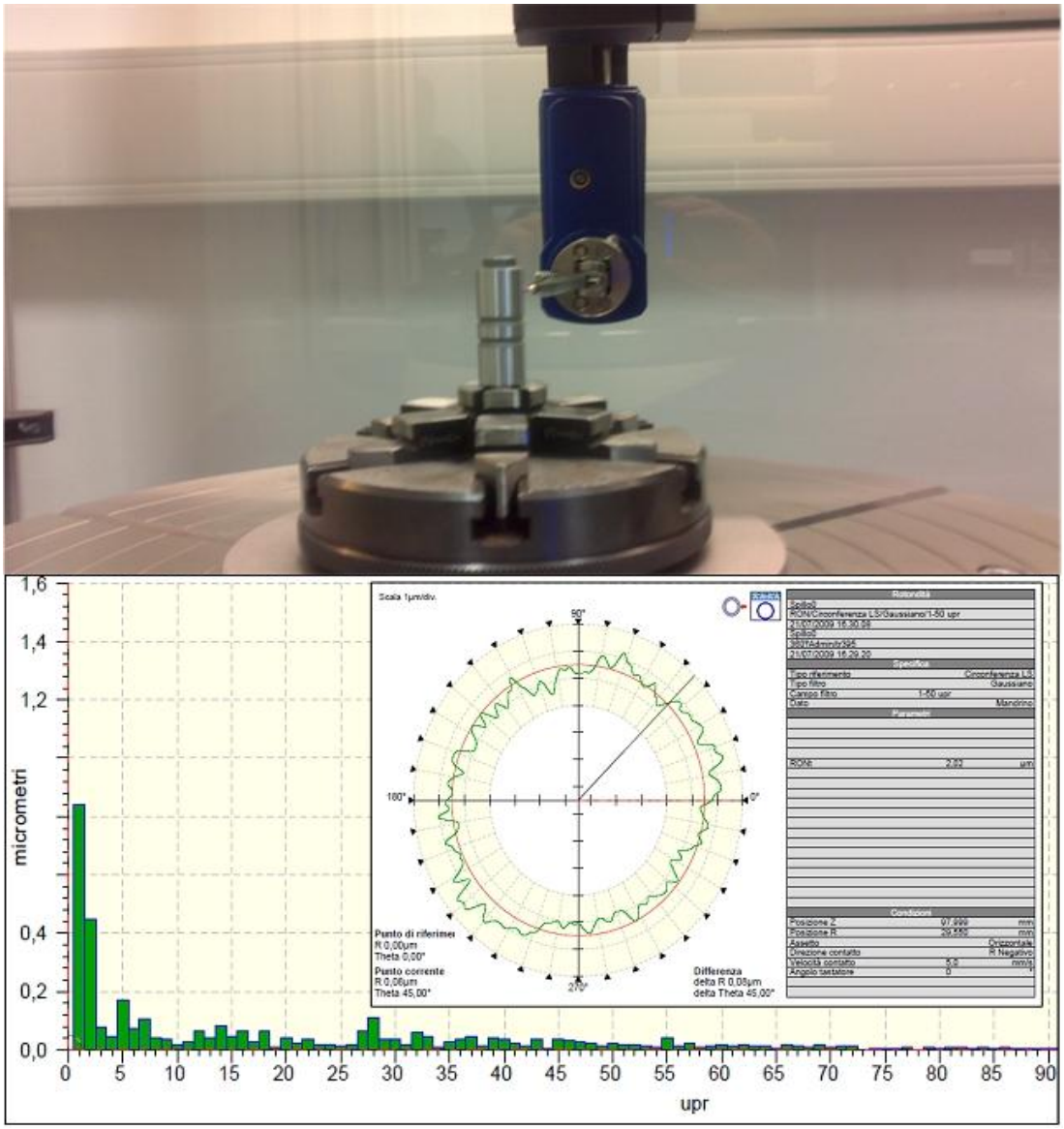

Figure 5-13 Example of roundness meter measuring configuration and output

5.6.2 Rounding action study: DoE

Since geometrical stability is deeply examined in previous par. 4.2.1 and optimal geometrical configuration can be established before the setting up of the machining operation, the present investigation applies a complete (2x2x3x2) DoE to investigate influencing parameters on the single roundness components (i.e. UPR), thus verifying the effectiveness of common practice workshop adjustments.
Investigated parameters and levels with a multistepped infeed cycle are the same as shown in table 5-2Table 5-2.

Table 5-2 Investigated DoE parameters for Roundness Characteristic analysis

Grinding wheel specification		Grinding wheel speed v_s[m/s]		Control wheel speed Ω_r[rpm]			Grinding wheel dressing overlap U_d	
1	2	35	45	25	45	65	6.3	12.6

5.6.3 Analysis of results

Considering the aim of this analysis to be the investigation of factors influencing the single lobes,
in table 5-3 the analysis of variance results are reported, in terms of p-values[61]. This results show that not all the investigated parameters affect the amplitude of lobing error.
From the reported robust geometrical analysis for the analysed configuration (figure 5-14), 3rd and 5th lobe order resulted to be the closest UPR to geometric instability. This is a typical case in centerless grinding. It is of particular interest to understand which machine parameters vary in order to reduce the error of each single waveform order.
From the obtained results, a variation of control wheel speed will not be significant on the 3 UPR amplitude. Instead, reducing the grinding wheel speed will reduce 3rd lobe amplitudes. Similarly the dressing speed can affect the UPR amplitudes.
This types of consideration may be particularly helpful in the eliminations of lobing issues arising typically at grinding wheel change, in which the spread of grinding wheel characteristics (e.g. the hardness, see cap. 2) may induce different behaviour in terms of roundness error UPR.

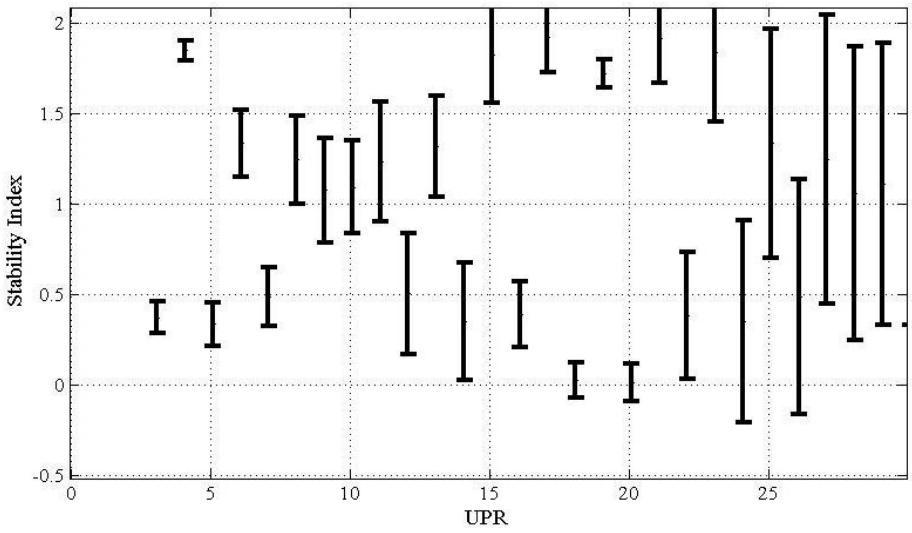

Figure 5-14 Robust stability indexes for investigated gap geometry H_0=10 mm; α_r=0.8 deg, L_{center} =65 mm, L_{min} =10 mm; L_{max}=35 mm.

[61] The threshold of significance for p-value was arbitrary chosen to be equal to 0.05.

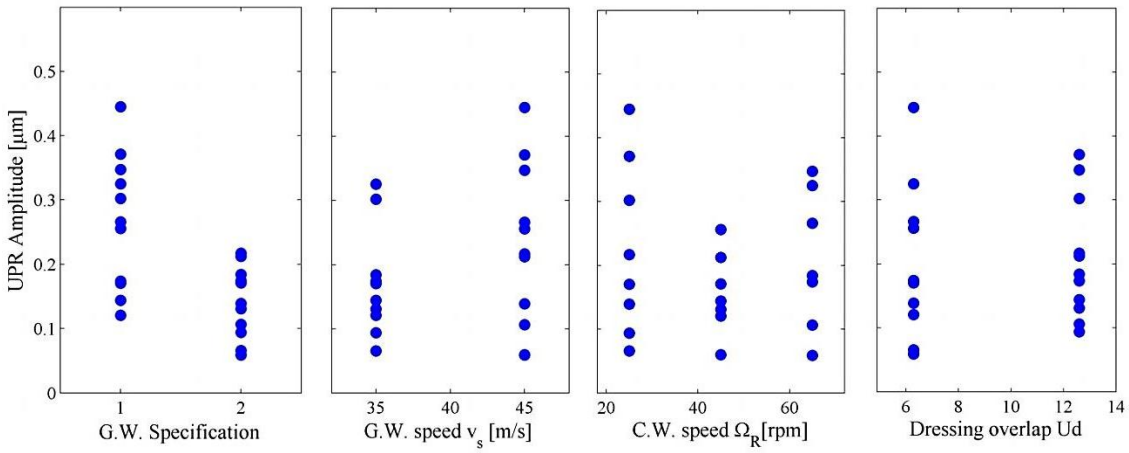

Figure 5-15 Scatter plot of 3rd UPR versus investigated parameters

Table 5-3 p-values from analysis of variance on UPR against investigated parameters

	UPR								
	3	**4**	**5**	**6**	**7**	**8**	**9**	**10**	**11**
G.W. Specification	0	0	0,0042	0,0001	0,0002	0	0,1182	0,0016	0
Dressing Overlap Ud	0,034	0,2077	0,1294	0,3322	0,8992	0,5727	0,1642	0,8727	0,0366
Vs	0,002	0,4739	0,0001	0,6285	0	0,9189	0,0024	0,0061	0,0237
Vw	0,665	0,3296	0,2061	0,1763	0,0235	0,0421	0,2168	0,3493	0,1694
	12	**13**	**14**	**15**	**16**	**17**	**18**	**19**	**20**
G.W. Specification	1E-04	0,0003	0	0,1777	0	0,231	0,0026	0,1602	0
Dressing Overlap Ud	0,136	0,922	0,5293	0,2326	0,0131	0,8085	0,2343	0,7485	0,1392
Vs	0,369	0,0316	0,448	0,0541	0,5974	0,0564	0,0015	0,1427	0,0455
Vw	0,01	0,0577	0,0734	0,7288	0,0222	0,623	0,005	0,6714	0,282
	21	**22**	**23**	**24**	**25**	**26**	**27**	**28**	**29**
G.W. Specification	0	0,0009	0,0015	0,4069	0,0001	0,0001	0,0194	0,0492	0,0036
Dressing Overlap Ud	0,426	0,3629	0,8577	0,3184	0,2695	0,2781	0,4129	0,0987	0,3042
Vs	0,005	0,0005	0,2527	0,7117	0,0057	0,0083	0,9662	0,1702	0,7572
Vw	0,084	0,0593	0,8686	0,0036	0,2497	0,2876	0,0022	0,0291	0,5051

Concerning the investigation aims and the most common critical UPR orders, from the displayed results the following conclusions may be outlined:

- 3 and 5 UPR amplitude variations do not depend on control wheel speed but rather on parameters such as grinding wheel specification, dressing parameter and grinding wheel speed for 3 UPR whilst grinding wheel specification and grinding speed only affect 5th UPR. Reduction of grinding wheel speed result to be more convenient to reduce their amplitude.

- 11 UPR amplitude depends on grinding wheel specification, dressing overlap and grinding wheel speed.

- 12 UPR amplitude is affected by control wheel speed and grinding wheel specification but not by grinding wheel speed.

- Generally speaking, low order UPR are strongly influenced by grinding wheel choice specification and cutting speed. Control wheel speed becomes statistically significant just for some lobing order.

5.7 Frequency domain analysis of roundness

5.7.1 Premises

In order to investigate more deeply the process characteristics and in order to find some possible way to monitor the roundness error, the frequency domain was investigated.
FFT built-in routine in Mathworks MATLAB was applied to process recorded signals with the aim of looking for some relationship with obtained roundness data (RonT and UPR).
Whilst AE_{rms} spectrum showed peaks at expected frequencies (e.g. rotating workpiece frequency, rotating grinding wheel frequency), power emission signal showed a frequency analysis not compliant to physical aspects, with marked peaks at non-interesting frequencies (see figure 5-16).
The non-conformance of power emission spectrum may be due to the belt coupling between grinding wheel spindle and its motor (which the power sensor is applied to); this seem to justify the low pass filtering effect on high frequency components.
In order to investigate the spectrum entities connected to roundness characteristics, a "clean" AE_{rms} signal was considered, i.e. spark-in and spark-out were neglected.
Later, in order to smooth the influence of multi-stepped infeed components, the signal was processed through the removal of linear component (due to multistepped nature of infeed rate) out of the AE_{rms}-signal.
Then, the FFT was carried out and its results analysed in the frequency domain:

- Since an high amount of noise at very low frequencies (<5 Hz) signal components directly related to control wheel rotation were rarely identified.

- Peaks corresponding to grinding wheel rotation and workpiece rotation are clearly identified. From workpiece rotation frequency the driving workpiece diameter resulted to be $\emptyset$10.

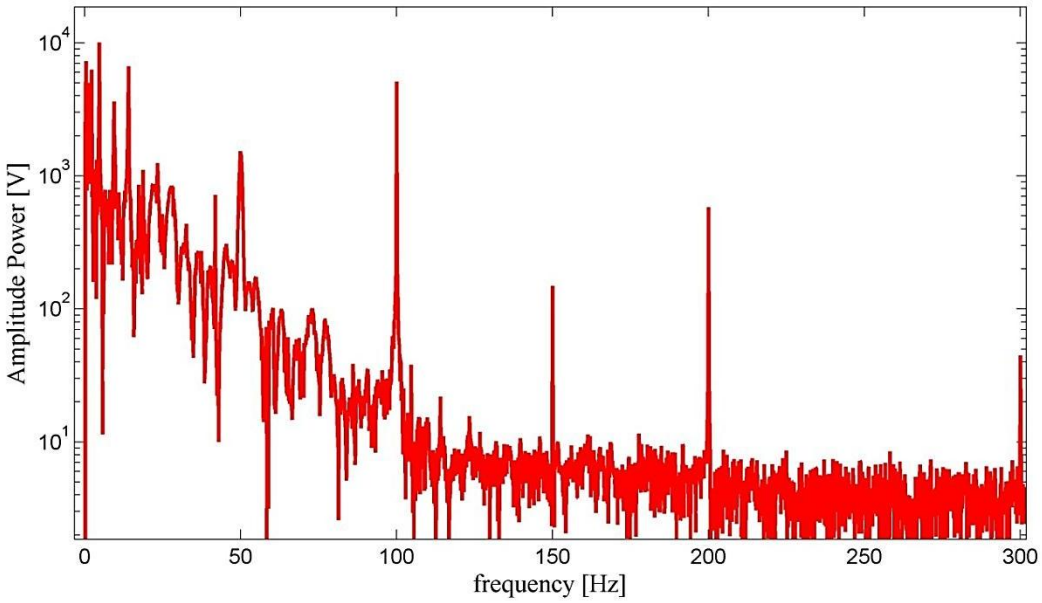

Figure 5-16 Example of FFT(PWR) for v_s =35 m/s (=1700rpm) and Ω_R = 45 rpm (i.e. Ω_w =15 Hz)

From AE spectrum analysis, repetitive peaks clearly appeared at frequency corresponding to multiples of workpiece and grinding wheel rotation frequency; the former are interpreted as due to the presence of multi-lobed part (see 5.6.1) and thus investigated as in following.

An experimental campaign was carried out to see the feasibility of roundness prediction through its monitored frequency features.

One roundness measurement was carried out to identify each parameter combination. Investigated parameter combination is the one reported in table 5-1.

In order to compare signal fft(AE_{rms}) amplitudes and roundness component amplitudes in a stiffer way, from fft analysis, peaks from two adjacent signals were extracted based on signal-to-noise level[62] and amplitude criteria.

The amplitudes and frequencies of the most robust and highest peaks with a bandwidth limited to 300 Hz were later identified as peaks occurring because of the rotational speed of the workpiece (i.e. due to its roundness error).

The extracted components were compared with UPR amplitudes in order to find some relationship between the two (an example is reported in figure 5-18).

[62] The signal-to-noise level is defined based on the repeatability level of the signal: if the harmonic component is relevant in two adjacent signals and its difference in the two is <20% then the peak is considered robust.

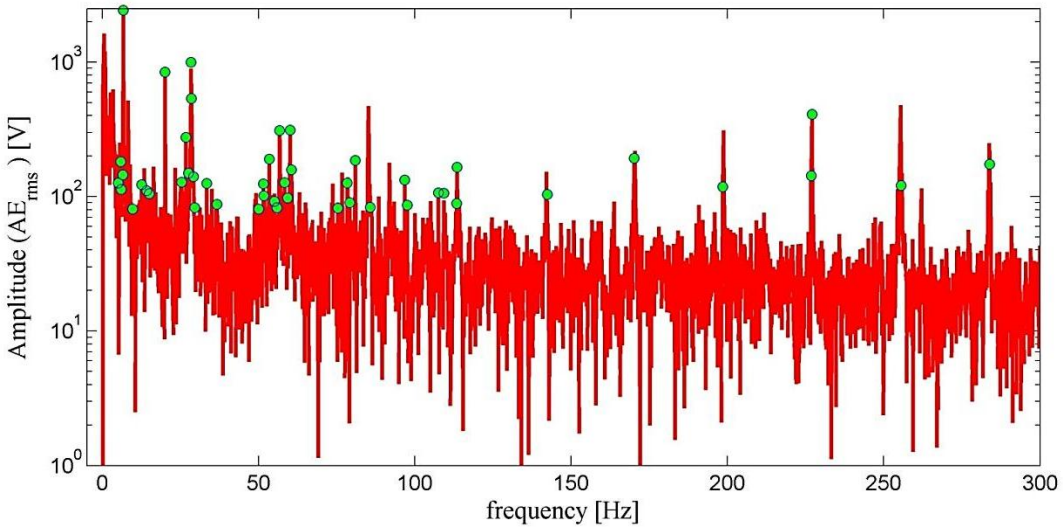

Figure 5-17 Example of extracted robust peaks for v_s =35 m/s (1700 rpm) and Ω_R = 25 rpm (Ω_w = 8.3 Hz)

Further, from analysed AE_{rms} signal, no relevant peaks apart from kinematical one were observed. This demonstrated the absence of any dynamic influence on the machining operation[63].

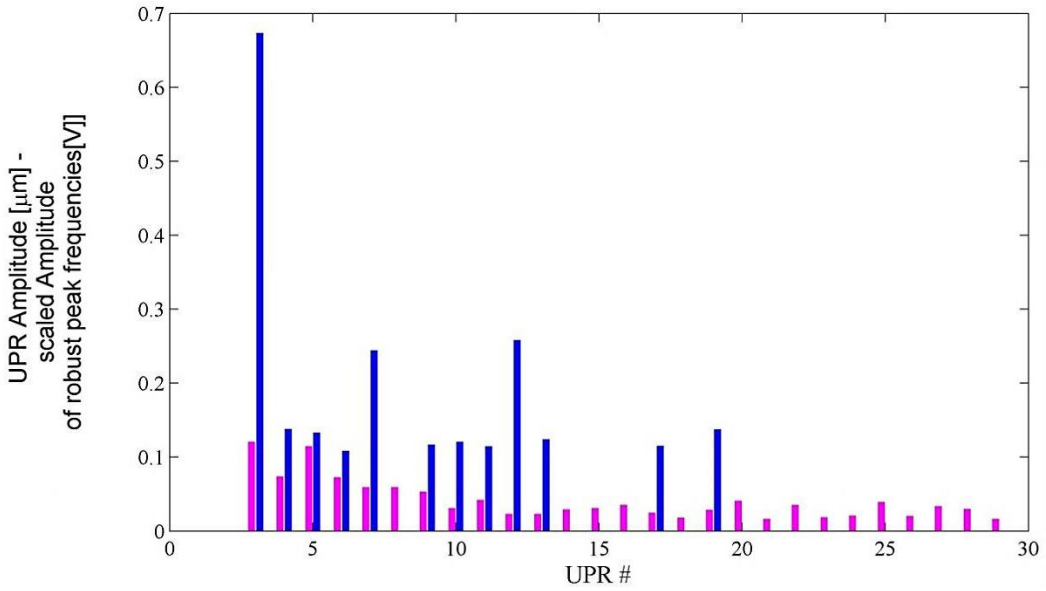

Figure 5-18 Comparison of roundness features (UPR) and scaled FFT(AE_{rms}) amplitudes features of robuts peaks

5.7.2 Analysis of results

The relationship between the AE_{rms} spectral content and the roundness content seems to be relevant in terms of correlation coefficient for a limited number of data and, in particular, for only one given GW specification.

[63] The grinding wheel 1st resonance was found to occur in the proximity of 160 Hz.

In table 5-4 the correlation coefficient and corresponding p-values values obtained from the comparison of roundness and AE_{rms} frequency features are reported.

Table 5-4 Correlation coefficient r and p-values for roundness and fft (AE_{rms}) component

GW speed V_s [m/s]	CW speed V_r [rpm]	Dressing Overlap U_d	GW spec 1		GW spec 2	
			R	p-value	R	p-value
45	25	12.6	0.07	0.72	0.67	0
45	45	12.6	0.91	0	0.38	0.047
45	65	12.6	0.72	0	0.74	0
45	25	6.3	0.71	0	0.32	0.1
45	45	6.3	0.80	0	0.14	0.5
45	65	6.3	0.55	0.0003	0.4	0.04
35	25	12.6	-0.11	0.58	0.51	0.01
35	45	12.6	0.18	0.37	0.01	0.98
35	65	12.6	0.30	0.121	0.22	0.27
35	25	6.3	-0.18	0.37	0.31	0.11
35	45	6.3	0.51	0.007	-0.03	0.86
35	65	6.3	0.15	0.44	0.5	0.009

Hence, despite the fact that AE_{rms} spectrum can give information about qualitative aspects (i.e. dynamic or kinematic frequencies), no useful outcomes are obtained.
Hence, it is suggestible to verify the performance of the measurement and UPR repeatability before collecting further data.

5.8 Relationship between roundness and infeed phase parameters

The roundness investigation proceeded to find any process parameter to be put in relation with roundness parameter for a real multistepped infeed process[64].

[64] The multistepped infeed cycle is the same considered for roundness components investigations. Once the final machining point is found, based on set infeed speed and runs it was possible to establish phase boundaries.

The cycle was divided in its different phases, in order to determine if a relationship exists between sub-phases monitored characteristics mean(AE_{rms}), mean(PW), $\sigma(AE_{rms})$, σ (PW)) and roundness. Cycle has been divided in sub-phases according to set infeed rates (figure 5-19)

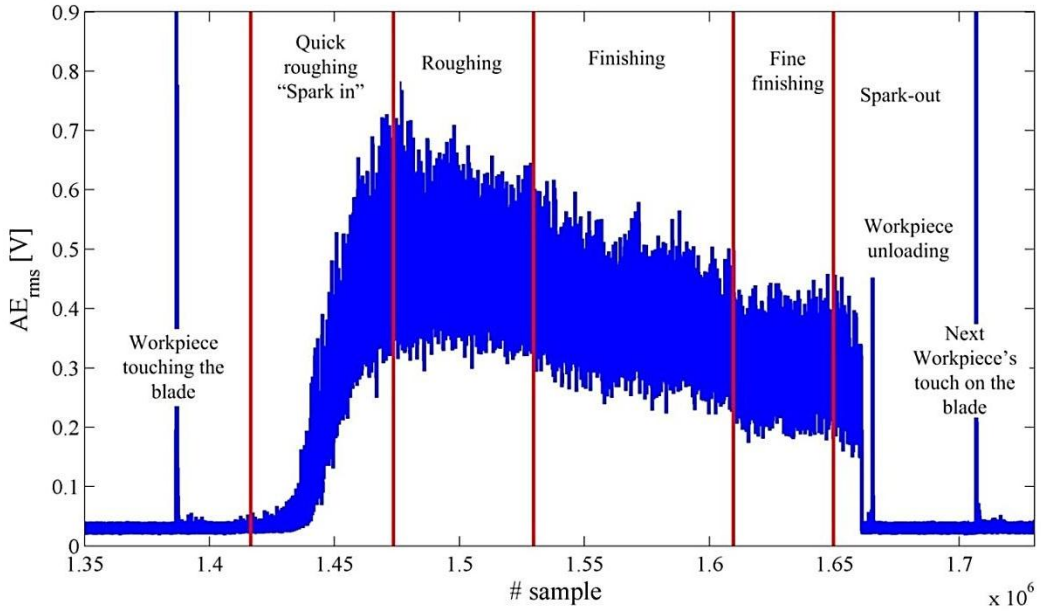

Figure 5-19 Signal subdivision for phase parameters investigation

From the analysed data, the correlation factor showed a significant relationship between the power signal mean and the roundness error. Anyway, this relationship seemed to be the corresponding of the relationship considered between cutting speed and single UPR values.
No meaningful differences in correlation factor appeared in considering power means from different phases (see figure 5-20).

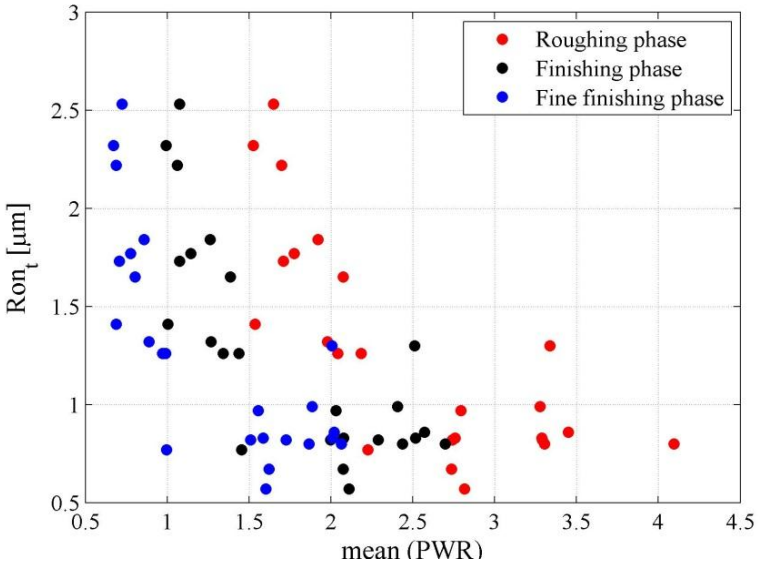

Figure 5-20 Roundness against mean(Power) for different infeed phases

5.9 Conclusions

From the data analysis carried out for a practical case study the following issues were highlighted:

- The time constant is a significant parameter and, for a correct cycle design, should be investigated with special attention in order to overcome and prevent its varying nature over short dressing stint or over the whole wheel life.

- The model proposed in literature for the sparkout evolution and study have been confirmed.

- The time constant is highly dependent on grinding wheel specification and, based on that, other parameters may result significant.

- The literature model of time constant depending on workspeed is not verified. An improvement was obtained using the equivalent chip thickness dynamic model for the determination of the time constants. Further improvements are needed to understand the varying nature of time constant based on grinding wheel specification.

- The monitoring of AE_{rms} signal is a promising technique for centerless ground components with demanding tolerances in terms of superficial finishing

- The study of AE_{rms} signal spectra showed that no chatter occurred throughout the investigated parameter range. The main peaks occurred at frequencies multiple of workpiece speed and grinding wheel speed.

- The study of roundness UPR components were not successful. Further study are needed, especially to investigate the repeatability of UPR amplitude throughout the cycle and AE_{rms} spectrum components characteristics.

6 Conclusions

The centerless infeed grinding system has been analyzed with the aim of reviewing the actual state of art and developing new tools for the cycle design and the output monitoring, with the following conclusions.
From the analysis of state of art literature concerning the centerless infeed system and the analysis of other aspects involved in the machining system, the major outcomes are:

- the simulation tools developed in literature (both in frequency domain and in time domain) do not give a quantitative prediction of the roundness error but can be used to compare and evaluate different aspects (linear and non-linear) affecting the machining system;

- the dynamic force model used in centerless grinding analysis are over-simplified and application of state of art models can give better representation of system varying parameters and behaviours, such as wheel speed effects on time constants;

- grinding wheels have Young's moduli spread up to two hardness grades under the same wheel specification due to their production cycles; wheel hardness affects the cutting stiffness and contact stiffness.

- rubber control wheels have Young's moduli spread up to 45%, based on literature data; the Young's modulus have an effect on control wheel wear rate, on roundness filtering effects and on contact stiffness;

- there is a lack in considering effect of tool variances to evaluate robust system simulations.

From the analysis of practical aspects of centerless grinding and the build-up of process analysis tools:

- a number of rules of thumb can be used to roughly estimate machining cycle time;

- a number of rules of thumb can be used to assess boundaries for the cycle kinematical parameters;

- a number of different setup rules and normograms does exist to set up the machine based on fixed tool diameters;

- the changes in tool dimensions have an impact on stabilities indexes over the whole process life; hence a tool for the robust geometrical stability prediction was developed to overcome the diameter variability problem;

- the cycle time evaluation depends on the system time constant τ that has to be evaluated experimentally;

- the developed tool for the cycle time evaluation can predict variances due to incomplete recover in the system deflections (insufficient sparkout phase);

The system monitoring permitted to achieve the following results:

- system time constant τ is heavily dependent on grinding wheel specification and, based on that, other parameters may be significant;

- system time constant τ is not dependent on the workpiece speed for centerless grinding operations;

- system time constant τ varies as wheel wear occurs over time between dressing;

- roughness monitoring for high quality demands trough AE_{rms} is a promising in-line solution;

- roundness components (UPR) have different behaviour and dependencies based on their order;

- for the investigated geometry and control wheel speeds chatter did not occur;

- the spectral analysis of the AE_{rms} signal did not show any significant peak in correspondence of the first grinding wheel resonance peak;

- there is no evidence that workpiece roundness components can be predicted by means of spectral analysis of AE_{rms} or Power signal trough the applied methodology; future investigations on repeatability of correlated entities are suggested;

- roundness values do not have any statistically significant relationship with mean values nor standard deviation of any sub-phase of AE_{rms} signal.

The obtained results highlight some perspectives for future works.
Process monitoring is getting an increasing importance due to the zero-defect production target. With this aim, it is of particular interest to perceive the investigation of reliable ways to detect roundness defectives. Based on author's gathered experience, it will be fundamental to consider the nature of the relationship between roundness and the characteristics of the AE_{rms} signal; in particular, it seems suggestible to fully evaluate the impact of noisy components in it, investigating the part of signal related to roundness. At the same time, deep understanding of repeatability of UPR amplitudes on small batch of pieces should be investigated.

Other applications of AE_{rms} spectrum could concern the use of self-learning algorithms to detect, for example, deviations in spectrum magnitudes due to unexpected sudden variation.
Roughness correlation with AE_{rms} acoustic emission is an explored sector but, from examined literature, the main qualitative limits of this monitoring technique are not known. Future work should be focused on the investigation and possibilities of AE_{rms} to detect production defectives for high demanding application, especially considering the improvement rate in monitoring technologies.
On the other side, beside the huge amount of research over the past decades, there is a further need for centerless grinding modelling to consider aspects such as dressing, coolant, wheel specifications and, in particular, those with intrinsically varying properties. More sophisticated dynamic models have already been explored in other grinding operations but, at the moment, did not find wide application in centerless grinding; during this work, it has been shown how, for instance, that system varying characteristics could affect required cycle time (i.e. dimensional stability). The development of these tools could prevent the built up of excessively costly processes or processes lacking of robustness. All these efforts will be a significant step towards zero-defectives task.

Bibliography

Allanson D.R., Kelly S., Terry S., Moruzzi J.L., Rowe W.B., Coping with compliance in the control of grinding process, Annals of the CIRP, 38/1 (1989), 311-314

Allanson D.R., Rowe W.B., Chen X., Boyle A., Automatic dwell control in computer numerical control plunge grinding, Proc. Of the Institution of Mechanical Engineers Part B, 211/7 (1997), 565-575

Atlantic Gmbh, Control wheels for centerless thru feed and plunge in B ED9 – Bonding, Information Brochure (2009)

Badger J.A., Torrance A.A., A comparison of two models to predict grinding forces from wheel surface topography, Int. J. of Machine Tools & Manufacture, 40 (2000) 1099-1120

J.Badger, Grinding: a pictorial odyssey, CTE Magazine, 61/2, (2009

Barrenetxea D., Alvarez J., Madariaga J., Gallego I., Stability analysis and time domain simulation of multiple diametetr parts during infeed centerles,, CIRP Annals, 60 (2011), 351-354

Barrenetexea D., Marquinez J.I., Bediaga I., Uriarte L., Continuous workpiece speed variation (CWSV): Model based practical application to avoid chatter in grinding, CIRP Annals, 58 (2009), 319-322

Bhateja C.P., Current state of the art of workpiece roundness control in precision centerless grinding, Annals of the CIRP, 33/1 (1984) 199-203

Bhateja C.P., Lindsay R.P., The importance of abrasive grinding wheel hardness control for the productivity of production grinding operations, CIRP Annals, 30/1 (1981), 247-249

Bocca Malandrone, www.boccamalandronesunebo.it, last access 13/10/2012

Brecher S., Hanning S., Simulation of plunge centerless grinding Process, Prouduction enginerring Research and development, 2 (2008), 91-95

Brown R.H., Saito R.H., Shaw M.C., Local elastic deflections in grinding, Annals of the CIRP, 19 (1971), 105-113

Bueno R., Zatarain M., Aguinanagalde J.M., Geometric and dynamic stability in centerless grindin, Annals of the CIRP, 39/1 (1990) 395-398

Challen j.M., Oxley P.L.B., An explanation of the different regimes of friction and wear using asperity deformation models, Wear, 53 (1978) 229–243

Cheng X., Rowe W.B., Analysis and simulation of the grinding process, Part II, Int. J. Mach. Manufact., 36/8 (1996) 883-896

Chen X., The sharpness of grinding wheel: an important measure of wheel behaviour, Proceedings of the Institution of Mechanical Engineers, Part B: Journal of Engineering Manufacture , 216/ 5 (2002), 829-832

Cheng K., Machining dynamics: Fundamentals, Applications and Practices, London, Springer-Verlag, 2009

Choi T., Shin Y.C., Generalized intelligent grinding advisory system, International Journal of Production Research, 45/8 (2007) 1899–1932

Cibaldi C., I criteri di scelta e di trattamento degli acciai da costruzione e da utensili: metallurgia di base, vol.1, AQM, 2006

Cincinnati Milling Machine Co., The, Grinding machine division, Pubblication N° G 758-5M-
12.1.61.B

Davies J.R., ASM Handbook, Volume 16: Machining, ASM international, ASM International, Metals Park, Ohio, USA (1989)

Decneut, R. Snoeys, J. Peters, Sonic testing of grinding wheels, CRIF Report MC36, 1970

Durgumahanti U.S. Patnaik, Singh V., Rao P.V., A new model for grinding force prediction and analysis, Int. Journal of machine tools and manufacture,50/3 (2010), 231-240

Furukawa Y., Myiashita M., Shiozaki M., Vibration analysis and work-rounding mechanism in centerless grinding, Int. Journal of Machine Tool design and research, 44 (1970), 145-175

Gallego I., Intelligent Centerless grinding: Global solution for Process instabilities and optimal cycle design, Annals of the CIRP, 56/1 (2007), 347-352

Garitaonandia, M.H. Fernandes, J. Albizuri, J. M. Hernandez, D. Barrenetxea, A new perspective on the stability study of centerless grinding process, Int. Journal of Machine Tools and Manufacture, 50 (2010) 165-173

Ghiringhelli (G&G Service), M200SP500CNC4A, Machine Handbook, 2011

Guo C., Malkin S., Kovach J.A., Laurich M., Computer simulation of below center and above center centerless grinding machines, Machining science and technology, 1/2 (1998), 235-249.

Hahn R.S., Price R.L, A non destructive method of measuring local hardness variations in grinding wheels, Annals of the CIRP, 26 (1968), 19-29

Hahn R.S., Lindsay R.P., Principles of grinding-part1 Basics relationships in precision grinding, Machinery, July-November 1971

Hahn R.S., The influence of threshold forces on Size, Roundness and contour errors in precision grinding, Annals of the CIRP, 30/1, (1981) 251-254

Hashimoto F., Kanai A., Myiashita M., Growing mechanism of chatter vibrations in grinding processes and chatter stabilization index of grinding wheel, Annals of the CIRP. 33/1 (1984), 259-263

Hashimoto F., Gallego I., Olivera J.F.G., Barrenetxea D., Takahashi M. , Sakakibara K., Stålfelt H. Staadt G., Ogawa K., Advances in centerless grinding technology, CIRP Annals Manufacturing Technology, 61 (2012), 747–770

Hashimoto F., Lahoty G.D., Miyashita M., Safe operation and friction characteristics of regulating wheel in centerless grinding, Annals of the CIRP, 47/1 (1998) 281-286

Hashimoto F., Zhou S.S., Stability diagram for chatter free centerless gridning and its application in machine development, Annals of the CIRP, 49/1 (2000), 225-230

Hermes Schleifkoerper Gmbh, Bonded Abrasives, Information Brochure (2010)

Hou Z.B., Komanduri R., On the mechanics of the grinding process, International Journal of machine tools and manufacture, 43 (2003), 1579-1593

ISO 13942: 2000 Bonded abrasive products: Limit deviations and runout tolerances

ISO/TS 12181-1:2003: Geometrical Product Specifications (GPS) – Roundness – Part 1: Vocabulary and parameters of roundness

ISO/TS 12181-1:2003: Geometrical Product Specifications (GPS) – Roundness – Part 2: Specification operators

Inasaki I., Regenerative Chatter in Grinding, Proceedings of the 18th MTDR Conf. (1977) 423-429.

Jameson J.R., Farris T.N., Equilibrium and compatibility simulation of plunge centerless grinding, Proceedings of the institution of Mechanical Engineers: Part B, 222/7 (2008), 747-757

Johnson K.L., Contact mechanics, Cambridge University Press, 1985

Kanappan S., Malkin S., Effects of grain size and operating parameters in the mechanics of grinding, Transactions of the ASME Journal of Engineering for Industry, 94 (1972), 833-842

Kim K., 2 dimensional modeling of centerless grinding – infeed (plunge) process, International Journal of the KSPE, 4/4 (2003), 25-31

Klocke F., Manufacturing Processes 2: Grinding, Honing, Lapping (RWTHedition) , Berlin, Springer-Verlag, 2009

F. Klocke, D. Friedrich, B. Linke, Z. Nachmani; Basics for in-process roundness improvement by a functional workrest blade, CIRP Annals, 53/1 (2004), 275-280

Konig, W | Follinger, H, Elastic Modulus of Grinding Wheels and Its Impact on Their In-Process Behavior – Part I, Ceram. Forum Int. Vol. 64, no. 6-7, (1987) 220-224

Konig, W | Follinger, H, Elastic Modulus of Grinding Wheels and Its Impact on Their In-Process Behavior – Part II, Ceram. Forum Int. Vol. 64, no. 6-7, (1987) 296-300

Kranjnik P., R. Drazumeric R., Meyer B., B. Kopac B., Zeppenfeld C., Simulation of workpiece forming and centre displacement in plunge centerless grinding, International Journal of machine tools and manufacture, 48/7-8, (2008), 824- 831

Li H., Shin Y.C., Time domain dynamic simulation model for stability prediction of infeed centerless grinding process, Journal of manufacturing science and engineering, 129/3, (2007) 539-551

Lichun L., Jizai F., Peklenik J., A study of grinding force mathematical model, Annals of the CIRP, 29/1, (1980), 245-249

Lin X., Modelling and Simulation of grinding processes based on a virtual wheel model and microscopic interaction analysis, PHD Thesis, Worcester Polytechnic institute, 2010

Lizarralde R., Barrenetxa D., Gallego I., Practical application of new simulation methods for elimination of geometric instabilities in centerless grinding, Annals of CIRP, 54/1 (2005), 273-276

Malkin S., Cook N.H., The wear of grinding wheels, Trans. ASME B, 93/4, (1971), 1121-1133

Malkin, S. and Guo, C. Grinding technology - Theory and applications of machining with abrasives, (2008), New York, Industrial Press

Marinescu I.D., Rowe W.B., Dimitrov, B., Inasaki I., Tribology of Abrasive Machining Processes, (2004), New York, William Andrew Publishing

Marinescu I.D., Hitchiner M., Uhlmann E., Rowe W.B., Inasaki I., Handbook of machining with grinding wheels, (2008), CRC Press, Boca Raton

Metcut research associates, Machining data handbook, vol.2, 3rd ed., (1980), MDC, Cincinnati, Ohio

Miyashita M., Hashimoto F., Kanai A., Diagram for selecting chatter free conditions of centerless grinding, Annals of the CIRP, 31/1 (1982), 221-223

Mikrosa, Kronos S125, Machine Handbook, (2005)

Modler, Grinding technology: concepts, solutions, applications, Catalogue of Johann Modler GmbH, (2005)

Monzesi Rettifiche, 400CNC, Machine Handbook, (2000)

Peters J., Snoeys R., Decneut A., Sonic testing of grinding wheels, Proc. 9th Int. Conf. MTDR, Manchester, England. Pergamon Press (1968).

Qi H.S., Rowe W. B., Mills B., Contact length in grinding – part 2: evaluation of contact length models, Proceedings of the Institution of Mechanical Engineers. Pt.J. Journal of Engineering Tribology. 211/J1 (1997), 77-85

Rammerstorfer F.G., Hastik F., Der Dynamische E-modul von Schleifkorpen, Werkstatt und Betrieb, 107 (1974) , 527-533

Rowe W.B., Barash M.M., Computer Method for investigating the inherent accuracy of centerless grinding, Int. J. Machine Tool design Research, 4, (1964), 91-116

Rowe W.B., Richards D.L., Research Note: Geometric Stability charts for the centerless grinding process, Journal of Mech. Engineering Science, 14/2 (1972), 155-158

Rowe W. B., An experimental investigation of grinding machine compliances and improvements in productivity, Proceedings of 14th Int. MTDR Conference, Manchester, 1973, 479-486

Rowe W.B., Miyashita M., Koenig W., Centerless grinding research and its application in advanced manufacturing technology, Annals of the CIRP, 38/2 (1989), 617-625.

Rowe W.B., Morgan M.N., Qi H.S., Zheng H.W., The effect of deformation on the contact area in grinding, Annals of the CIRP, 42/1 (1993), 409-412

Rowe W.B., Principles of modern grinding technology, (2009),Oxford, William Andrews

Shaw M.C., Principles of abrasive processing, (1996), Oxford, Oxford University Press

Shen C.H., Grinding wheel screening by the grindo sonic method, GMMD report, 1981

Shimizu T., Inasaki I., Yonetsu S., Studies on the force vibration during grinding, Bullettin of the JSME, 20/142 (1977) 475-482

Snoeys R., Wang I.C., Analysis of the static and dynamic stiffnesses of the grinding wheel surface, Proceedings of the 9th Int. MTDR Conference, vol 2 (1968), 1133-1148

Snoeys R., Brown D., Dominating parameters in grinding wheel and workpiece regenerative chatter, Proceedings of the 10th Int. MTDR Conference (1969), 325-348

Snoeys R., Peters J., Decneut A., The Significance of chip thickness in grinding (Keynote), Annals of the CIRP, 23/2 (1974), 227-237

Spur G., Stoferle T., in Enciclopedia delle lavorazione meccaniche, Tecniche Nuove, vol.4, pag 129

Takasu S., Masuda M., Heavy-Duty centerless grinding for multi-diameter shafts, Annals of the CIRP, 37/1 (1988), 323-326

Tang J., Du J., Chen Y., MOdeling and experimental study of grinding forces in surface grinding, Journal of materials processing Technology, 209 (2009) 2847-2854

Tooe S., Umino K., Shinozaki N., Study on grinding characteristics of Grinding wheel (1st report), Bull. Jap. Soc. of Prec. Engg., 21/4 (1087), 245-250

Tonshoff H.K., Peters J., Inasaki I., Paul T., Modelling and Simulation of grinding processes, Annals of the CIRP 41/2 (1992) 677-688

Tsasch H., Applied machining technology, (2009) , Springer

Werner G., Influence of work material on grinding forces, Annals of the CIRP. 27/1, (1978), 243-248

Williams J.A., Xie Y., The generation of wear surfaces by the interaction of parallel grooves, Wear 155 (1992) 363–379

Wintherthur Group, Handbook of Centerless Grinding, Wintherthur Group booklet, (2005)

Winter Group, Catalogue No. 5: Dressing Tools: WINTER Diamond Tools for Dressing of Grinding Wheels, (2012)

Webster J., Tricard M., Innovations in abrasive products for precision grinding, CIRP Annals, 58/2, (2004), 597-617

Younis M., Saadek M. M., T. El-Wardani, A new approach to development of a grinding force model, J. Eng. Ind. (Trans. ASME), 109/4, (1987) 306-313

Yamada T, Lee H, Morita H. Study on the contact stiffness of grinding wheels due to the difference of dressing condition, Proceedings of The Twenty-first Annual Meeting
of The American Society for Precision Engineering 21st; 2006.

Yang W.Y., Cao W., Chung T.S., Morris J., Applied numerical methods using MATLAB, 1st ed J. Wiley, 2005

Zhou S.S., Gartner J.R., Howes T.D., On the relationship between setup parameters and lobing behaviour in centerless grinding, Annals of the CIRP, 45/1 (1996), 341-346

Zhou S.S., Gartner J.R., Howes T.D., Lobing behaviour in centerless grinding- part I: stability estimation, Jorunal of dynamic systems, measurement and control, 119 (1997), 153-159

Zakharov O.V., Rotational stability of blank in centerless grinding with longitudinal supply, Russian engineering research, 28/6 (2008) 588-591

Appendix

Table of dynamic parameters

Symbol	Measuring units	Name
F_n	[N]	Grinding force in radial direction
F_t	[N]	Grinding force in tangential direction
$F_x^{'}$	[N/mm]	Grinding force in "x" direction per unit of width
λ		Grinding force ratio
R_b	[N]	Blade normal reaction force
R_r	[N]	Control wheel reaction force
μ_b	-	Blade kinetic friction coeficient
μ_r	-	Regualting wheel kinetic friction coefficient
μ_{r0}	-	Regualting wheel static friction coefficient
K_{eq}	[N/µm]	Equivalent system stiffness
K_s	[N/µm]	Cutting stiffness
k_s	[N/µm/mm]	Specific cutting stiffness
k'_s	[N/µm/mm]	Specific cutting index
K_{cr}	[N/µm]	Contact stiffness between workpiece and regulating wheel
K_{cg}	[N/µm]	Contact stiffness between workpiece and grinding wheel
k_{cx}	[N/µm/mm]	Specific contact stiffness between workpiece and "x" wheel
K_m	[N/µm]	Static machine stiffness
Δr_w	[mm]	Cumulative radius defect

Table of kinematic parameters

Symbol	Measuring units	Name
v_s	[m/s]	Grinding wheel speed
v_w	[m/s]	Workpiece speed
v_R	[m/s]	Control wheel speed
Ω	[rpm]	Workpiece rotational speed
Ω_R	[rpm]	Control wheel rotational speed
a_e	[µm]	Actual depth of cut
a	[µm]	Machine set depth of cut
v_{fr}	[mm/min]	Infeed speed
v_{far}	[mm/min]	Dressing traverse speed
b_d	[mm]	Dressing active width
b	[mm]	Grinding contact width
U_d	-	Dressing overlap
h_{eq}	[µm]	Equivalent depth of cut
q	-	Speed ratio
Q_w	[mm^3/min]	Stock removal rate
Q_w'	[mm^3/mm/min]	Stock removal rate per unit of width
G	-	Grinding ratio

Geometrical parameters table

Symbol	Measuring units	Name
D_w	[mm]	Workpiece diameter
D_s	[mm]	Grinding wheel parameter
D_r	[mm]	Regulating wheel parameter
d_e	[mm]	Equivalent diameter
H	[mm]	Center height
H_0	[mm]	Center height at the tilting focus
α	[deg]	Center height angle
α_r	[deg]	Control wheel tilting angle
β	[deg]	Actual depth of cut
β_r	[deg]	Angle between the centerline and the direction connecting control wheel center to the workpiece center (clockwise)
β_s	[deg]	Angle between the centerline and the direction connecting grinding wheel center to the workpiece center (counter clockwise)
γ	[deg]	Center height angle (equivalent notation)
θ	[deg]	Blade angle
b_d	[mm]	Dressing active width
b	[mm]	Grinding contact width
K_1	-	Geometrical coefficient for imperfection at blade contact
K_2	-	Geometrical coefficient for imperfection at regulating wheel contact
lc	[mm]	Contact length
lg	[mm]	Geometrical contact length
Rr	-	Rough contact correction parameter
Δr_w	[mm]	Cumulative radius defect
Δr_{wg}	[mm]	Radius defect due to geometrical issues
Δr_{wk}	[mm]	Radius defect due to system dynamic deflections
Δr_{wd}	[mm]	Radius defect due to vibration generated during the centerless grinding process

Acronyms table

Acronym	Name
OP	Machining operation type
OD	Outside Diameter grinding
ID	Inner Diameter grinding
S	Surface grinding
CF	Creep feed grinding
CW (=RW)	Control wheel (=Regulating wheel)
GW	Grinding wheel
SiC	Silicium Carbide
PCD	Polycristalline diamond
Al_2O_3	Aluminium oxide
UPR	Undulation per revolution
AE	Acustic Emission

List of figures

List of tables